https://doi.org/10.1016/j.ensm.2019.12.011

Aqueous Metal-Air Batteries: Fundamentals and Applications

Qianfeng Liu[†,1,3], Zhefei Pan[†,2], Erdong Wang*[,1], Liang An*[,2], Gongquan Sun*[,1]

[1] Division of Fuel Cell & Battery, Dalian National Laboratory for Clean Energy, Dalian Institute of Chemical Physics, Chinese Academy of Sciences, Dalian 116023, China

[2] Department of Mechanical Engineering, The Hong Kong Polytechnic University, Hung Hom, Kowloon, Hong Kong SAR, China

[3] University of Chinese Academy of Sciences, Beijing 100049, China

[†] Equal contribution.

* Corresponding authors.

Email: edwang@dicp.ac.cn (E.D. Wang)

Email: liang.an@polyu.edu.hk (L. An)

Email: gqsun@dicp.ac.cn (G.Q. Sun)

Abstract

Aqueous metal-air batteries have gained much research interest as an emerging energy storage technology in consumer electronics, electric vehicles, and stationary power plant recently, primarily due to their high energy density derived from discarding the bulkier cathode chamber. In addition, abundant raw materials, low cost, high safety, and environmental friendliness are intrinsic advantages of metal-air batteries as well. Motivated by the desirable characteristics, the significant progress has been made in promoting the promising electrochemical performance and improving the long-term stability in aqueous metal-air batteries in recent years. This review article starts with a general description of the features and working principles of aqueous metal-air battery systems. Then, the air cathode structures are introduced and compared, as well as the electrochemical catalysts applied in the air cathode are comprehensively summarized, including noble metals, alloys, metal oxides, hydroxides or sulfides, carbon materials, as well as composite materials such as metal (oxides)/metal oxides and (metal) oxides/carbon materials. In addition, the chemistries and major issues of metal anodes, e.g. aluminum, zinc and magnesium, are reviewed and respective strategies to alleviate these issues are offered as well. Afterwards, detailed discussions have been provided on the recent progress towards the electrolytes and separators, both of which are crucial components in

the battery configuration. From the system point of view, innovative single-cell and stack system designs are also presented. Finally, the challenges and perspectives for the future development of aqueous metal-air batteries are highlighted.

Keywords: Metal-air batteries; Aqueous electrolytes; Bi-functional electrocatalysts; Separators; System designs

1. Introduction

The growing demands in energy supply and the awareness of climate change have facilitated the inevitable transition from burning fossil fuels to clean and efficient energy conversion technologies such as fuel cells [1-6]. In spite of the power-generating processes, the storage of the energy generated from renewable energy sources, such as solar and wind power, is a parasitic and crucial process for the energy sustainability [7-12]. Given the adequate but intermittent solar and wind power, it is urgent to develop energy-storage systems to reserve the renewable energy, which are essential components in the future energy network to buffer the unpredictable energy generation and supply [13-18]. The advantages of energy-storage systems can be summarized as: (1) store the energy at off-peak times and release the energy during peak times to reduce the overall generation from power plants; (2) make the intermittent solar and wind power a stable power source; and (3) accelerate the electrification of transportation, reduce fuel consumption and promote a low carbon economy [19]. Batteries, one kind of energy-storage systems, penetrated every corner of our daily life have been well-known for their excellence in converting and storing energy. Particularly, first reported in 1991, lithium-ion batteries have been widely used in portable electronic devices and electric vehicles [20]. In order to meet the demand to electrify transportation and promote grid-scale stationary energy storage, the energy density and power density of the Li-ion batteries are required to be continuously improved [9, 21]. Unfortunately, it is generally accepted that an increase of at most 30% in energy density can be made in Li-ion battery technology, indicating intercalation chemistry-based conventional lithium-ion technology is approaching its performance upper limit [13]. In addition, the disadvantages of high cost, especially for the insufficient supply of lithium and cobalt, and blemished safety issues have held back the large-scale applications of Li-ion batteries [10].

Recently, metal-air batteries have received ever-increasing research interest as an emerging energy storage technology in consumer electronics, electric vehicles, and stationary power plants [14, 18, 22-29]. It can be seen from Fig. 1 that the publications associated with metal-air batteries show a remarkable increase from 62 publications in 2011 to 874 publications in 2018, indicating the ever-increasing research interest has been paid to this field. In addition, China and USA play the

leading role in this research direction, as 44.7% and 17.6% of the publications published by the researchers from China and USA, respectively. The two pioneer countries are followed by South Korea, Japan, Germany, Australia, Canada, Singapore, India, and UK, which suggests that worldwide attention has been attracted by this technology. Unlike the conventional batteries where the reagents are stored within the cells, metal-air batteries utilize oxygen from the atmosphere at the cathode, thus they are consequently thought as a hybrid of batteries and fuel cells. Due to the air-breathing structure discarding the bulkier cathode chamber, they have high theoretical energy densities (energy per unit weight) in the range of 1353-11429 Wh kg^{-1} (calculated by the common Zn-, Al-, Mg- and Li-air batteries), which are about 3-30 times higher than that of lithium-ion battery [13]. In general, the metal-air battery consists of a metal anode saturated with appropriate electrolyte, a porous air cathode absorbing the surrounding air, as well as a proper separator mechanically disconnecting the anode and cathode. The metal anode can be alkali metals (e.g., Li), alkaline earth metals (e.g., Mg), earth abundant metals (e.g., Al), or first-row transition metals (e.g., Zn) with good electrochemical equivalence. With regard to the traditional non-aqueous electrolyte, it brings about four concerns hindering its wide applications: (1) the inherent safety issue attributed to the flammable organic electrolytes; (2) the low ionic conductivity around 1-10 mS cm^{-1}; (3) the high cost due to the rigorous manufacturing requirements; and (4) the potential environmental pollution [30]. As a contrast, aqueous electrolyte is of particular attraction in terms of high operation safety, great ionic conductivity of approximately 1 S cm^{-1}, low cost, and environmental benignity [31]. Because of the aqueous electrolyte, Li, Na, and K in the metallic form are plagued by their inherent instability to react with water [10]. In addition, differing from the air cathode made of bare porous carbon materials in non-aqueous metal-air batteries, a homogenous distribution of catalyst on the substrate is required to maximize the performance via increasing the cycling efficiency by lowering the voltage gap between charge and discharge processes in aqueous metal-air batteries.

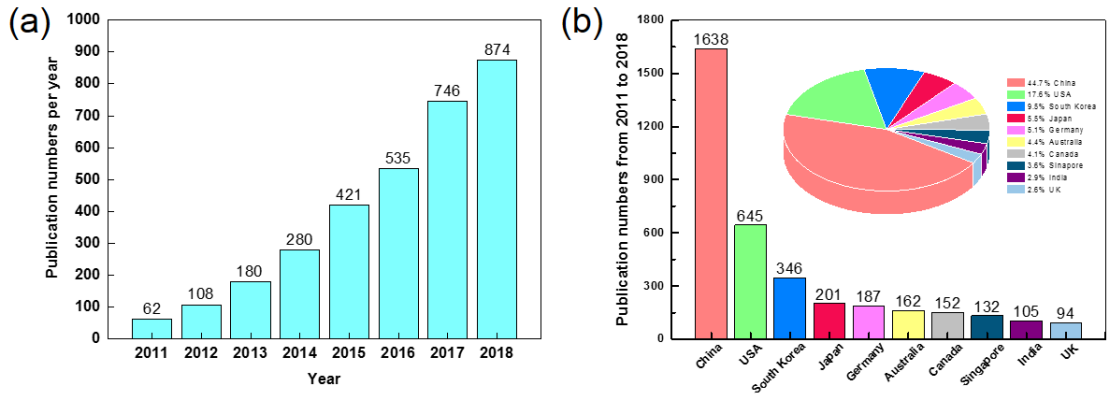

Fig. 1. (a) Publications related to metal-air batteries per year from 2011 to 2018, and (b) the top 10 countries publishing the most publications from 2011 to 2018.

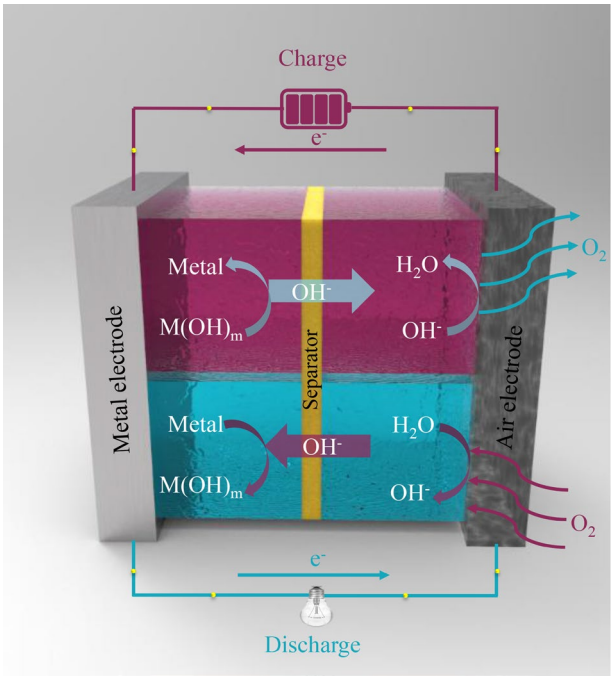

Fig. 2. Working principle of aqueous metal-air batteries.

Basically, the working principle of aqueous metal-air batteries are illustrated in Fig. 2. On the anode, the metal is oxidized to release electrons and the metal ions combine with hydroxide ions to form metal hydroxide during discharge process:

$$M + nOH^- \rightarrow M(OH)_n + ne^- \quad (1)$$

where M presents the metal (e.g., Zn, Al, or Mg) and n is the valence of metal ions. The released electrons transport through the external circuit and reach the cathode to participate in the oxygen

reduction reaction (ORR). On the cathode, oxygen molecules from the atmosphere combining the coming electrons and water are reduced to hydroxide ions:

$$\frac{n}{4}O_2 + ne^- + \frac{n}{2}H_2O \rightarrow nOH^- \quad (2)$$

The generated hydroxide ions transport through the separator from the cathode to the anode to complete the current loop. Combining the Eq. (1) and (2), the overall reaction can be obtained:

$$M + \frac{n}{4}O_2 + \frac{n}{2}H_2O \rightarrow M(OH)_n \quad (3)$$

It should be mentioned that currently, only Zn-air batteries can be electrically rechargeable in aqueous electrolyte, while the Al- and Mg-air batteries need to be recharged via mechanically changing the metal anodes, which cannot be directly reduced from ions to metals in aqueous electrolyte [32]. In charge process, the reaction steps are inverse with the discharge as shown in Fig. 2.

The objective of this review is to provide a general description of aqueous metal-air batteries, summarize the recent advances in electrode structures and novel catalysts of air cathodes and metal anodes (Zn, Al, and Mg), conclude the latest progress in electrolytes and separators, as well as discuss the single-cell and stack system designs. Finally, conclusions are given followed by a brief future perspective.

2. Air electrode

The air cathodes are one of the key components for metal-air batteries, and the well-established air electrodes ensure efficient and stable operation of metal-air batteries. Generally, an efficient air electrode should possess fast oxygen diffusion while prevent water permeating, high electrochemical activity for oxygen reduction in primary metal-air batteries, both of oxygen reduction and oxygen evolution in rechargeable ones, quick migration of OH^-, a stable physical structure in alkaline condition and good electrochemical stability (especially under high potentials). These complicated and self-contradictory requirements entangle the design of air electrodes. According to the literatures, therefore, the main interest in metal-air batteries over the past 50 years is focused on achieving better catalytic activity, longer life and lower cost of fabrication methods and materials for air electrodes. In this section, the air electrode holistic architecture, detailed material and design aspects of gas diffusion layer and catalyst layer are reviewed.

2.1. Air electrode architecture

The architecture of a conventional air electrode is composed by three components: a catalyst layer (or an active catalyst layer), a current collector and a gas diffusion layer as shown in Fig. 3. Generally, the gas diffusion layer is assembled at the outside of the air electrode, then pressed with the current collector layer and catalyst layer successively with a sandwich structure. This classical structure is built by Heise and Schumacher of the National Carbon Company in 1932 used for Zn-air battery, which has been almost unchanged since then [33]. The outside gas diffusion layer has various pores to ensure the fast diffusion of oxygen. Meanwhile, these pores must be hydrophobic enough to avoid the electrolyte leakage. The current collector layer is always bedded between the gas diffusion layer and catalyst layer to transfer the electrons from or to the catalyst layer. The catalyst layer is the place for oxygen reduction or evolution, which plays the most crucial role for high performance of air electrode. To maximize the oxygen diffusion rate, all these three layers of the air electrode are porous. During the operation of air electrodes for ORR, the oxygen in the air diffuses from the porous gas diffusion layer and current collector layer to the catalyst layer. At the same time, the electrons from the metal anode transfer through the current collector layer to the catalyst layer and combine with the oxygen at the catalyst active sites. For oxygen evolution reaction, the paths of oxygen and electrons are inverse. Although the architecture of the air electrodes of different kinds of aqueous metal-air batteries contain some difference, such as arrangement of the three layers, the air electrodes possess the same function to keep the battery running.

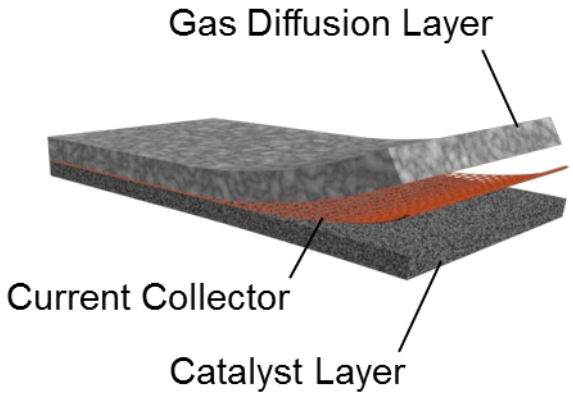

Fig. 3. Schematic of the air electrode configuration.

2.1.1. Gas diffusion layer

The gas diffusion layer plays a vital role in the performance of the metal-air batteries, especially for high current density discharge and durability of the electrode determined by the gas diffusion rate and electrolyte leakage time. To facilitate oxygen transport in the air electrode, the gas diffusion layer should be thin, porous and hydrophobic [34]. The hydrophobic pores and channels provide fast oxygen transport pathways and avoid flooding, which can be adjusted by hydrophobic agents, such as polytetrafluoroethylene (PTFE), polyvinylidene fluoride (PVDF), and fluorinated ethylene propylene (FEP) [35]. Although the higher percent of hydrophobic agent will enhance the waterproofness, it reduces the porosity and hinders the gas diffusion [36]. Therefore, to balance the waterproofness and gas diffusion rate, the proper PTFE content is 30-70 wt.% [37]. One of typical fabrication methods is uniformly blending PTFE with carbon black [38] (e.g. AD-200 [39], XC-72 [40, 41], acetylene black [42]), active carbon [42] or/and carbon fiber [43-46] in alcohol, then the mixture is dried to pasty and rolled to be film or scratched to the current collector. The other typical architecture of gas diffusion layer is directly using PTFE porous film to proof water and diffuse air [47-50]. To avoid being punctured by the current collector, the PTFE film and current collector are separated by a thin microporous layer, such as carbon powder and some part of catalyst layer.

Although the conventional fabrication technology is relative maturity, it is also complicated for the researchers in laboratory to assemble a desired testing metal-air battery [51]. Fortunately, Toray Industries, Inc. in 1980 developed a successful commercial gas diffusion layer for polymer electrolyte fuel cell by Toray carbon paper [34], which is also suitable for metal-air batteries as the gas diffusion layer directly [52] or simply treated with PTFE [53]. The woven carbon cloth, similar to the carbon paper, also has the continuous macropores and is widely applied to flexible Zinc-air batteries in laboratories because of the excellent mechanical flexibility [54-62]. Additionally, the good electroconductivity of the carbon paper and cloth makes themselves as the current collectors. However, they are quite brittle to handle as large area electrodes because of the high possibility of leakage, which is not permitted to keep the metal-air battery running, and the relative high cost also limits the wide application for metal-air batteries. To solve the leakage of primary zinc batteries, Wang et al. designed a new kind of cathode with continuous hydrophobic pores based on carbon felt and PTFE, combined with commercial manganese-based ORR catalyst. The resulting battery

equipped with this durable cathode can stably discharge over 3600 h in air with an average potential of 1.1 V at 50 mA cm^{-2} [63].

For primary aqueous metal-air batteries, the different kinds of electrolytes (alkaline or neutral solutions) and discharge current densities require different types of gas diffusion layers. For example, the permeability of neutral solution (NaCl) is much lower than that of alkaline solutions (KOH and NaOH). Therefore, the hydrophobicity of the gas diffusion layer for neutral electrolyte can be designed relative lower [41, 64], and some researchers even using the hydrophobic catalyst layer as the gas diffusion layer [65]. However, the Mg-air battery with neutral electrolyte also needs high hydrophobic gas diffusion layer for longtime operation. For example, Wang et al. [44] designed a high-performance cathode based on carbon fiber felt for Mg-air battery. When the proportion of PTFE is 20 wt.% in the catalyst layer and about 70 wt.% in gas diffusion layer is proper for the Mg-air battery with higher power density and durability of 1100 h discharge. Under low discharge current density (<100 mA cm^{-2}), the PTFE loading in the gas diffusion layer makes a negligible change [36, 47, 66].

For rechargeable aqueous metal-air batteries, mainly referring of Zinc-air batteries, the gas diffusion layer requires higher potential corrosion resistant materials, such as high-graphitized carbons (e.g. graphene [67], reduced graphene oxide [68], and carbon nanotubes [69]) and porous metal materials [70-73]. These high corrosion resistant materials as the gas diffusion layer can efficiently solve the corrosion problems causing by the carbon paper [74-87] and carbon cloth [88-92], such as the loss of active surface area due to the carbon corrosion, and the interlocking degeneration of uniform distribution of current, even severe leakage. For example, Sun et al. [93] designed a carbon-free and binder-free cathode with hierarchical porous 3D $MnCo_2O_4$ nanowire bundles obtained by hydrothermal method, which kept the porous structure after 300 cycles during 2 months.

2.1.2. Current collector

The main role of the current collector is collecting electrons, and another is a physical support to avoid being teared, especially for large area cathodes. As a collector, it should be conductive enough; and as a support, it should be tough enough. Additionally, the current collector is always assembled at outside of the catalyst layer, which means it must be porous enough to transfer oxygen. Therefore,

the materials of current collector focus on metal foam, metal mesh (such as nickel foam [49, 94-116], copper foam [117, 118], nickel mesh [119, 120], stainless steel mesh [121, 122]) and carbon cloth [28] or paper [74-87]. Recently, some new kinds or concepts of current collectors have been designed [123-127]. For example, Liu and co-workers [126] reported a current-collector-free cathode with a 3D foam-like composite composed of Mo_2C nanorods decorated by high electroconductive N-doped carbon. Nickel foam, with good NaCl-corrosion-resistance performance, is the main material as current collector for Mg-air battery [41, 45, 64, 65, 128-130]. But for the other metal-air batteries, the materials of current collector are multitudinous as previously described.

2.1.3. Catalyst layer

Catalyst layer, the place for oxygen reduction and evolution, is the key component for air electrodes, which determines the performance of metal-air batteries on charge-discharge efficiency and durability. Because of the limitation of in-situ characterization technologies, the atomic ORR process remains unclear [131-133]. Based on the experience and theory model, the ORR process on "three phase interface" is widely accepted [134-139]. Although the true model of ORR is a "two phase interface" process of solid and electrolyte (because the oxygen must dissolve in the electrolyte so that it can be reduced on catalyst) [135], the researchers still chronically call it "three phase interface". As oxygen has low solubility and diffusivity in aqueous electrolytes, oxygen in the ORR process is mainly in the form of gas phase before it dissolving in the electrolyte. Therefore, to fast diffuse the oxygen, the porous catalyst layer should possess proper hydrophobicity to avoid flooding or forming thick electrolyte film [140]. The hydrophobicity is adjusted by the content of PTFE owing to its capable of water repellent and stability [37]. And the porous structure is always supplied by porous carbon materials with good conductive, high stability, low cost and abundant sources [133, 141-147]. For traditional fabrication method of catalyst layers, the active catalyst and substrate is always bonded by PTFE binder. To avoid the binding catalysts falling from the substrate, the catalysts are better to directly grow on substrate. If the substrate with self-supporting catalyst is a continuous electroconductive net, such as carbon fiber [148-155] and nickel foam [110-112, 116], the PTFE mainly acts as the hydrophobicity adjuster. Although different kinds of aqueous primary metal-air batteries discharge in alkaline or neutral electrolytes at various current density with multitudinous kinds of ORR catalysts, the architectures are similar as described.

Compared to primary aqueous metal-air batteries, the significant change of catalyst layers for electrically rechargeable ones (mainly Zn-air batteries) is transformed ORR catalysts to bi-functional oxygen catalysts except for tri-electrode structure [156]. The bi-functional oxygen catalysts consume oxygen during battery discharge and reversely evolve oxygen while charging. During charging process, the potential of catalyst layer is always above 1.5 V vs. RHE, which is too high for the carbon materials to endure [37]. Therefore, the materials in bi-functional catalyst must be more robust than that of ORR materials, such as the high-graphitized carbons [147, 157-160], carbon fiber materials [148-155] and porous metal [116, 117, 161]. Additionally, it is better to design the binder-free catalyst layer, which can reduce the ohmic polarization to lower the potential of OER and avoid the exfoliation of catalyst by the oxidation or degradation of binders [162]. For instance, Zhong et al. [58] developed a facile and binder-free method for the *in situ* and horizontal growth of ultrathin mesoporous Co_3O_4 layers (ORR catalyst) on carbon cloth as a high-performance bi-functional air electrode for a flexible Zn-air battery (as shown in Fig. 4). The contact area of the mesoporous Co_3O_4 layers and conductive support was maximized, facilitating the rapid electron transport and preventing the aggregation of ultrathin layers. Compared with the traditional method of carbon fibers supported Co_3O_4 nanoparticles with binder, the grown ultrathin mesoporous Co_3O_4 layers exerted over 10 times of mass activity for ORR and OER. Additionally, the Zn-air battery equipped with the corresponding of Co_3O_4 layers was operated without obvious degradation under serious deformation and even during the cutting process.

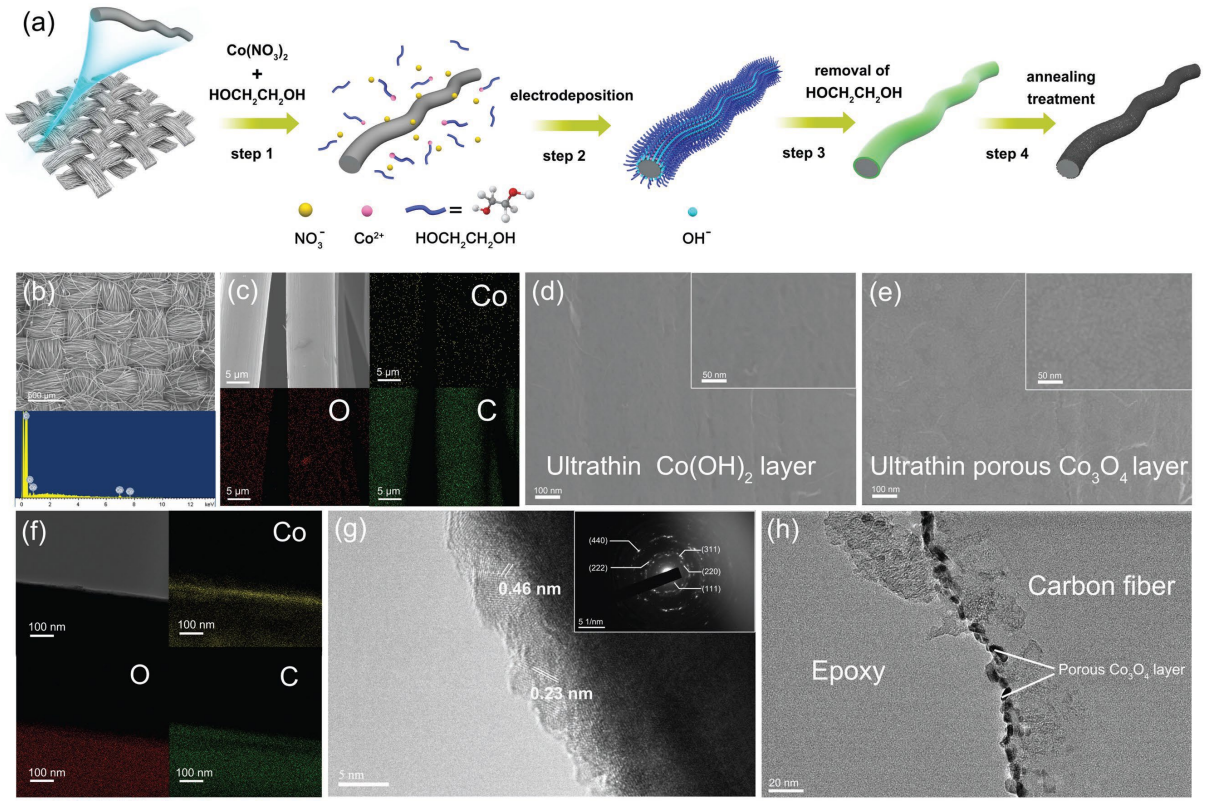

Fig. 4. (a) Schematic diagram of the preparation of the air electrode. (b) SEM image and the EDS of an as-prepared ultrathin $Co(OH)_2$/CC. (c) SEM image and the elemental mapping of an ultrathin $Co(OH)_2$/CC. (d) SEM image of the surface of an ultrathin $Co(OH)_2$/CC. (e) SEM image of the surface of the ultrathin Co_3O_4/CC. (f) STEM image at the edge of a carbon fiber with an ultrathin $Co(OH)_2$ layer and the elemental mapping of Co, O, and C. (g) HRTEM image of the edge of a carbon fiber with an ultrathin Co_3O_4 layer. (h) Cross-sectional TEM image of a carbon fiber with an ultrathin Co_3O_4 layer. [58] Copyright 2017 John Wiley and Sons.

2.2. Oxygen catalyst

The oxygen electrocatalysts applied for metal-air batteries must take the activity, stability, conductivity, mass transfusion and cost into overall consideration. So far, the materials that have been explored for ORR electrocatalysts or ORR/OER bi-functional electrocatalysts include noble metal, alloys, metal oxide, hydroxide or sulfide, carbon materials, as well as the corresponding of composite materials, such as metal (oxide)/metal oxide, (metal) oxide/carbon material. In view of the mechanism of ORR and OER that has been reviewed in detail [131, 132, 158, 163-167], in this

section, it will be introduced concisely. Additionally, the oxygen catalysts will be classified by the functions for ORR and ORR/OER based on materials, and the difference between the different kinds of metal-air batteries will be introduced simply.

2.2.1. Reaction mechanism for ORR and OER

ORR mechanism In alkaline conditions, the ORR intermediates involve diverse oxygen-containing species, such as OOH*, OH* and O*, resulting complicated multistep electron-transfer processes. Generally, these processes can be classified into two pathways, direct four-electron pathway and two-electron pathway. For the former, one oxygen molecular receives 4 electrons and is reduced to 4 OH^-. For the latter, the oxygen molecule is first reduced to intermediate of H_2O_2 or HO_2^-, then the intermediate transfers into electrolyte or is further reduced to OH^- via receiving 2 electrons (which is also named of indirect four-electron pathway) [168]. Presently, plentiful materials have been investigated for the ORR electrocatalytic mechanisms, involving noble metals, alloys, metal oxides/carbides/nitrides, carbon nanomaterials and their composites [132]. Generally, the direct four-electron pathway favors noble metal-based electrocatalysts, while the two-electron pathway is apt to carbon nanomaterials. However, the ORR pathways are changed with the variation of materials, including the species, composition, specific crystal surfaces and even the experimental conditions [169]. For example, Pt electrode in acid media undergoes direct four-electron pathway via inner-sphere model, while undergoes both direct four-electron and two-electron pathways in alkaline media because of coexistence both of inner- and outer-sphere model. For non-noble metals, the dominated outer-sphere electron transfer process impels the two-electron pathway in alkaline media. Owning to the outer-sphere mechanism, a nonspecific adsorption for oxygen molecular, it is possible for using a wide range of non-noble metals and their oxides as ORR electrocatalytic materials in alkaline media [170].

OER mechanism OER is the reverse reaction of ORR. Expectedly, the excellent ORR catalysts should display outstanding performance for OER, such as Pt, however, this is not always observed by experiment [132]. As a multi-electron pathway, OER also contains complicated intermediates (such as OOH*, OH* and O*), which are similar to that of ORR resulting to high overpotential [6]. The corresponding potential gap between ORR and OER changes the adsorption energy of these intermediates at the same substrate to change the reaction kinetics. Therefore, the proper ORR

catalysts are always not suit for OER. Additionally, under the high positive potential of OER, the metal elements in ORR catalysts could be oxidized to higher valence, such as Pt and NiFe LDHs, which also alters the surface conditions to change the reaction kinetics [6]. The complicated intermediates make the OER reaction mechanism diverse too. However, most of the mechanisms suggest that the substrate (M) adsorbs OH- to form of M-OH firstly, then transferred to M-O. The intermediate M-O produces oxygen molecular through two pathways, one is direct combination of two M-O to produce, the other one involves the formation of M-OOH to decompose to oxygen molecular [6]. To describe the activity tends, a number of descriptors have been presented in type of volcano plots, such as ΔG_O-ΔG_{OH} [171], the number of d-electrons in the e_g orbital [172] and coordinatively unsaturated metal cation (M_{CUS}) [173]. However, these trends are complex due to various influence factors, including differences in electrochemically active surface area, electrical conductivity, surface chemical stability and composition [174].

2.2.2. Oxygen reduction catalyst

Noble metals Pt, one of noble metals, has been recognized as the most active electrocatalyst for ORR, and it remains the benchmark (commercial Pt/C) in the evaluation for new electrocatalysts. To reduce the cost caused by the high price, the methods to reduce the load or enhance the activity of the Pt-based catalysts are continuous exploiting, including decreasing the particle size [175], reducing the thickness of Pt layers [176], alloying with transition metals [177, 178] and enhancing the synergistic effect [175]. In addition, the other noble metals such as Pd [138, 179, 180], Ag [181], Au [182] and their alloys [178, 183, 184] have received considerable attention in recent years. Silver is particularly attractive [148, 185-195] due to its relatively lower cost (only ~1% of the price of platinum), proper activity [196, 197] and better long-term stability [198]. Especially in high concentration of KOH or NaOH, the metal-air batteries equipped with Ag-based catalysts even exhibited better performance than that of Pt/C [181, 186, 189, 199, 200]. Benefiting from the high surface and facilitated mass transportation in the 3D interconnected porous structure, the np-Ag fabricated via electrodeposition by Sun's group [201] displayed 130 times enhancement in ORR catalytic activity than that of the flat polycrystalline silver, and even outperformed the commercial Pt black catalyst in 0.1 M NaOH.

Metal oxides and the hybrids Metal oxides are considered as good as non-noble metal catalysts due to their low-cost and considerable high activity in alkaline electrolytes [143, 202-205], which mainly focus on Mn-based oxides [50, 190, 206, 207], such as MnO_2 [193, 206, 208, 209], Mn-based perovskite [137, 210-216] and spinel [219-219]. For example, $LaMnO_3$, one of typical perovskites (ABO_3), possesses good intrinsic activity for ORR. When the valance state of Mn increased, the structure became $LaMnO_{3+\delta}$, which exhibited excellent ORR activity closed to Pt/C with over 3 times higher than that of $LaMnO_3$ [210]. To obtain the high activity of the metal oxide, it must be fabricated with optimal design, such as size, morphology, crystallographic structure and composition control. Therein, hybridization (doping and defecting), the special kind of composition control, is an effective method to enhance the intrinsic activity by optimizing the electron structure. For instance, Liu et al. [216] designed the $(La_{1-x}Sr_x)_{0.98}MnO_3$ (LSM) by appropriate doping with Sr and introducing A-site deficiencies to effectively tailor the Mn valence and increase the oxygen adsorption capacity of LSM, which exhibited high activity for ORR.

Carbon materials Due to the reasonable balance between catalytic activity, durability, electroconductivity, specific surface area and cost, carbon materials (especially heteroatoms doped carbons) have been applied widely in metal-air batteries as catalysts [220-231] and supports [37, 132, 133, 141, 159, 166, 232-235], such as N, O, P, S and B doped graphene, carbon nanotube, carbon fiber and carbon black, and graphitic carbon nitride. The sp^2-type carbon materials without or with little heteroatoms doping possess high electroconductivity, which are suitable for supports of catalysts. Additionally, the porous carbon can fast transfer oxygen to reduce the mass transfer polarization. For example, Zhou et al. [236] successfully fabricated hierarchically porous carbon microspheres (HCMs) with fully open and interconnected super-macropores. When it supported Pt nanoparticles as ORR catalyst for Zn-air battery, it promised a nearly 100% Pt utilization and showed a higher activity and better durability than the commercial Pt/C both in the rotating disk electrode (RDE) and Zn-air battery. When the carbon materials are doped with heteroatoms, especially for N atom, they can exhibit high activity for ORR to act as metal-free catalysts [227, 230, 237-239]. Li et al. [228] fabricated N-doped microporous carbon as an exceptional metal-free catalyst from banana peel, exhibiting a comparable ORR activity and much better stability than that of Pt/C. When the N-doped carbon materials are anchored with translation metal atoms, such as Fe

[240-250], Co [251-254] and Cu [255-257], the ORR activity will be obviously further enhanced. For example, inspired by fibrous string structures of bufo-spawn, Cheng et al. [243] reported a scalable synthesis of atomic Fe–N_x coupled open-mesoporous N-doped-carbon nanofibers (OM-NCNF-FeNx) as shown in Fig. 5. In neutral phosphate-buffered saline (PBS), the ORR activity of OM-NCNF-FeNx was close to Pt/C and much higher than that of OM-NCNF.

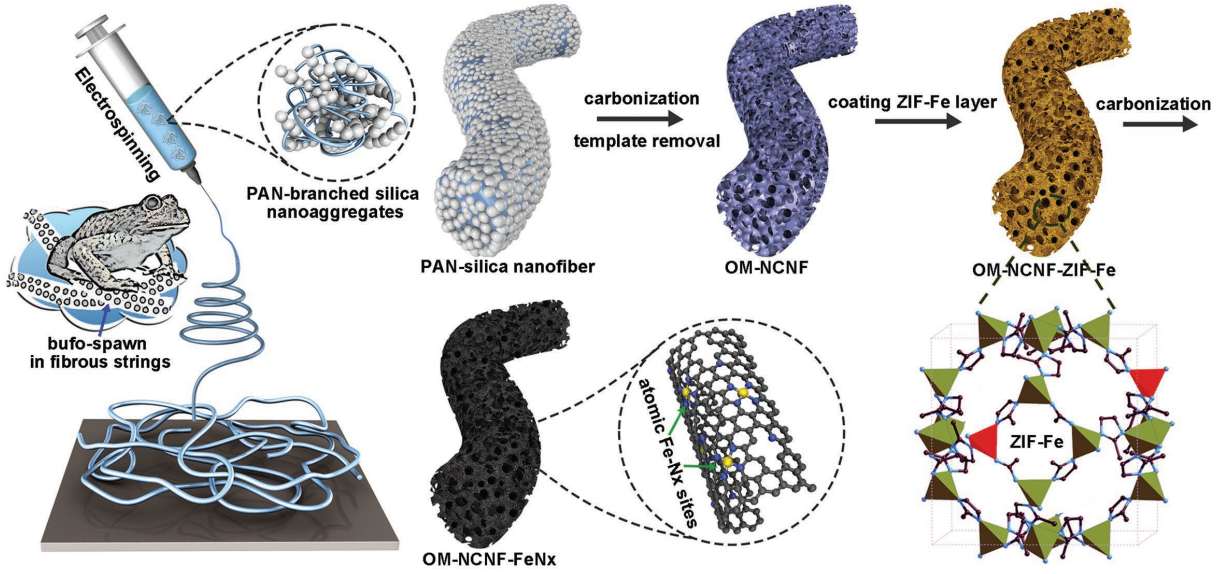

Fig. 5. Schematic representations of the fibrous string structures of bufo-spawn inspired fabrication towards the open-mesoporous CNFs. [243] Copyright 2018 John Wiley and Sons.

Composite materials Composite materials combine the different functional materials to stimulate their merits together, such as the high activity of metal oxides, high specific area, porosity and conductivity of carbon materials and porous metals. As is well-known, commercial Pt/C is one of typical composite materials, which combines highly active Pt nanoparticles with porous and conductive carbon. As the multiple demands for electrocatalysts, such as good activity, durability, conductivity, mass transfusion and low cost, carbon materials are the suitable choice. Therefore, carbon materials have been applied widely for ORR catalysts as composite materials recently. For instance, the pores of carbon, such as carbon black (XC-72, Ketjenblack carbon) and active carbon [258, 259] provide firm sites to anchor active materials. However, the anchored active materials exposed in solution are unavoidable to be dissolved, split, corroded and agglomerated. Carbon-coated materials can solve these problems and avoid the loss of activity by controlling the layer numbers of carbon [260, 261]. Additionally, the covering carbon provides high speed electron

pathways for active materials to lower the ohmic polarization. For example, Lee et al. [262] prepared 1D N-doped porous carbon nanotubes (CNTs) embedded with core-shell Co@CoOx nanoparticles (Co@CoOx/NCNTs), which exhibited excellent ORR kinetic current and stability due to the uniform interconnected nanotube network, facilitated electron transport, and an enlarged electrochemically accessible surface area in the unique 1D porous tubular structure. To get uniform pore distribution and large pore volume, metal organic framework (MOF) [254, 257, 258, 263] and zeolitic imidazolate frameworks (ZIF) [199, 231, 264-267] -derived heteroatom-doped carbon-based electrocatalysts have attracted tremendous attention and exhibited superior activity. Mu et al. [255] prepared Fe, Cu-coordinated ZIF-derived carbon framework (Cu@Fe-N-C) by introducing Fe^{2+} and Cu^{2+} during the growth of ZIF-8 as shown in Fig. 6. Due to the bimetallic active sites, large surface area, high nitrogen doping level, uniform Fe-N_x distribution, and conductive carbon frameworks, the Cu@Fe-N-C exhibited excellent ORR performance. Furthermore, the composite materials always not only combine the advantages of each material, but also bring synergistic effects to enhance the ORR process, including the metal oxide/metal oxide [199, 211, 217, 258, 259, 268, 269], metal oxides/carbon materials [42, 217, 225, 261, 269-273] and carbon materials doped with atoms [52, 220, 222, 242, 274-276]. For example, Shao et al. [211] found the Co_3O_4-CeO_2/ketjenblack (KB) showed much better electrocatalytic performance than both Co_3O_4/KB and CeO_2/KB due to the synergistic effects between Co_3O_4 and CeO_2. Because of the strong coupling effect and synergistic effect, the composite materials of inorganic/nanocarbon exhibited higher ORR performance than that of each one. Similarly, Shao and co-workers [217] found the strongly coupled Mn_3O_4 quantum dots (QDs)/N-doped carbon skeleton exhibited synergistic effect between Mn_3O_4 QDs, nitrogen and carbon nanotubes because of the strong polarization and electronic interaction between Mn_3O_4 QDs and N-doped graphene, which was also confirmed by density functional theory (DFT) calculations. In addition, with the help of DFT method, Wu et al. [220] calculated that the graphene doped with Py-N and P at the same time lowered the energy difference between lowest unoccupied molecular orbital (LUMO) and highest occupied molecular orbital (HOMO) of triplet oxygen molecule, indicating the P-doping and graphitic-N has a synergistic effect on promoting ORR reaction. Besides, based on ORR performance and DFT calculations, Wen et al. [263] found the same kind of atom with different types, such as Py-N and graphitic-N also exhibited synergistic effect.

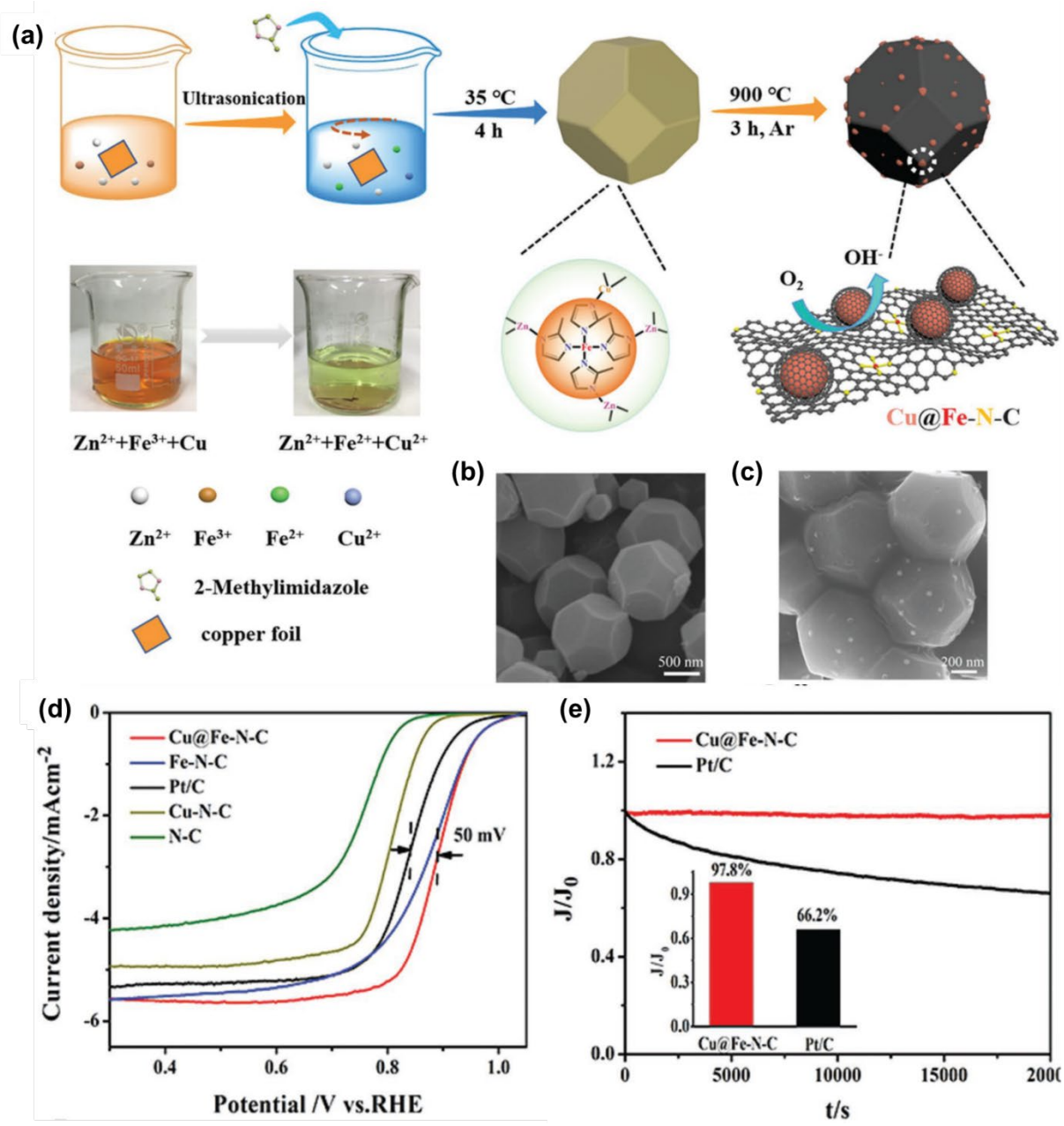

Fig. 6. (a) Schematic of the synthesis procedure of Cu@Fe-N-C. SEM images of (b) FeCu-ZIF, and (c) Cu@Fe-N-C. (d) LSV curves of Cu@Fe-N-C, Fe-N-C, Pt/C, Cu-N-C, and N-C in O_2-saturated 0.1 m KOH solutions. (e) The i–t chronoamperometric responses of Cu@Fe-N-C and Pt/C. [255] Copyright 2018 John Wiley and Sons.

In the recent years, based on *Web of Science Core Collection*, the ORR electrocatalysts for primary aqueous metal-air batteries were focused on Zn-air (~65%) and Al-air (~25%) battery, and the typical examples of which are summarized in Table 1 and Table 2. For primary Zn-air batteries,

the ORR catalysts are concentrated on composites of metal oxides/porous heteroatoms-doped carbon materials from mechanism discussion to application methods. The ORR catalysts of Al-air batteries are mainly related to Ag-based and Mn-based catalysts to reduce the cost and enhance the performance. Although the researches of ORR catalysts have been widely investigated in alkaline environment, the attention paid on the development for neutral solutions is limited. Fortunately, the performance of catalysts in neutral solution is comparable to that in weak alkaline solution [277], which makes some catalysts of Mg-air batteries directly come from Zn-air and Al-air batteries [41, 64, 65, 138, 178, 199, 243, 278-281]. For aqueous Li-air batteries, the electrolyte of cathode is similar to alkaline metal-air batteries, which makes the catalysts similar to the alkaline metal-air batteries [282].

Table 1 The performance of some typical ORR electrocatalysts and the responding Zn-air Batteries

Catalyst	**E_0/V vs. RHE**	**$E_{1/2}$/V vs. RHE**	**Durability**	**Battery performance**	**Ref.**
O-PdFe@Pt/C	~1.0	~0.88	62.5% at 0.9V after 10k cycles	P_{max} 293 mW cm^{-2} 1.313V at 5 mA cm^{-2}	[176]
AgNW-GA	-0.072V vs. Ag/AgCl	-0.3V vs. Ag/AgCl	106% at -0.4V after 24 h	P_{max} 331 mW cm^{-2} 1V at 206 mA cm^{-2}	[186]
Co@CoOx/NCNTs	0.94	0.80	95% at 0.551 V after 30 h	P_{max} 353 mW cm^{-2} 1.0V at 237 mA cm^{-2}	[262]
MnO_2/N-HGS	0.94	0.84	85% at 0.77 V after 12 h	P_{max} 82 mW cm^{-2} 1.26V at 10 mA cm^{-2}	[271]
CoMn/pNGr	0.94	0.791	11 mV shift after 5000 cycles	P_{max} 210 mW cm^{-2} 1.50V at OCV	[283]
$LaMnO_{3+\delta}$	-	0.852	87% at 0.46 V after 6 h	P_{max} 198.6 mW cm^{-2} 1.255V at 10 mA cm^{-2}	[210]
Fe3C(Fe)@NG	-0.055 V vs Ag/AgCl	-0.152 V vs Ag/AgCl	82.5% at -0.3 V after 10 h	P_{max} 186 mW cm^{-2} 1.1V at 50 mA cm^{-2}	[270]
Fe-N-CNBs-600	1.03	0.875	83% at 0.7V after 12 h	P_{max} 275 mW cm^{-2} 1V at 171 mA cm^{-2}	[268]

Co-N/CNT	0.99	0.91	93% at 0.7V after 3600s	1.0V at 215 mA cm^{-2} 1.22V at 50 mA cm^{-2}	[284]
NPC/G	0.9	0.81	70% at 0.81V after 20000s	P_{max} 267 mW cm^{-2} 1.0V at 161 mA cm^{-2}	[285]

Table 2 The performance of some typical ORR electrocatalysts and the responding Al-air Batteries

Catalyst	**E_0/V vs. RHE**	**$E_{1/2}$/V vs. RHE**	**Durability**	**Battery performance**	**Ref.**
Ag_2MnO_4	0.9	0.8	~87%@0.85V 25000s	P_{max} 105.2 mW cm^{-2} 0.9V@100 mA cm^{-2}	[189]
Ag-MnO_2	0.83	-	91%@0.5V 50000s	P_{max} 204 mW cm^{-2} 1.0V@199 mA cm^{-2}	[190]
Ag/CFP	-0.07 V vs. MMO	-	-	P_{max} 109.5 mW cm^{-2} 1.56V@30 mA cm^{-2}	[148]
LaSrMnO	0.903	~0.65	97.1%@0.4V 10000s	P_{max} 191.3 mW cm^{-2} 1.29V@100 mA cm^{-2}	[216]
Cu-Ce-O oxide	-0.23 V vs. MMO	-0. 37 V vs. MMO	Hardly changes after 2000 cycles	P_{max} 78.1 mW cm^{-2} 0.78V@100 mA cm^{-2}	[286]
CuN_xC_y/KB-400	-	0.82	5 mV shift after 2000 cycles	1.53V@40 mA cm^{-2}	[258]
Ni-Co-S @G/NSC900	0.901	0.826	±0.28%@150 mA cm^{-2} after 125h	P_{max} 261.3 mW cm^{-2} 1.23V@150 mA cm^{-2}	[287]
4.8% Ce-MnO_2/C	0.872	0.783	96.4%@0.43V 40000s	P_{max} 348.8 mW cm^{-2} ~1.6V@100 mA cm^{-2}	[209]
Fe-N-C	-0.09 V vs. Ag/AgCl	-0.23 V vs. Ag/AgCl	-	P_{max} ~105 mW cm^{-2} ~1.34V@50 mA cm^{-2}	[246]
NSC800	0.1 V vs. MMO	-	30 mV shift after 5000 cycles	P_{max} 46 mW cm^{-2} ~1.15V@20 mA cm^{-2}	[276]

2.2.3 Bi-functional oxygen catalyst

The complex multi-electron process makes the kinetics of electrocatalytic oxygen reactions (ORR/OER) rather slow, which challenges the stable and efficient bi-functional oxygen electrocatalysts to practically usable levels in rechargeable aqueous metal-air batteries. Noble metal based catalysts exhibit excellent activity to ORR (Pt) or OER (RuO_2, IrO_2), however, they cannot electrochemical catalyze efficiently both of ORR and OER. Additionally, the poor durability and ultrahigh cost make the Pt, RuO_2 and IrO_2 based electrocatalysts hardly to large-scale application in metal-air batteries. To enhance the bi-functional activity, stability and lower the cost, alloying [117, 288-292] and hybridization [293-296] with the transition metal and the composites are widely applied. For example, Goodenough et al. [289] reported a bi-functional oxygen electrocatalyst consisting of porous metallic nickel-iron nitride (Ni_3FeN) supporting ordered Fe_3Pt intermetallic nanoalloy. In this hybrid catalyst, Ni_3FeN mainly contributes to the high activity for OER while the ordered Fe_3Pt nanoalloy for ORR. This method to compose two individual components with high activity for ORR and OER respectively is also available for some other non-noble metal catalysts, such as NiFe-layered double hydroxides (LDHs) with MnOx or Co-N-C, which exhibit high activity both for ORR and OER [297-300].

To restrain the irreversible change of ORR and OER catalysts causing by the wide potential window during charge/discharge operation of rechargeable metal-air batteries, tremendous efforts have been paid to further promote the activity and durability of the non-noble metal based bi-functional catalysts materials [35, 132, 140, 159, 204, 301, 302]. The spinel Co_3O_4, one of typical bi-functional oxygen catalysts, exhibits high activity for OER but relative low activity for ORR and electroconductivity. [303]. When it is doped with heteroatoms, such as Zn [304], Ni [305-307], Mg [308], Cu [309] and S [310, 311] to transform into $ZnCo_2O_4$, $NiCo_2O_4$, $MgCo_2O_4$, $CuCo_2O_4$ and Co_3S_4, as well as hybridized with other metal (oxides), such as Co [312-314], MnO_2 [315], or carbon materials [316-318], both of the ORR and OER activity can be obviously enhanced via valence/energy-level modification, conductivity enhanced and synergistic effect. For example, Song et al. [314] reported a Co_3O_4-doped Co/CoFe nanoparticles integrated with graphitic shells, which showed a surprisingly high bi-functional (ORR/OER) catalytic activity due to the core–shell structure via synergistically promoting the ORR performance while cobalt oxide doped on the metal surface boosting the OER performance, the carbon shell with high electrical conductivity effectively

impeding the aggregation and the further oxidation of Co/CoFe nanoparticles. Additionally, compared with the free-doped carbon materials, the N-doped carbons can further enhance the ORR/OER performance for Co_3O_4-based materials via stronger coupling/anchoring effect to active materials and modifying catching ability to intermediate products of oxygen redox reactions [91, 312, 313, 316, 319, 320]. These modification methods to promote the activity and durability of OER/ORR are also suitable for other metal oxides [321-323], such as perovskites [294, 322, 324-327], Mn-based oxides [297, 328-332], metal sulfides [333-336] and nitrides [289, 337-339]. For example, Peng et al. [328] designed a controllable large-scale synthesis of sulfur-doped $CaMnO_3$ nanotubes via an electrospinning technique followed by calcination and sulfurization. The resulting sulfur-modified $CaMnO_3$ (CMO/S) exhibited higher activity and stability for ORR and OER than that of pristine CMO due to the sulfur doping, which replaced oxygen atoms to increase intrinsic electrical conductivity and introduced abundant oxygen vacancies to provide enough catalytically active sites as shown in Fig. 7.

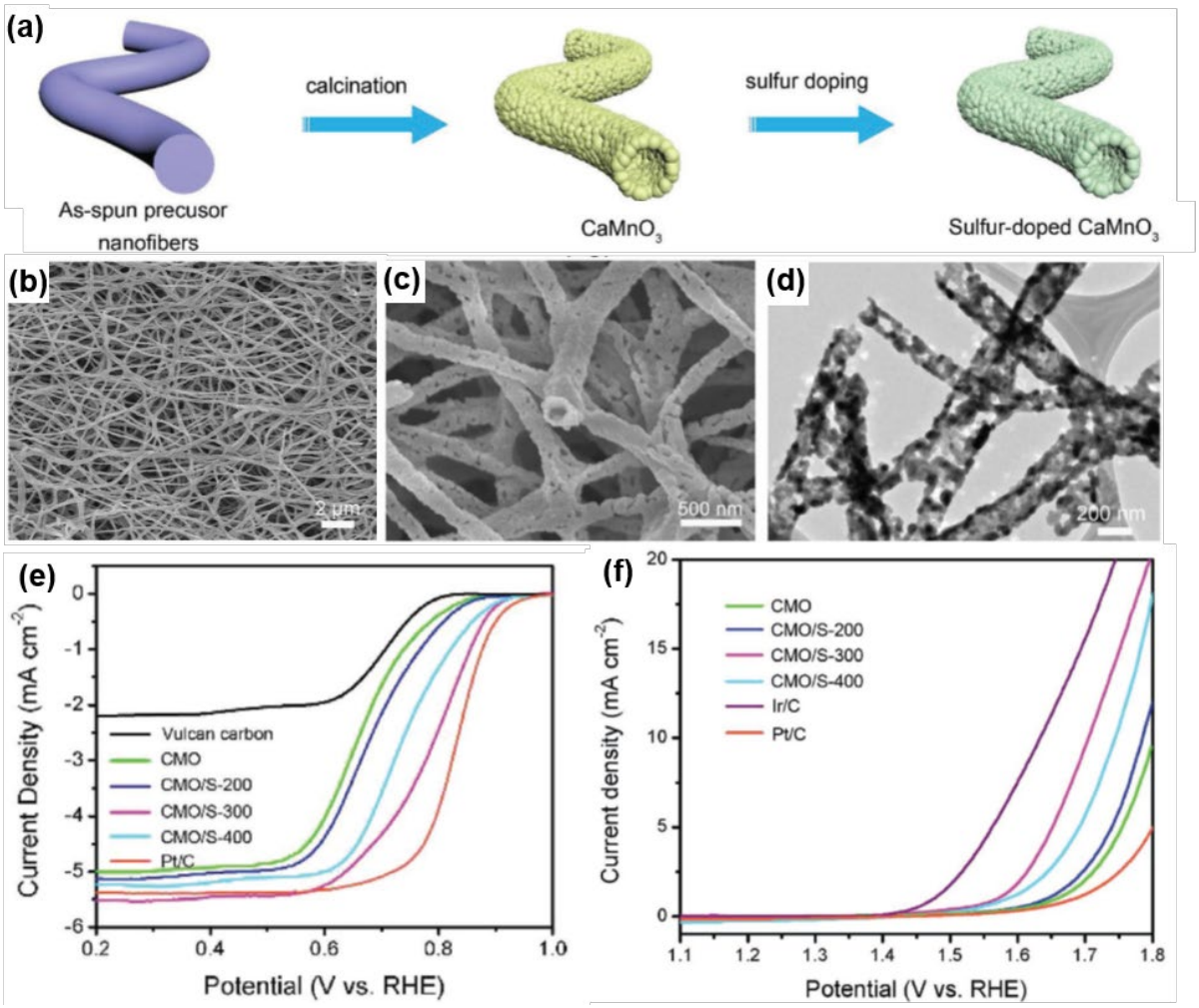

Fig. 7. (a) Scheme of the formation of CMO/S, (b-c) SEM, (d) TEM of CMO/S-300, respectively. (e) ORR polarization curves of XC-72, CMO, CMO/S-200, 300, 400 and Pt/C in O_2-saturated 0.1 M KOH. (f) OER polarization curves of CMO, CMO/S-200, 300, 400, Pt/C and Ir/C in N_2-saturated 0.1 M KOH. (g) Cycling performance of rechargeable zinc–air battery using CMO/S-300 as air electrode catalyst at 5 mA cm^{-2} with a duration of 400 s per cycle. [328] Copyright 2018 John Wiley and Sons.

Carbon materials are becoming one of the necessary additions for aqueous rechargeable metal-air batteries as the literature reported in recent years based on *Web of Science Core Collection*. Although a few kinds of bi-functional catalysts are fabricated without carbon materials, it must be aided by carbon paper or carbon cloth to assemble the air electrode [96, 332, 340, 341]. To slow the corrosion rate, the graphite carbons and carbon fibers are favored, such as graphene [342, 343], reduced graphene oxide [287, 327], carbon nanotube [308, 344, 345] and porous carbon fibers [149, 288, 346]. Besides for acting as additions and supported materials, the carbon materials also exhibit

proper activity for ORR and OER as metal-free materials when doped with N, O, P and S heteroatoms [347-352], but the OER activity is relative lower to IrO_2 and RuO_2. When the N-doped carbon is anchored with Fe or Co atoms to form Fe-N-C or Co-N-C structure, their OER activity can be compared with IrO_2 and RuO_2 [353, 354]. Additionally, the ORR activity is even better than that of Pt/C in alkaline condition [236, 355, 356]. For example, Pan et al. [354] developed a polymerization-pyrolysis-evaporation strategy to synthesize N-doped porous carbon with anchored atomically dispersed Fe-N_4 catalytic sites deriving from predesigned bimetallic Zn/Fe polyphthalocyanine. The Fe-N_4 exhibited superior bi-functional electrocatalytic performance for OER and ORR, high efficiency and extraordinary stability in rechargeable Zn-air batteries as shown in Fig. 8. Recently, ZIFs, a subclass of MOFs, have attracted extensive attention owing to their versatile surface geometry, flexibility, abundant pores, and high specific surface area. The structural adjustability offers rich platforms to design functional materials for ORR and OER in rechargeable batteries [57, 91, 357-362]. For example, Dai et al. [361] reported the Co@N-C materials (C-MOF-C2-T) from a pair of enantiotopic chiral 3D MOFs by pyrolysis. The C-MOF-C2-900 with a unique 3D hierarchical rodlike structure, consisting of homogeneously distributed Co nanoparticles encapsulated by partially graphitized N-doped carbon rings along the rod length, exhibited excellent electrocatalytic activities for ORR and OER. The rechargeable Zn–air batteries based on C-MOF-C2-900 exhibited an excellent cycling stability without polarization increase after 120 h test.

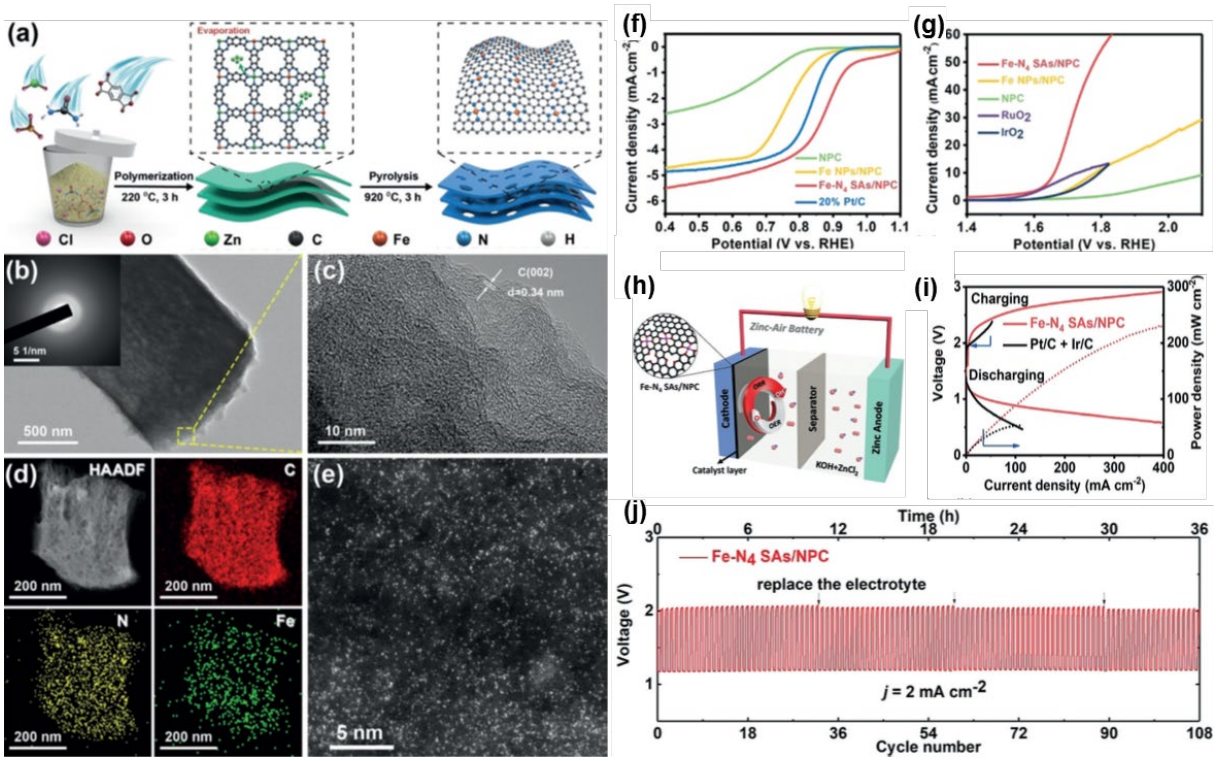

Fig. 8. (a) Synthesis, (b) TEM (inset: SAED image), (c) HRTEM, (d) HAADF-STEM and EDS mapping images (C red, N yellow, Fe green), and (e) AC HAADF-STEM of the Fe-N4 SAs/NPC. LSV curves for (f) ORR and (g) OER, representation of (h) Zn-air battery and (i) the charge–discharge polarization curve and power density plot, and (k) charge–discharge cycling performance. [354] Copyright 2018 John Wiley and Sons.

The aqueous rechargeable Zn-air batteries are summarized in Table 3 based on catalyst materials. The other kinds of metals for metal-air batteries, such as Li, Na, Al and Mg in aqueous solution cannot be reduced from metal ions or metal oxides to metal reversible, so the aqueous rechargeable metal-air focused on Zn-air batteries. However, the hybrid structure with organic electrolyte for anode and aqueous electrolyte for air cathode can resolve the irreversible problem. In this case, the catalysts react in alkaline aqueous solution is similar to the rechargeable Zn-air battery, so the catalysts applied in Zn-air batteries can also be suitable for some hybrid Li-air and Na-air batteries [275]. Recently, for Li-air [363-366] and Na-air [84, 367-370] batteries, the materials of bi-functional catalysts are focusing on perovskite and spinel oxides compositing with carbon materials.

Table 3 The performance of some typical bi-functional oxygen catalysts and the responding rechargeable Zn-air Batteries

Catalyst	$E_{ORR1/2}$/V vs. RHE	$E_{OER\ 10mA\ cm^{-2}}$/V vs. RHE	Voltage gap V @ mA cm^{-2}	Battery performance	Ref.
IrMn/Fe_3Mo_3C	0.89	1.52	1st 0.75 @ 10 100th 0.86 @ 10	Voltaic efficiency 56.1% after 100 cycle (200 h) at 10 mA cm^{-2}	[281]
$Ni_{46}Co_{40}Fe_{14}$ Nanoalloy	0.93	1.66	200th 0.63 @ 10	Voltaic efficiency ~65% after 200 cycle (3.3 h) at 50 mA cm^{-2}	[371]
$MnFe_2O_4$/ $NiCo_2O_4$	0.767	1.574	0.8 @ 10 1.1 @ 50	Voltaic efficiency 60.8% after 100 cycle (32 h) at 10 mA cm^{-2}	[372]
$La_x(Ba_{0.5}Sr_{0.5})_{1-x}Co_{0.8}Fe_{0.2}O_{3-\delta}$	~0.7	~1.7	100th 1.0 @ 10.5	Voltage gap increases 0.25V after 100 cycle (33 h) at 10.5 mA cm^{-2}	[373]
Co_3O_4/MnO_2-CNTs	~0.83	~1.7	1.0 @ 100	Voltaic efficiency <50% after 200 h at 10 mA cm^{-2}	[308]
$CaMnO_3$ nanotubes	0.68	1.7	0.67 @ 5	Voltaic efficiency ~58% after 120 cycle (16 h) at 5 mA cm^{-2}	[321]
S-GNS/$NiCo_2S_4$	0.88	1.56	1st 0.7 @ 10 150th 0.8 @ 10	P_{max} 216.3 mW cm^{-2} at 0.67 V	[374]
Ni3Fe/N-C sheets	~0.79	~1.63	1st 0.78 @ 10 105th 0.98 @ 10	Voltaic efficiency 51.8% after 105 cycle (420 h) at 10 mA cm^{-2}	[375]
Co–N_x/C nanorod array	0.877	1.53	0.68 @ 50	P_{max} 193.2 mW cm^{-2} at 0.70 V	[358]
pyridinic-N doped graphene	0.85	1.68	0.76 @ 10	P_{max} 115.2 mW cm^{-2} at 200 mA cm^{-2}	[347]
P,S-doped carbon nitride	0.87	1.56	0.8 @ 25	500 cycles beyond 100 h at 25 mA cm^{-2}	[348]

3. Metal electrode

3.1. Al anode

Al has been considered as an attractive source of the metal-air batteries primarily due to its inherent properties, including the third most abundant elements in the earth crust, the low cost of 1.9 USD kg^{-1}, the high theoretical volumetric energy capacity of 8056 mAh cm^{-3}, the high theoretical gravimetric energy capacity of 2981 mAh g^{-1}, the low density of 2.71 g cm^{-3}, as well as the negative standard electrode potential of -1.76 V vs. standard hydrogen electrode (SHE), as shown in Fig. 9. Its capacity per unit volume of 8056 mAh cm^{-3} is much higher than that of the widely used zinc (5857 mAh cm^{-3}). However, the Al-air battery is still not as popular as Zn-air battery [376-377]. The major hindrance is that Al anode exhibits some undesired properties, such as the formation of the protective oxide film, which is spontaneously formed on aluminum surface in air and aqueous solutions. Because of the presence of the protective oxide film, the corrosion potential of Al anode is shifted in the positive direction (about -0.8 V vs. NHE). Moreover, the active dissolution of aluminum is impeded considerably, which causes a significant loss of available energy and a low Al anode utilization. In addition, Al undergoes serious self-discharge reactions with the evolution of large amount of hydrogen gases in alkaline solutions [377].

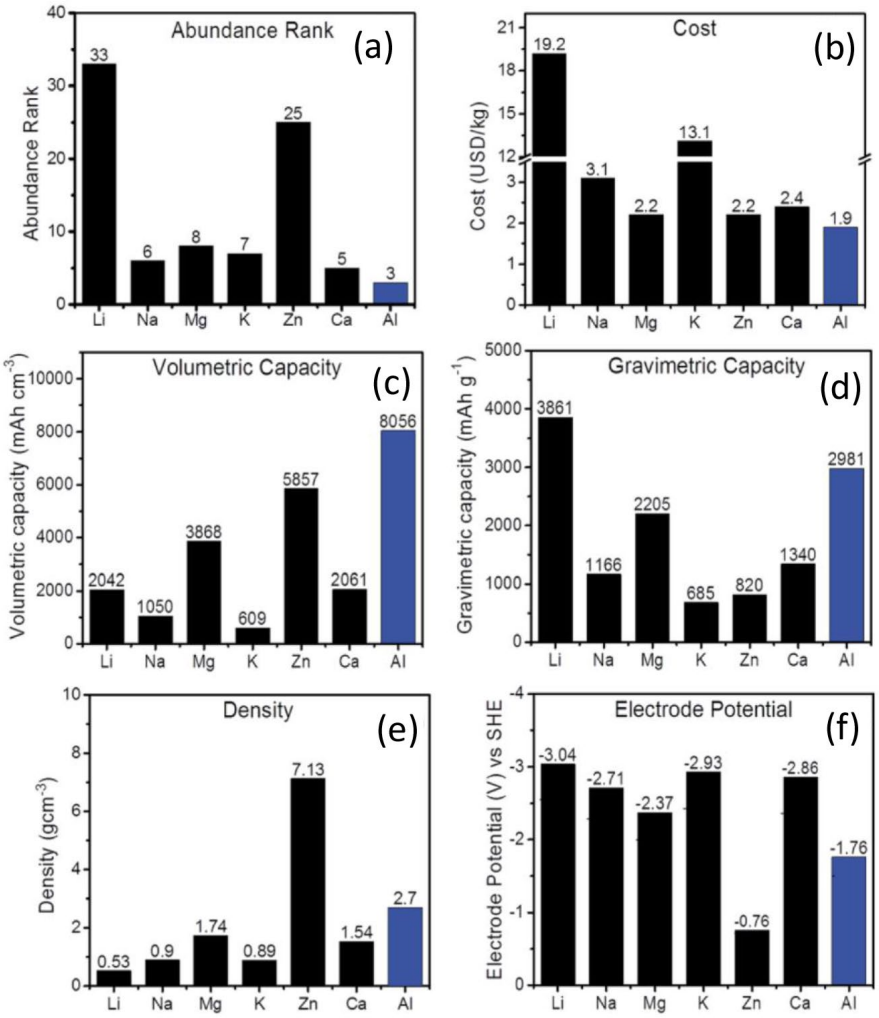

Fig. 9. Comparison of (a) abundance, (b) cost, (c) volumetric capacity, (d) gravimetric capacity, (e) density at 25°C and (f) electrode potential vs. SHE of Li, Na, Mg, K, Zn, Ca and Al. [378] Copyright 2017 Royal Society of Chemistry.

Muñoz-Torrero et al. [379] investigated the performance of anodes deposited by Al with different substrates such as Al, stainless steel, and expanded graphite. The cyclic voltammetry (CV) results indicated that the expanded graphite appeared as a promising alternative anode substrate for Al-air batteries. In addition, the expanded graphite possessed interesting properties for battery applications due to its lower cost, high electrical conductivity, low density, and high temperature resistance. Cho et al. [376] reported that a complex film containing Fe and Si impurities was formed when the purity of the Al anode was not high, which hindered the ion-exchange on the interface between the electrode and electrolyte, thus the discharge voltage decreased from 1.0 V to 0.8 V when the 4N high pure grade Al (99.99% purity) was changed to the 2N5 commercial grade Al (99.5% purity).

Nevertheless, the 2N5 grade Al showed the potential to replace the 4N grade Al to reduce the cost at the high-power discharge condition, because the complex film was dissolved at the high-power discharge condition so that the discharge current densities of 2N5 grade Al and 4N grade Al became similar. To alleviate the self-corrosion of the Al anode, Fan et al. [380] fabricated an ultrafine grained (UFG) aluminum anode using equal channel angular pressing (ECAP) at room temperature. In 4 M NaOH electrolyte, the UFG Al anode exhibited an energy density of 3525 mWh g^{-1} and an anode utilization of 77.4%, while the coarse-grained Al anode only showed the energy density of 2267 mWh g^{-1} and the anode utilization of 55.3%. The improvement was attributed to active dissolution of the UFG Al anode. They also studied the effect of crystallographic orientation on the Al anode performance [381]. It was indicated that the single crystal Al exhibited better electrochemical performance than the polycrystalline Al, because the polycrystalline Al suffered from galvanic corrosion and crystal defects. Among the single crystal Al, Al (001) showed the lowest corrosion rate and highest electrochemical activity, which was attributed to the low surface energy. Pino et al. [382] treated commercial Al alloy with carbonaceous materials, allowing the battery stably operated at 6 mA cm^{-2} for 27 h, which was three times higher than that of a bare Al anode. This was because the carbonaceous materials slowed down the adherence of the aluminate gel [$Al\text{-}Al_2O_3\text{-}Al(OH)_3$] on the Al anode significantly. Future research attention may be paid to alleviating Al passivation problem via the development of novel Al alloy and the modification of conventional Al anode, thus a longer lifetime and a higher Al utilization can be achieved.

3.2. Zn anode

Currently, in spite of the Al anodes, great attention has been paid to the Zn anodes, which are more popular than the Al anodes. This is mainly because Zn-air batteries are electrically rechargeable, thus it is capable to store the renewable but intermittent solar and wind power, while Al-air batteries can only be mechanically recharged by replacing Al anodes [19]. In addition, Zn metal has advantages of low cost and high energy density, making the Zn-air batteries promising energy storage devices. The successful demonstration of the primary Zn-air batteries motivates the researchers to realize the commercialization of secondary Zn-air batteries. However, four issues related to Zn anode still need to be addressed: (1) The dendrite formation derived from uneven deposition of Zn at active sites during charging causes the short circuiting; (2) The shape change of

Zn anode decreases effective surface area and limits cycle life due to the redistribution of active materials over the Zn electrode surface on cycling; (3) The anode passivation decreases Zn electrode utilization and battery capacity because of the limited mass transfer of soluble species to the anode as well as the dissolved Zn anode to the electrolyte; and (4) The self-discharge results in the anode corrosion and capacity loss owing to the more negative reduction potential than hydrogen [19]. It is important to prevent the transformation of $Zn(OH)_4^{2-}$ into ZnO that has a low solubility, low conductivity, and poor electrochemical reversibility, thus the reversibility of the Zn redox reaction can be enhanced in Zn-air batteries [383]. In addition, the self-discharge of Zn anode material is identified as a main factor that limits the energy density of alkaline Zn-air batteries [384]. To diminish the self-discharge problem, Lee et al. [384] coated the Zn powders with a Al_2O_3 layer via chemical solution process. The coating layer prevented Zn from exposing to the KOH electrolyte, thus the hydrogen evolution reaction was hindered. It was demonstrated that the 0.25 wt.% Al_2O_3 coating Zn anode showed a discharge time of more than 10 h, while the pristine Zn only showed a discharge time of 7 h at 25 mA cm^{-2}. Similarly, Jo et al. [385] coated Zn anode with polyaniline (PANI) to prevent directly swelling the Zn particle in the aqueous electrolyte, aiming at reducing the corrosion of anode and hydrogen evolution reaction (HER). The treated anode inhibited 85% corrosion compared to bare Zn anode and retained 97.81% capacity, while the capacity retention of bare Zn anode was 74.40%. Schmid et al. [386] coated zinc particles with silica in order to reduce early formation of irreversible ZnO passivation layers during discharge, as shown in Fig. 10. Eq. (4) and (5) explains that swelling the silica layers in aqueous KOH electrolyte leads to the formation of a $Si(OH)_4$ gel, which controls the zinc dissolution by shifting the solubility limit of zincate ions.

$$Zn_2SiO_4 + 2H_2O \rightarrow Si(OH)_4 + 2Zn \quad (4)$$

$$SiO_2 + 2H_2O \rightarrow Si(OH)_4 \quad (5)$$

Two coating methods, *i.e.*, chemical vapor deposition (CVD) and chemical solution deposition (CSD) were tested. It was shown that both the CVD-coated zinc (69% zinc utilization) and CSD-coated zinc (62% zinc utilization) possessed improved discharge capacity compared to bare zinc (57% zinc utilization) at C/20 rate, which was attributed to reducing the supersaturation of zincates.

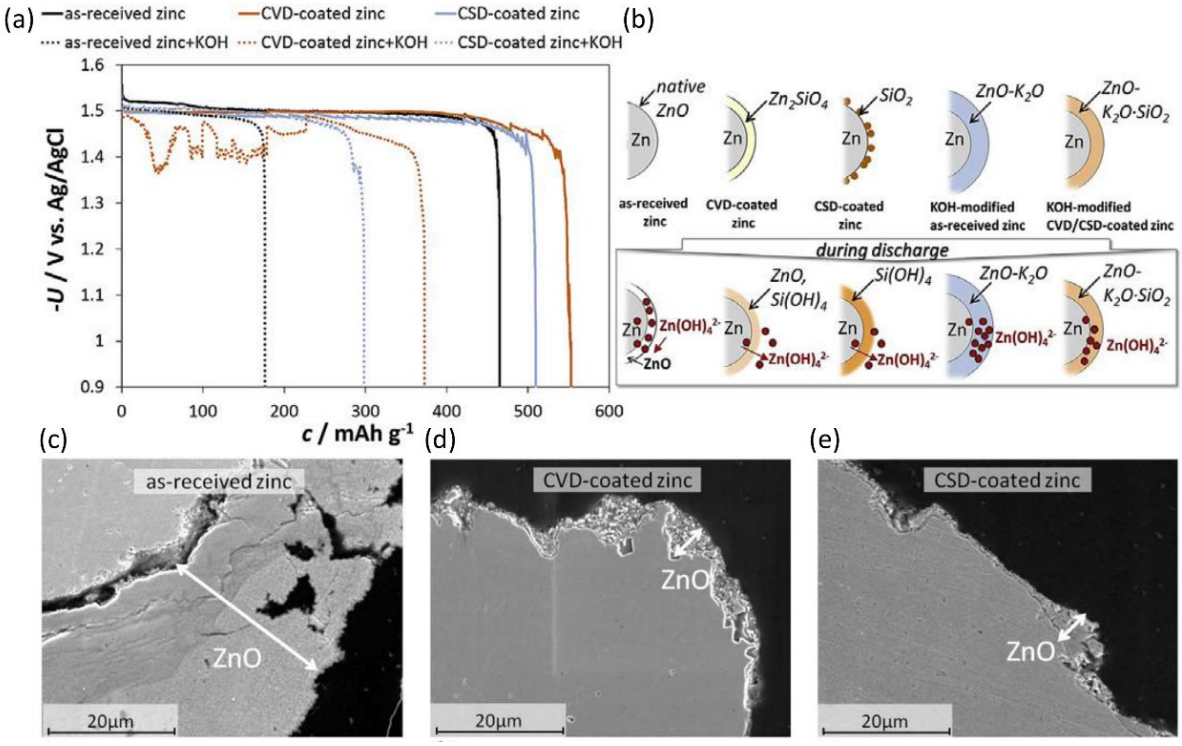

Fig. 10. (a) Discharge curves of the 1st cycle of zinc particles (as-received zinc, CVD-, CSD-coated zinc) with and without KOH modification, (b) schematic illustration during the discharge process, and SEM images of the cross section of (c) as-received zinc, (d) CVD-coated zinc, (e) CSD-coated zinc after discharge. [386] Copyright 2015 Elsevier.

Stock et al. [387] coated Zn anode with an anion-exchange ionomer (AEI), allowing the hydroxide ions to pass but confining the $Zn(OH)_4^{2-}$ between the surface of the Zn anode and the AEI. As a result, the CV cycling of coated Zn anode reached more than 70 cycles, showing a long-term stability, which was six times as that of a pristine Zn anode. In view of the electrical rechargeability after complete discharge, Schmid et al. [388] coated zinc particles with bismuth oxide based glasses, resulting in a cyclic stability of 20 full cycles, whereas bare zinc particles only achieved one complete discharge. Theoretically, the zinc utilization could be promoted to 465% after coating, however, the practical improvement of the zinc utilization was 85% due to the electrolyte limitation. Despite the coating method, Titscher et al. [389] used copper weave and copper foam as current collector, on which zinc particles were coated. It was indicated that this structure increased the active surface area by the multidimensional current collectors, effectively reducing local current densities and significantly alleviating the surface passivation problem. The results showed that the anode with

a higher degree of structuring and a thinner particle coating possessed better electrochemical properties. In addition, extensive efforts have been paid to zinc anode for others alkaline rechargeable batteries, such as Zn-Ni, Zn-Ag batteries. Yan et al. [390] fabricated three-dimensional Zn/Cu foam electrodes by pulse electro-deposition of zinc on copper foam, which showed superior cycling stability and high rate capability. Zhang et al. [391] prepared Bi-doped Zn-Al layered double hydroxides (Zn-Al-Bi LDH) via the constant pH hydrothermal method and used it as the anodic material. It was reported that the addition of Bi could decrease polarization, maintain the electrochemical activity, and enhance the discharge capacity of Zn-Al LDH. Sun et al. [392] synthesized ZnO with a uniform and complete coating of reduced graphene oxide. It was indicated that the RGO layer as a protective film could effectively inhibit the dissolution of ZnO into the alkaline electrolyte, and Zn could be uniformly formed on the RGO surface with a high utilization in the charge process due to the good conductivity and surface adsorption properties. Yang et al. [393] prepared a polydopamine (PDA)-coated nanosized ZnO as an anode material. The battery showed a high specific capacity of 364.3 mA h g^{-1} at 1 C after 200 cycles due to the efficient diffusion of OH^- into the inner electrode and the prevention of shape change. Zamarayeva et al. [394] proposed rechargeable silver-zinc wire batteries. A cathode architecture with silver nanoparticle ink embedded into the conductive thread was implemented. The battery showed a specific discharge capacity of 1.4 mAh cm^{-1} at 0.5 C discharge rate, with a capacity retention of above 98% after 170 cycles. The wire battery could maintain this capacity after repeated flexing to a bending radius of 5 mm. Li et al. [395] reported a solar charged planar flexible quasi-solid-state aqueous rechargeable Ag−Zn battery using metal−organic framework -derived Ag nanowires on carbon cloth as a binder-free cathode. It was demonstrated that Ag−Zn battery yielded a remarkable energy density of 1.87 mWh cm^{-2} because Ag nanowires provided abundant reaction sites and shorted electron and ion diffusion paths. In order to develop a reversible zinc anode, structural modification and compositional modification by means of additives, electrodeposition, chemical doping, and advanced casting have been demonstrated to be feasible ways to deal with the above mentioned issues.

3.3. Mg anode

Mg is another popular anode material attracting much attention because of high theoretical gravimetric capacity of 2200 mAh g^{-1}, high specific energy density of 6.8 kWh kg^{-1}, and relatively

low cost of 2.2 USD kg^{-1}. In addition, it has second-most negative electrode potential of -2.37 V vs. standard hydrogen electrode (SHE) [396]. Although aqueous Mg-air batteries are not electrochemically rechargeable currently, the replacement of exhausted Mg anodes for fast mechanical recharging allows this technology to have numerous applications [397]. However, Mg suffers from severe self-corrosion during discharge in aqueous electrolyte, lowering the anode utilization efficiency and the specific energy density of anode. Moreover, the practical voltage of Mg-air batteries (1.6 V) is much lower than the theoretical voltage (3.1 V) due to the sluggish kinetics of electrode reactions. To solve these issues, novel anode materials are in urgent need of development. Wang et al. [398] demonstrated that the Mg-Li-Al-Ce-Y-Zn alloy exhibited superior anodic efficiency than that of the state-of-the-art AP65 (Mg-6 wt.% Al-5 wt.% Pb) magnesium alloy. It was explained that the Zn distributed in the β-Li phase brought about three advantages: (1) weak the micro-galvanic couple between the α-Mg and β-Li phases, reducing the corrosion current density; (2) promote the formation of more Al-Li particles in the β-Li phase, accelerating the self-peeling of the discharge products; and (3) favor the uniform dissolution of Mg-Li-Al-Ce-Y-Zn alloy, reducing the self-discharge. Xiong et al. [399] reported that the hot extruding and subsequent annealing treatment of Mg-6wt.%Al-1wt.%Sn alloy showed positive effect on the performance of Mg-air primary battery. After treatment, the precipitation of second phases was facilitated and spherical Mg_2Sn phases with typical sizes of 50-100 nm were uniformly distributed in the Mg-Al-Sn alloy. This microstructure contributed to improving the self-peeling of the corrosion products, increasing the discharge voltage at the high current density, thus a higher power density of 94.1 mW cm^{-2} was achieved comparing to AZ31, Mg-Li-Al-Ce, and Mg-Al-Pb alloy anodes. Li et al. [400] indicated that adding indium (In) into Mg anode enhanced Mg dissolution through synergistic effects, which involved increasing the second-phase amount, generating less-protective products, promoting products self-peeling, and dissolution-reprecipitation of indium. Liu et al. [401] investigated the effects of magnesium anodes with different phase constitutions on the discharge performance. The results showed that the Mg-11Li-3Al-1Zn-0.2Y (LAZ1131) anode mainly containing the single β-Li (bcc) phase exhibited the highest discharge capacity and anodic efficiency are 1478 mAh g^{-1} and 62.1%, respectively. It was attributed to the active β-Li phase matrix, providing high cell voltage and soluble surface product. Moreover, the fine and dense precipitates kept the β-Li peel away in the

form of small and dense particle clusters, which contributed to a uniform corrosion. Deng et al. [396] proposed that Mg-0.1 wt.% Ca alloy was a promising candidate as anode material of primary Mg-air batteries. The addition of Ca was beneficial for improving the discharge performance, which was ascribed to the high electrochemical activity of Ca and the induced grain refinement. While too high Ca addition showed negative effects on the anode utilization efficiency and discharge potential, is was due to the increasing amount of Mg_2Ca phase. The Mg-air battery using Mg-0.1 wt.% Ca alloy as anode yielded an open circuit voltage of 2.0 V and a peak specific energy of 1800 Wh kg^{-1}. In summary, common approach to improve the discharge performance is using magnesium alloys to replace pure magnesium as the anode.

4. Electrolyte

4.1. Alkaline electrolyte

In general, a suitable electrolyte is crucial for the battery system to achieve a satisfactory performance, because the electrolyte plays a dominant role in the battery electrochemistry, which effectively determines its rechargeability and the cell voltage [19]. KOH has been primarily used as the electrolyte for Zn-air batteries due to its excellent ionic conductivity, high oxygen diffusion coefficient, low viscosity, as well as good activity for both Zn anode and air cathode [402]. Fig. 11 shows the conductivity of KOH solution in terms of its concentration and temperature. Because the 30 wt.% KOH solution (about 7 M) exhibits a good conductivity of 640 mS cm^{-1} at 25°C, it is widely adopted in many studies. In addition, 37 wt.% KOH solution (9 M) is widely used in many modern alkaline batteries, because it shows high conductivity and low corrosion gassing [19].

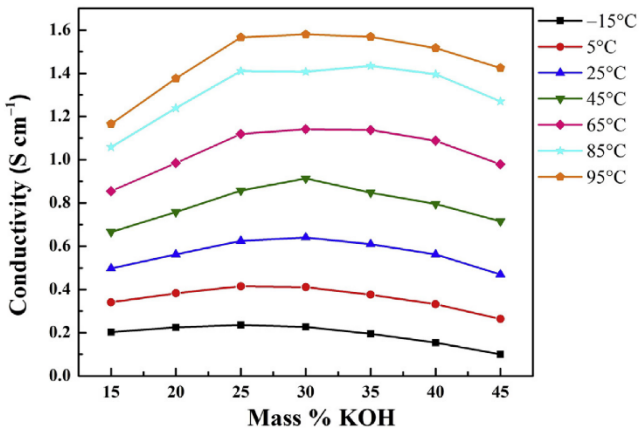

Fig. 11. Conductivity of KOH at different concentrations and temperatures. [19] Copyright 2016 Elsevier.

However, in Al-air batteries, the use of alkaline electrolyte, generally NaOH solution, will cause the self-corrosion of Al electrodes and the parasitic hydrogen evolution during battery discharge, which is the major defect resulting in the degradation of the battery performance according to Eq. (6) [403]

$$2Al + 6H_2O \rightarrow 2Al(OH)_3\downarrow + 3H_2\uparrow \quad (6)$$

To address the self-corrosion of the Al anode, Ma et al. [377] added ethanol into 4 M NaOH solution. The hydrogen evolution reaction hardly occurred because the proton of ethanol was much less active than that of water. Similarly, Wang et al. [404] added L-cysteine and cerium nitrate into 4 M NaOH solution to protect the Al anode. Due to the synergistic effect between the L-cysteine and cerium nitrate, they could form a complex film on Al anode surface, preventing the HER and enhancing the Al utilization. Liu et al. [405] reported that the AA5052 Al anode corrosion in alkaline electrolyte was effectively restrained by adding small amount of carboxymethyl cellulose (CMC) and ZnO. This was attributed to the formation of a complex between CMC and Zn^{2+} ions on the alloy surface, thus improving the battery capacity. Deyab et al. [403] demonstrated that the addition of ionic liquid [1-Allyl-3-methylimidazolium bis(trifluoromethylsulfonyl)imide] (IL) into electrolyte contributed to the inhibition of anode corrosion and hydrogen evolution as well as the promotion of battery capacity. In the presence of ILs, the adsorption of H_2O on the anode was prevented, thus the HER was hindered. In addition, the Al reacted with ILs to for a complex and the complex fell into the battery electrolyte leaving the reaction surface at the Al anode, as shown in Eq. (7).

$$Al + IL^+ + e^- \rightarrow Al(IL) \quad (7)$$

In summary, limited attention was paid to the electrolyte, which has a significant effect on the battery performance. Hence, modification and replacement of the conventional alkaline electrolyte are necessary with the purpose of improving metal-air battery performance and facilitating its applications.

4.2. Neutral electrolyte

Despite the desirable properties, the use of alkaline electrolyte in metal-air batteries brings about several technical problems [406-408]. One issue is related to the carbonate problem referring to the phenomenon that the hydroxide ions react with carbon dioxide in the air to form the insoluble carbonates, which is a severe problem in alkaline hydrogen fuel cells as well [409-411]. The carbonates eventually precipitate on the cathode catalyst covering the active sites and blocking the pores within the cathode, thus the long-term performance of the battery will degrade. The other issue is associated with the corrosion of carbon-based air cathode in concentrated alkaline electrolyte according to Eq. (8) [412]:

$$C + 6OH^- \rightarrow CO_3^{2-} + 3H_2O + 4e^- \quad (8)$$

The corrosion of the substrate will result in the severe catalyst loss due to the absence of the support material, which is also disadvantageous for the long-term stability. Therefore, neutral electrolytes that are environmentally friendly have attracted attention recently, due to remediating the corrosion problem related to the use of alkaline electrolytes. For the zinc-air batteries, Sumboja et al. [413] reported that the zinc-air batteries with neutral chloride-based electrolyte and manganese oxide catalyst exhibited satisfactory voltage profile (discharge and charge voltage of 1 and 2 V at 1 mA cm^{-2}) and excellent cycling stability (around 90 days of continuous cycle test) as shown in Fig. 12, which was attributed to the reduced carbon corrosion of the air cathode and decreased carbonation in neutral electrolyte.

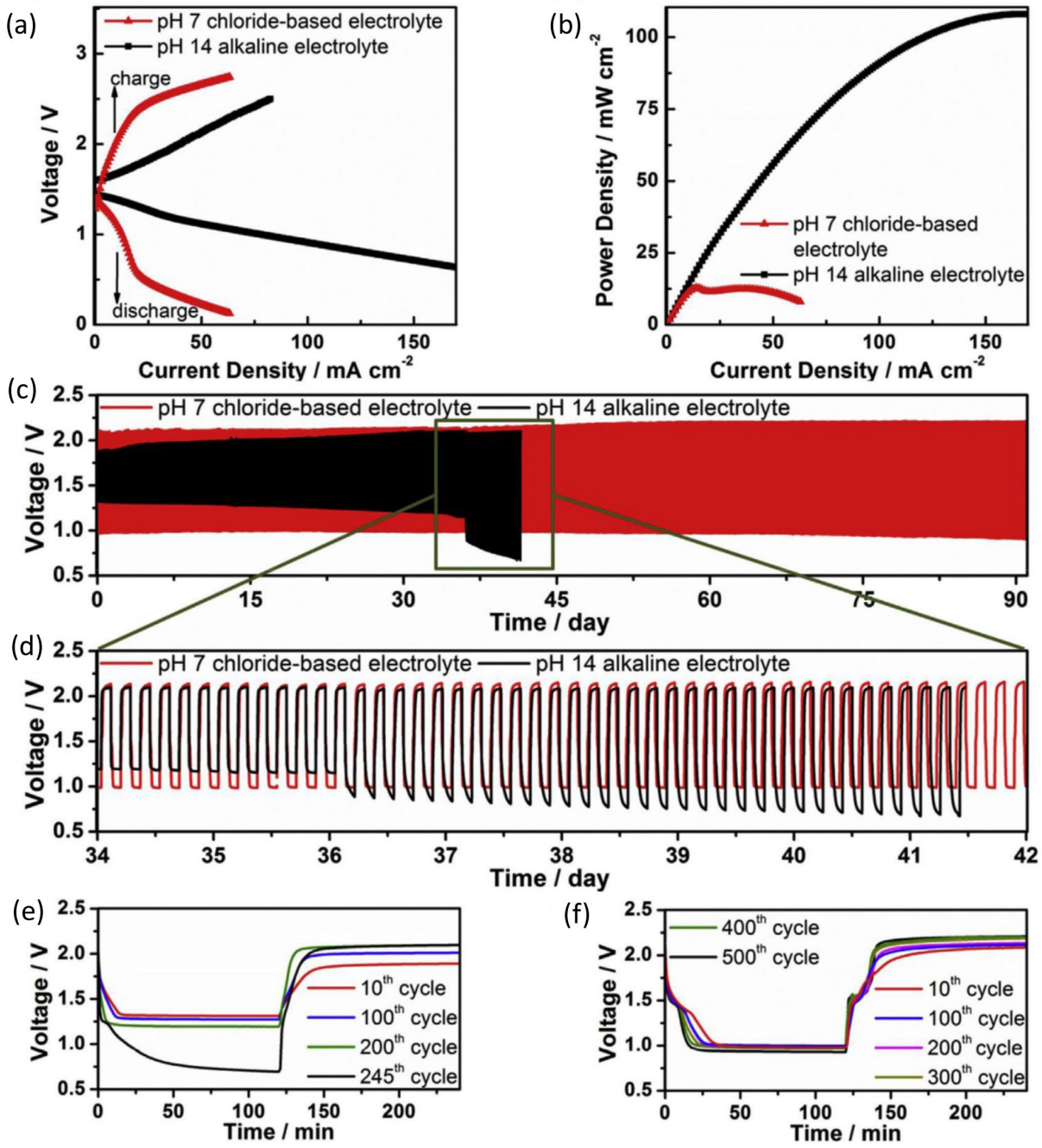

Fig. 12. Performance of Zn-air batteries with alkaline and pH 7 chloride-based electrolyte. (a) Galvanodynamic discharge and charge polarization curves. (b) Power density plots extracted from galvanodymanic discharge curve. (c, d) Cycling stability. Discharge/charge curves during selected cycles in: (e) alkaline and (f) pH 7 chloride-based electrolyte. [413] Copyright 2016 Elsevier.

Wang et al. [414] prepared concentrated Zn-ion electrolyte with a supporting salt at a high concentration [1 m $Zn(TFSI)_2$ + 20 m LiTFSI (where m is molality (mol kg^{-1}); TFSI, bis(trifluoromethanesulfonyl)imide)] for Zn-air batteries, which was neutral and capable of retaining

water in an open atmosphere. As the Zn^{2+} is surrounded by $TFSI^-$ instead of water, the H_2 evolution was hindered effectively, resulting in a reversible and dendrite-free Zn plating/stripping (coulombic efficiency ≈ 100%). The Zn-air battery using this electrolyte delivers a high energy density of 300 W h kg^{-1} for 200 cycles. It is widely accepted that the formation of ZnO derived from $Zn(OH)_4^{2-}$, which has low conductivity, low solubility, and poor electrochemical reversibility, is one of the main obstacles to the commercialization of Zn-air batteries. Lee et al. [383] added alcohols into the electrolyte as additives to react with $Zn(OH)_4^{2-}$ to form the modified zincate $Zn(OH)_{4-n}(OR)_n^{2-}$. Because the transformation of $Zn(OH)_{4-n}(OR)_n^{2-}$ into ZnO was slower than that of $Zn(OH)_4^{2-}$, the reversibility of the anode and retention of capacity could be improved in cycle tests.

For the magnesium-air batteries, Mg anode shows a high corrosion rate in alkaline electrolyte, thus the neutral sodium chloride solution is adopted as electrolyte. Dinesh et al. [415] used water soluble graphene (WSG) as inhibitor in 3.5% NaCl electrolyte to protect the Mg anode as well as serve as a catalyst. It was indicated that the discharge current density increased from 13.24 to 19.33 mA cm^{-2} due to the enhanced electrochemical activity and the specific discharge capacity increased from 822.85 to 1030.71 mAh g^{-1} due to the subdued anode corrosion with the immersion of WSG. Similarly, Deyab et al. [416] adopted decyl glucoside (DG) as electrolyte additive into 3.5% NaCl electrolyte, inhibiting the anode corrosion reaction. The results showed that the inhibition efficiency increased from 21% to 94% with an optimal DG concentration of 2.5 mM, which was attributed to the increased activation energy of the corrosion reaction. Richey et al. [417] investigated the effect of different electrolytes on the battery performance. They reported that $NaNO_3$ exhibited faradaic Mg^{2+} efficiencies more than 20% higher than the NaCl and HNa_2PO_4, while the open circuit voltage (OCV) was 1.45 V, which was lower than that of NaCl (1.65 V). It was suggested that using of either mixed aqueous/nonaqueous or protic/aprotic electrolytes could hinder Mg anode corrosion without impeding Mg^{2+} dissolution. Zhao et al. [418] tested the effects of phosphate and vanadate as additives in the 3.5 wt.% NaCl electrolyte on the performance of Mg-air batteries. The corrosion current densities of AZ31 anode in the blank, phosphate-containing, and vanadate-containing electrolytes were 79.43, 1.98, and 22.38 μA cm^{-2}, respectively, indicating that the phosphate possessed the best inhibiting effect on anode corrosion. In addition, under constant-current intermittent discharging, the anodic efficiencies of the Mg-air batteries with the blank,

phosphate-containing, and vanadate-containing electrolytes were 59.7%, 72.5%, and 68.8%, respectively. Although the neutral chloride electrolytes provide a more robust alternative to alkaline electrolytes, the sluggish electrochemical kinetics for both the ORR and OER need to be addressed by developing novel catalysts with higher catalytic activity. In addition, poorer conductivities of neutral electrolytes are also required to be substantially increased as well.

5. Separator

It is a promising strategy to separate the liquid-phase or gas-phase electrodes with a solid electrolyte, *i.e.*, the separator, which not only avoids the reactant crossover, but also completely circumvents the metal dendrite concerns [419]. Moreover, in order to realize the flexible applications of rechargeable batteries, transferring the aqueous electrolytes to shape-conformable solid-state electrolytes is of great significance, which greatly simplifies the design and fabrication process of the batteries [420]. As a critical component showing a great effect on battery performance, the separator is supposed to possess the capability of shuttling ions between the electrodes, as well as have sufficient chemical resistance in alkaline electrolytes for a longer lifetime, low ionic resistance and high electrical resistance for a better performance. In addition, the porous separator is required to have a high absorption capacity and appropriate porosity to sustain electrolytes in the pores. However, the selective transport of target ions is not satisfactory, which results in the crossover of soluble metal ions, *e.g.*, the zincate ions in zinc-air batteries, from the separator to the air electrode. This undesired phenomenon will significantly decrease the capacity and cycling efficiency of the battery [20]. Hwang et al. [421] minimized porosity of the membrane to reduce the zincate ion migration by utilizing novel anionic exchanging coating on commercial polypropylene (PP) membranes by copolymerization of ionic liquid monomers of 1-[(4-ethenylphenyl)methyl]-3-butylimidazolium hydroxide (EBIH) and butyl methacrylate (BMA) monomers. It was indicated that the battery using the modified separator exhibited a drastic 281% increase in lifetime and with 1.4% slightly higher initial energy efficiency. Lee et al. [422] synthesized an electrospun nanofiber mat-reinforced permselective composite membrane by impregnating polyvinyl alcohol(PVA) into electrospun polyetherimide (PEI) nanofiber mat as shown in Fig. 13. It was found that the 2nd discharge capacity (~213 mAh g^{-1}) of this membrane was almost

7 times higher than that (~34 mAh g^{-1}) of the Celgard 3501, which was attributed to the suppressed the bulky zincate ion crossover without impairing the OH^- conductivity.

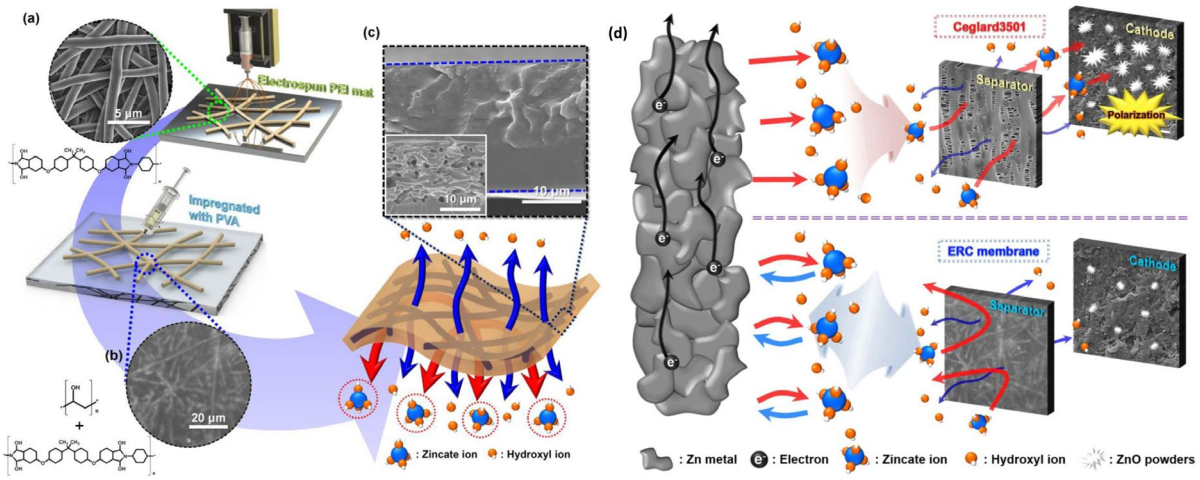

Fig. 13. Schematic of stepwise manufacturing procedure and morphological characterization (FE-SEM images) of ERC membrane: (a) electrospun PEI nanomat, (b) impregnation of PEI nanomat with PVA, (c) ERC membrane and conceptual illustration depicting its unique permselective transport behavior, and (d) permselectivity comparison between the ERC membrane and the conventional microporous polyolefin separators. [422] Copyright 2016 Elsevier.

Similarly, Kim et al. [423] prepared a separator with an anion-conducting continuous phase [electrospun PVA/polyacrylic acid (PAA) nanofiber mat] and an anion-repelling continuous phase (Nafion with pendant sulfonate groups) for zinc-air batteries as show in Fig. 14. As a result, the zincate ion crossover was suppressed by the anion-repelling continuous phase due to Donnan exclusion effect, while the OH^- conduction was slightly impaired due to the presence of the anion-conducting PVA/PAA nanofiber mat. Particularly, the battery with this membrane showed electrochemical rechargeability over 2500 min (at 20 mA cm^{-2} and 10 min cycle period), compared to the cell with the Celgard 3501 (900 min).

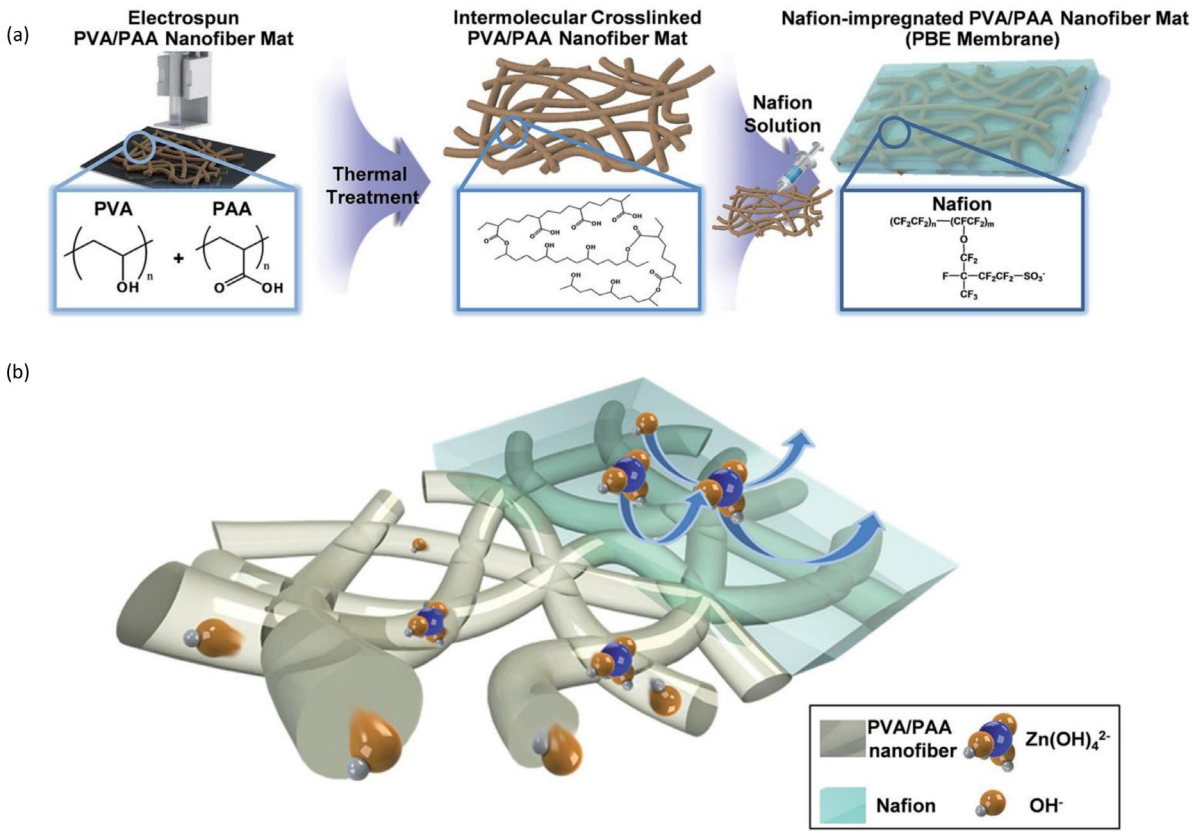

Fig. 14. (a) Schematic representation depicting the overall manufacturing procedure of the PBE membrane. (b) Conceptual illustration underlying the unique function of the PBE membrane as a selective ion transport channel. [423] Copyright 2016 Royal Society of Chemistry.

Yu et al. [419] developed a mediator-ion solid-electrolyte separator, through which the sodium ions shuttled to support the charge transfer and sustain the redox reactions at the anode and cathode. For the zinc-air battery application, the conventional alkaline cathode could be replaced by an acid cathode, thus the acidic electrolyte provided a higher redox potential of 1.23 V than that of alkaline electrolyte (0.40 V) for the ORR. As a result, the Zn-air battery could provide an OCV as high as 2.48 V and eliminate the carbonate problem existing in alkaline Zn-air batteries. Fu et al. [420] fabricated a thin, ultra-flexible and hydroxide ion conductive, nanofibrous cellulose electrolyte membrane with high water retention for zinc-air battery. The elimination of the aqueous electrolyte made it possible to develop a flexible device. In summary, the major research direction for the development of separator is to impede the crossover of anode soluble metal ions through the separator form the anode to the cathode, which will significantly decrease the capacity and cycling

efficiency of the battery. Meanwhile, negative effect on the conductivity of shuttle ions should be minimized.

6. Single cell and stack system design

6.1. Single cell design

The aqueous metal-air batteries can be simply divided into two main configuration types of non-flow batteries and flow batteries. The non-flow battery is designed for high specific density and portability, such as conventional Zn-air button battery for hearing-aid. While the flow battery is designed for longer operation time and higher stability. For instance, Al-air battery is main for exchange of the hot and preventing of precipitate, Mg-air battery is main for product separation and rechargeable Zn-air battery is for inhibiting dendritic.

A proper laboratory metal-air battery test setup is necessary for efficiently investigation of batteries. Fig. 15 (a) shows a schematic representation of battery test setup with installable structure and observable acrylic plates. In this test setup, the waterproof gaskets are assembled between electrodes and electrolyte by acrylic plates and electrodes. The current collectors coated by stainless steel or nickel are inlayed in the reserved grooves with fully contacted with the responding electrodes to reduce the contact resistance and avoid electrolyte leakage. To combine the representativeness of large scale and the conveniences in laboratory, the effective working area of air electrode or metal anode is always 1-4 cm^2. To study the performance of individual electrode, a common circumstance for electrochemical test of batteries, it should set up the reference electrode in the electrolyte filling hole as shown in Fig. 15 (a). As described before, the main research of metal-air batteries is focus on catalyst materials. To simplify the configuration of the battery and make a comparable result for the catalysts, the air electrode is fabricated by spraying catalysts on carbon paper or cloth [37, 424], while the anode is always chosen with high pure metal plate or commercial alloys. For flow batteries, the electrolyte is always input at the bottom and output at the top powered by peristaltic pumps to exchange the electrolyte efficiently and avoid of gas retention [226].

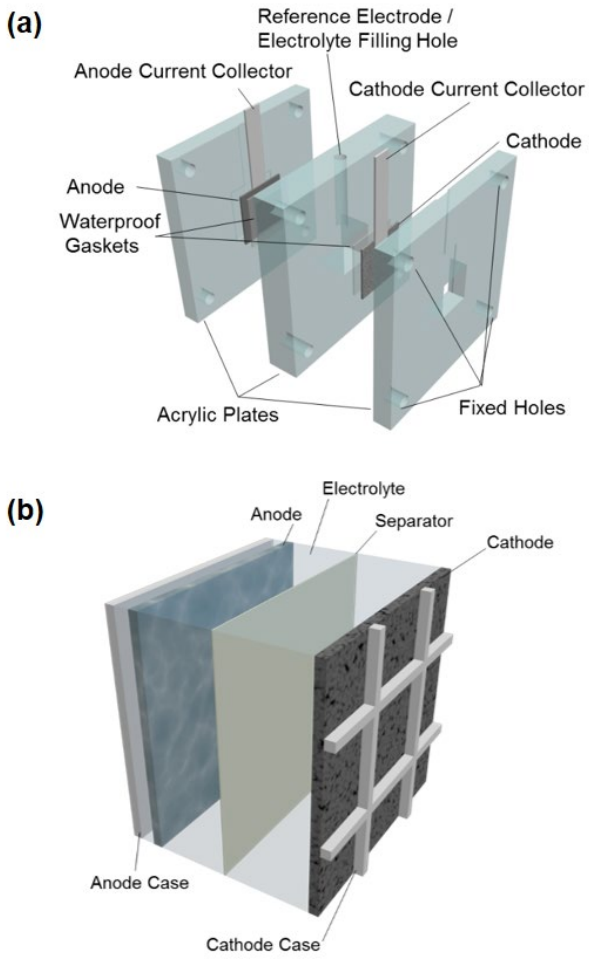

Fig. 15. Schematic representation of (a) a laboratory metal-air battery test setup formed by acrylic plates, the top hole is using for reference electrode and the electrolyte filling, (b) aqueous metal-air battery for application design.

When designing batteries for application, the structure is always changing with the application environments and specific requirements, such as vehicle power supply, which requires for high safety, high power density, high specific energy and good portability. In all these complex cases, the designing principles are still traceable. Firstly, the battery must be designed as a whole system. For instance, a whole battery consists of anode, cathode and electrolyte, no matter how a new kind of battery is defined and expressed [425]. Otherwise, the so-called battery cannot work. For example, the Mg-air battery under storage state cannot work before excited due to the lack of electrolyte. Secondly, the battery needs rational layout to promote the performance. For example, the proper gas passageways are formed by the cathode (as shown in Fig. 15 (b)) to facilitate gas diffusion. Additionally, the cathode should be tough enough to avoid the shape change of the air electrode [33].

For non-flow batteries, the distance between the cathode and anode is as short as possible to enhance the volumetric specific energy and reduce the ohmic resistance of electrolyte, but the proper distance must be reserved for volume change during charge/discharge process. When it comes to flow batteries, the distance is the main match for proper flow electrolyte [108, 426]. Finally, the application scenes determine the design and kind of metal-air battery. Thus, the versatile designs make metal-air batteries widely applied [33]. For example, the vehicle power source employs the flow Al-air battery, household reserve power source uses the neutral low-corrosion Mg-air battery, grid energy storage adopts the flow rechargeable Zn-air battery, and wearable devices utilizes flexible solid-state metal-air batteries.

As a typical example of non-flow metal-air batteries, primary Zn-air button cell is widely applied in hearing aids as for its high specific density and low price [427]. In Zn-air button cell, the micron order zinc powder is infiltrated with the gelled KOH electrolyte [33]. In order to maximize the specific energy, the button cell is filled with zinc powder as much as possible and directly using the metal casing and cap as the current collector. Generally, the cap is opened with one to three holes with millimeter-level diameter to feed oxygen, which is covered by sticky paster under storage state to avoid electrolyte volatilization and lengthen the storage life. For example, the primary Zn-air button battery designed by Power One (type p675) [427] can reach over 500 Wh kg^{-1} with storage life to 3 years. Flexible battery, another kind of non-flow battery, has become a major research with the requirement of flexible electronics in recent years [228, 428-430]. According to the literature reports [228, 430], the flexible batteries focus on Zn-air batteries due to the low cost and high safety. These batteries are designed to cable-like or thin-film “wearable” structure as shown in Fig. 16. In flexible batteries, the electrolyte is more desirable for solid-state or gelled electrolyte without fluidity, avoiding leakage and evaporation onto the electronic equipment or human skin.

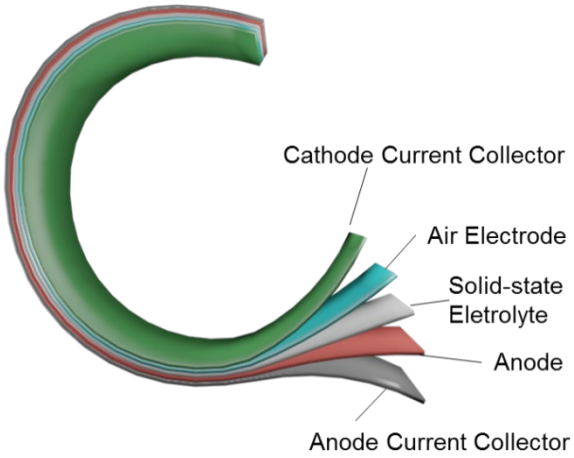

Fig. 16. Schematic representation of thin-film wearable flexible metal-air battery.

Metal-air flow batteries are equipped with a single electrolyte channel to exchange the electrolyte in the chamber of battery [226]. The flowing-electrolyte design helps to enhance the performance and lengthen the lifetime via managing the heat, separating the products and inhibiting the dendrites. For Al-air batteries, the vast heat can be carried with the flowing electrolyte and cooled by the heat exchange system, in which to manage the heat and control the reaction temperature. Additionally, the flowing electrolyte can also output or diluent the product to keep the high ionic conductivity or low viscosity of the electrolyte in the reaction chamber to delay the degradation. Fig. 17 shows a typical Al-air battery fabricated by Joint Institute for High Temperatures of the Russian Academy of Sciences [431]. The battery, designed for stack system, consisted of a body with inlet (bottom) and outlet (upper) channels for electrolyte circulation. During circulation, the electrolyte was supplied through the bottom inlets and exited out the upper outlets, mixed with hydrogen bubbles. The Al anode (size of 100 mm × 200 mm, thickness of 3.7-3.8 mm) is installed between a pair of parallel connected cathodes with the suitable size to anode. To facilitate the quick exchange, the Al anode held with anode current collector is installed into the anode mount with a waterproof sealing gasket plug and commutating elements.

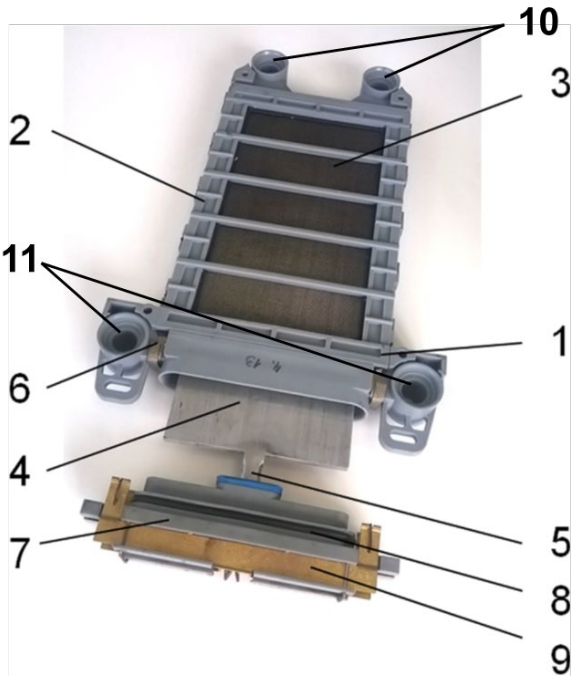

Fig. 17. Photograph of Al-air battery designed by Joint Institute for High Temperatures of the Russian Academy of Sciences: 1-cell body; 2-clip; 3-gas diffusion cathode; 4-anode; 5-anode current collector; 6-cathode current collector; 7-anode mount; 8-sealing gasket; 9-commutating elements, 10-elctrolyte inlets, 11-electrolyte outlets. [431] Copyright 2017 Elsevier.

6.2. Stack system design

The purpose of stack system design is to optimize the performance of battery system to achieve expected requirements, such as power, capacity, lifetime, safety, cost, operability and environmental suitability [432]. For example, to obtain the required voltage, current and power for applications, some metal-air single cells are stacked in series and parallels to raise the voltage and current, respectively. Generally, the cells are stacked with monopolar and bipolar arrangements. Although bipolar arrangement is a more efficient package method in fuel cells due to the absence of external wiring, the relatively low current of metal-air batteries ignore this advantage. Therefore, the metal-air cells in stack system are always designed to the sandwich structure that the metal anode is sandwiched with two externally connected parallel air electrodes to improve the space utilization. As the different applications need various design, it is difficult to summarize the stack system design with a simple description. Hence, some typical stack systems will be reviewed to reveal the design skills and ideas, such as Mg-air storage batteries, Zn-air remote application auxiliary batteries,

oxygen recycling rechargeable Zn-O_2 non-flow batteries, grid energy storage Zn-air flow batteries and Al-air vehicle power supply batteries.

Mg-air Battery A kind of two cells in series of Mg-air battery (type of AM-180) designed by Dalian Institute of Chemical Physics, Chinese Academy of Sciences (DICP, CAS) is produced by the co-partnership company as shown in Fig. 18 [433]. This battery is designed for LED light and charging the mobile phone via 5 V USB with energy of 180 Wh and weight of 428 g without electrolyte. Owing to the durable cathodes, the battery can be stored for 10 years with working life of about 1200 hours during -20 °C and 55 °C. The Mg anodes are inset in groove with a proper distance to cathodes to storage enough product of $Mg(OH)_2$, which lengthen the work time to 8 hours under 1.8 W output during each replace of electrolyte. Additionally, for fast replace of Mg anodes, the Mg plates are connected with quick connectors to electronic control.

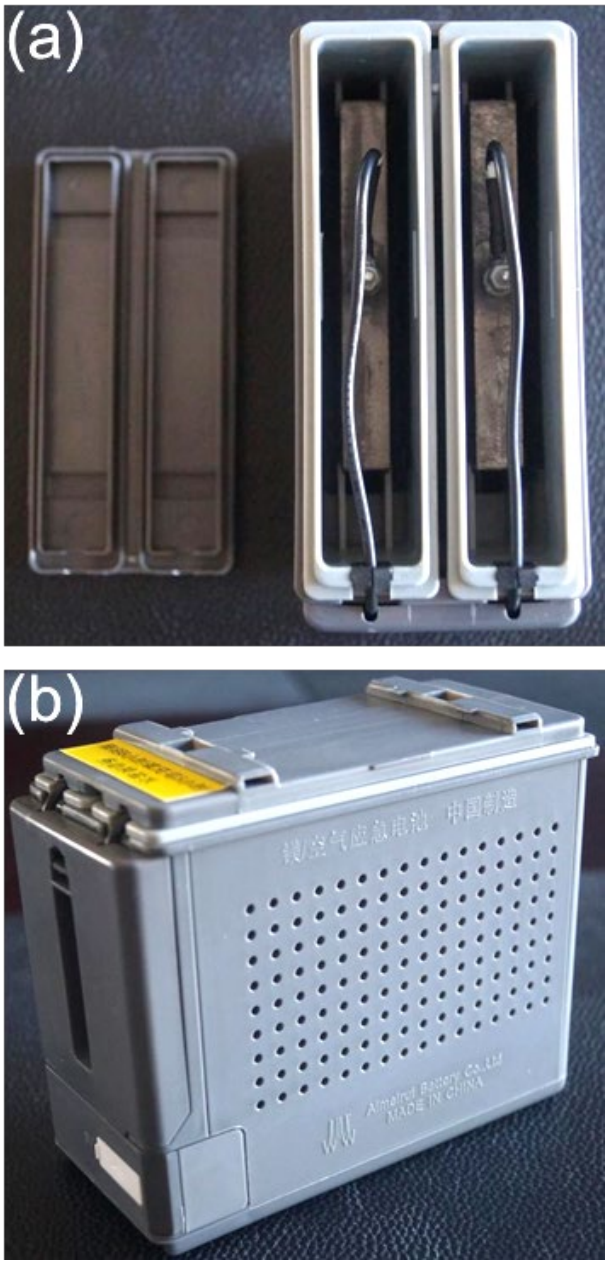

Fig. 18. Photographs of a two-cell in series of Mg-air battery of (a) inner structure and (b) appearance designed by DICP, CAS. [433]

Zn-air Battery Primary Zn-air battery is an attractive choice for many portable electronics due to the high specific energy, low cost and high safety, especially for working time during 1 to 14 days. For example, the type of BA-8180 primary Zn-air battery is designed by Electric Fuel Corp with capacity of 30 Ah and nominal voltage of 28 V for remote application as auxiliary power [33]. The 2.4 kg and 3.5 L battery is stacked by 24 in series cells with 500 Wh kg^{-1} and 1250 Wh L^{-1}, the anode and cathode of which is bonded by adhesive technology. To permit air access to the provisioned cathodes

(the key parameter required by current), the battery has a fan and air channels to provide positive pressure air.

The electrically rechargeable Zn-air/oxygen battery is a competitive candidate for grid storage energy because of the low cost, high safety and good environmental friendliness. However, the poor cyclic performance and relative low energy efficiency restrict the development caused by zinc dendrite, cathode corrosion, carbonate and slow kinetics. Wang et al. [434] deigned a separated three-electrode 1 kW/1 k Wh Zn-O_2 battery system with low cost oxygen recycling system to resolve the electrode corrosion and carbonate, which can efficiently extend the cyclic number and enhance the energy efficiency as shown in Fig. 19. The single cell of the system has a stable 1500 cycles with an average energy density of 60% and elimination of carbonates, and the system oxygen cost is only 0.2 ¢ kWh^{-1} per cycle. Amunátegui et al. [156] demonstrated a 1 kW-4 kWh zinc-air flow battery divided in three different stacks connected in parallel, which exhibited lower coulombic efficiency of 18.3% than expected of 13% due to shunt current losses as shown in Fig. 20. Additionally, the shunt current also makes zinc built-up and short-circuiting to restrict the cyclic performance, although the single cell can reach to 2000 cycles. For rechargeable Zn-air flow battery, the bi-functional oxygen electrode and shunt current is still the main engineering challenges to be overcame.

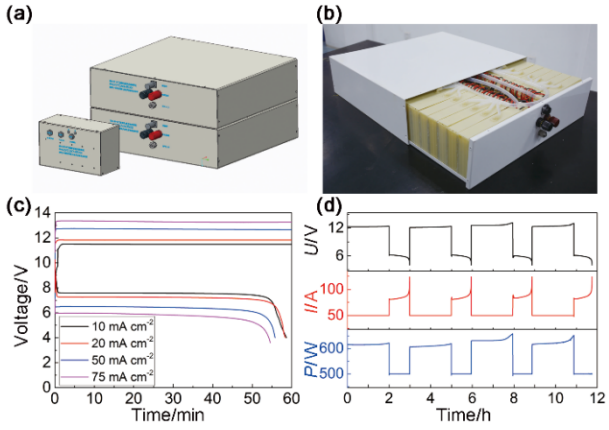

Fig. 19. (a) Design of the Zn-O_2 battery system. (b) Photograph, (c) charge-discharge curves and (d) cyclic results of a 500 W/500 Wh Zn-O_2 battery module. [434] Copyright 2018 John Wiley and Sons.

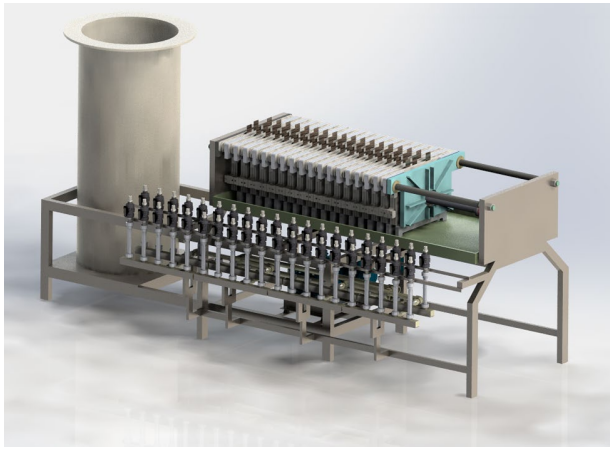

Fig. 20. One of the electrolyte tank and cell stack for the 1 kW-4 kWh zinc-air flow battery. [156] Copyright 2018 Springer Nature.

Al-air battery Al-air battery, due to the low cost, high specific capacity and negative potential anode of Al, has attracted much attention, which is always designed as flow battery to manage the heat and water [435]. For example, Phinergy combined with Alcoa [436] demonstrated an Al-air battery with in series 50 cells to provide enough energy to power an electric vehicle for up to 1000 miles by water and anodes fill-up every 200 miles. Owing to the special gas diffusion film to keep out CO_2 into electrolyte, the carbonate problem is reduced to lengthen the lifetime of cathode and system. However, 200 miles for each time is relatively short for vehicles, so the Phinergy promotes their Al-air battery as a trip extender, rather than a means of powering commuter trips.

7. Conclusion and outlook

The aqueous metal-air batteries, particularly of rechargeable Zn-air battery, primary Zn-air battery and Al-air battery, have gained significant attention during the last few years. This review outlines the research progress on the key components of the metal-air batteries including air electrodes, anodes, electrolytes and separators, designs of single cell and stack system. Focusing on the materials challenge of bi-functional catalysts and anodes, the performance of the electrocatalytic activity and durability for catalysts and coulombic efficiency and utilization for anodes are enhanced obviously via testing in laboratory. Despite the positive progresses are discussed, there are still enough further advancement to aqueous metal-air batteries on materials science and engineering as follows:

1) Advanced and low cost air electrode, which includes fabrication of catalysts, gas diffusion layer and design of air electrode, requires further development. The demand for catalysts is that the ORR electrocatalytic activity in primary metal-air battery can be compared with 20% Pt/C, and the bi-functional activity in rechargeable metal-air battery should be better for the hybrid catalyst of 20% Pt/C with RuO_2/C. The durability matches with gas diffusion layer, particularly of long running rechargeable batteries including electrical recharge and mechanical replacement, which can be stored at least of 5 years with electrolyte or 10 years in dry, and keep working at least of several hundreds of hours without obvious degradation. Additionally, a reliable relationship of activity performance between laboratory test and application conditions should be built to guide the engineering based on laboratory data. The thin gas diffusion layer must not only be versatile enough to prevent leakage, diffuse oxygen and keep out of CO_2 for alkaline electrolyte, but also be excellent in oxidation resistance for bi-functional oxygen electrodes. Currently, the outstanding performance of air electrodes with small size can be fabricated in laboratory, however, how to keep the performance during large-scale continuous production for application via low cost methods is still an intractable engineering challenge. Except for performance and fabrication demand, the catalyst and electrode polarization process also need more deeply understanding, such as the process of ORR and OER under electronic and atomic level on the active sites/area of the catalysts, the polarization percent for the three kind polarization for the three structure layers and the more meticulous and near-realistic models for oxygen transfer. These can help the researchers to enhance the performance of catalysts and air electrodes on the key points.
2) For electrically rechargeable Zinc-air batteries, the reversible zinc electrodes are supposed to meet these requirements: (1) a high anode utilization, (2) a high efficiency when recharging, and (3) at least several hundred charge/discharge cycles without obvious capacity degradation. To deal with these issues, structural modification and compositional modification by means of additives, electrodeposition, chemical doping, and advanced casting have been demonstrated to be feasible ways. In order not to reduce the overall zinc capacity, the additives should be effective in small quantities. For the primary Al-air and Mg-air batteries, which only can be recharged by mechanical change the anode, high utilization of the anode is the most critical

parameter influencing the battery performance. However, both the Al and Mg anode suffer from the sever anode passivation problem, which significantly reduces the utilization of the anode active materials. Therefore, future research attention can be paid to alleviating anode passivation problem via the development of novel anode alloy and the modification of conventional anode, thus a longer lifetime and a higher anode utilization can be achieved.

3) Using the aqueous electrolyte is of great significance for large-scale energy storage due to its intrinsic advantages, including the high power output due to higher ionic conductivity, high safety for abandoning the flammable organic electrolytes, low cost derived from using good availability of salts, and environmental friendliness. For the conventional alkaline electrolytes, modification by mixing them with novel electrolyte candidates is necessary due to the intrinsic problems such as anode corrosion, side reactions, and dendrite formation. The addition of room temperature ionic liquids (RTILs) is promising, because they are not only able to alleviate the dendrite formation, but also able to maintain the high ionic conductivity. For the neutral electrolytes, although it avoids the carbonate issue and substrate corrosion, poorer conductivities are required to be substantially increased to achieve a satisfactory power output. In addition, developing novel bi-functional catalysts with higher catalytic activity is of great significance, because the electrochemical kinetics for both ORR and OER are more sluggish in the neutral electrolytes than in the alkaline electrolytes.
4) Single cell and stack system designs need further optimization. Proper design of single cell and stack system is not only to keep battery work normally, but also important to assure the operation safe, reliable and optimum. Although almost all engineering single problem can be resolved by the responding methods, the induced methods always bring new troubles. For example, flowing electrolyte structure can resolve the zinc dendrite problem efficiently to lengthen the cyclic performance, but the flowing channels inducing of connecting electrolyte will result in shunt current or short-circuit current, consequentially, which leads to build-up zinc and lower coulombic efficiency. In addition, the flowing system also adds the extra power consume and cost. Therefore, the design of stack system must be considered as a whole from every component based on materials to the all system. However, the practical design is always to optimize an optimal balance with the solution and the responding new troubles. For example,

the closer cathode distance between metal-air cells in stack is, the better to obtain high volume power density via reducing volume in theory. But the closer distance makes higher resistance of oxygen transmission, which may result in the stack sink in anoxic state to enlarge the oxygen mass transfer polarization. So it needs to balance the distance with oxygen transfer by theoretical calculation and practical tests. Regrettably, the system design of metal-air battery is lacking of systematic and detailed reports, which may draw lessons from hydrogen fuel cells.

Recently, the non-aqueous and hybrid metal-air batteries, such as Li-air and Na-air batteries, have received most attention according to the literatures base on *Web of Science Core Collection* due to the high theoretical specific energy. However, synthetically compared with cost, safety and technical maturity, the aqueous metal-air batteries also exhibit obvious superiority. Therefore, the aqueous metal-air batteries combined with good safety, low cost and high specific energy are a promising candidate to support the increasing energy needs based on low-carbon and environmentally friendly energy structure.

Acknowledgement:

This work was supported by the National Key Research and Development Program (2017YFC0306403), the Strategic Priority Research Program of the Chinese Academy of Sciences (XDA09030104, XDA22010601), the Youth Innovation Promotion Association of the Chinese Academy of Sciences, Joint Sino-German Research Project (Grant No. GZ1364), and the Research Grants Council of the Hong Kong Special Administrative Region, China (Project No. 15222018).

References

[1] Z.F. Pan, L. An, C.Y. Wen, Recent advances in fuel cells based propulsion systems for unmanned aerial vehicles, Appl. Energy, 240 (2019) 473-485.

[2] M. Winter, R.J. Brodd, What Are Batteries, Fuel Cells, and Supercapacitors?, Chem. Rev., 104 (2004) 4245-4270.

[3] B.C.H. Steele, A. Heinzel, Materials for fuel-cell technologies, Nature, 414 (2001) 345.

[4] Z. Pan, R. Chen, L. An, Y. Li, Alkaline anion exchange membrane fuel cells for cogeneration of electricity and valuable chemicals, J. Power Sources, 365 (2017) 430-445.

[5] M. Armand, F. Endres, D.R. MacFarlane, H. Ohno, B. Scrosati, Ionic-liquid materials for the electrochemical challenges of the future, Nat. Mater., 8 (2009) 621-629.

[6] N.T. Suen, S.F. Hung, Q. Quan, N. Zhang, Y. J. Xu, H.M. Chen, Electrocatalysis for the oxygen evolution reaction: recent development and future perspectives, Chem. Soc. Rev., 46 (2017) 337-365.

[7] Z.F. Pan, H.R. Zhuang, Y.D. Bi, L. An, A direct ethylene glycol fuel cell stack as air-independent power sources for underwater and outer space applications, J. Power Sources, 437 (2019) 226944.

[8] Z.F. Pan, Y.D. Bi, L. An, Performance characteristics of a passive direct ethylene glycol fuel cell with hydrogen peroxide as oxidant, Appl. Energy, 250 (2019) 846-854.

[9] B. Dunn, H. Kamath, J.M. Tarascon, Electrical Energy Storage for the Grid: A Battery of Choices, Science, 334 (2011) 928-935.

[10] J. Fu, Z.P. Cano, M.G. Park, A. Yu, M. Fowler, Z. Chen, Electrically Rechargeable Zinc-Air Batteries: Progress, Challenges, and Perspectives, Adv. Mater., 29 (2017) 1604685.

[11] Z. Pan, Y. Bi, L. An, Mathematical modeling of direct ethylene glycol fuel cells incorporating the effect of the competitive adsorption, Appl. Therm. Eng., 147 (2019) 1115-1124.

[12] D. Lin, Y. Liu, Y. Cui, Reviving the lithium metal anode for high-energy batteries, Nat. Nanotechnol., 12 (2017) 194.

[13] Y. Li, J. Lu, Metal-Air Batteries: Will They Be the Future Electrochemical Energy Storage Device of Choice?, ACS Energy Lett., 2 (2017) 1370-1377.

[14] P.G. Bruce, S.A. Freunberger, L.J. Hardwick, J.M. Tarascon, Li-O_2 and Li-S batteries with high energy storage, Nat. Mater., 11 (2011) 19.

[15] F. Cheng, J. Chen, Metal-air batteries: from oxygen reduction electrochemistry to cathode catalysts, Chem. Soc. Rev., 41 (2012) 2172-2192.

[16] G. Girishkumar, B. McCloskey, A.C. Luntz, S. Swanson, W. Wilcke, Lithium-Air Battery: Promise and Challenges, J. Phys. Chem. Lett., 1 (2010) 2193-2203.

[17] X.Y. Yu, X.W. Lou, Mixed Metal Sulfides for Electrochemical Energy Storage and Conversion, Adv. Energy Mater., 8 (2018) 1701592.

[18] J. Pan, Y.Y. Xu, H. Yang, Z. Dong, H. Liu, B.Y. Xia, Advanced Architectures and Relatives of Air Electrodes in Zn-Air Batteries, Adv. Sci., 5 (2018) 1700691.

[19] M. Xu, D.G. Ivey, Z. Xie, W. Qu, Rechargeable Zn-air batteries: Progress in electrolyte development and cell configuration advancement, J. Power Sources, 283 (2015) 358-371.

[20] P. Gu, M. Zheng, Q. Zhao, X. Xiao, H. Xue, H. Pang, Rechargeable zinc-air batteries: a promising way to green energy, J. Mater. Chem. A, 5 (2017) 7651-7666.

[21] J. Lu, Z. Chen, Z. Ma, F. Pan, L.A. Curtiss, K. Amine, The role of nanotechnology in the development of battery materials for electric vehicles, Nat. Nanotechnol., 11 (2016) 1031.

[22] J. Zhang, Z. Zhao, Z. Xia, L. Dai, A metal-free bifunctional electrocatalyst for oxygen reduction and oxygen evolution reactions, Nat. Nanotechnol., 10 (2015) 444.

[23] R. Raccichini, A. Varzi, S. Passerini, B. Scrosati, The role of graphene for electrochemical energy storage, Nat. Mater., 14 (2014) 271.

[24] K. Zhang, X. Han, Z. Hu, X. Zhang, Z. Tao, J. Chen, Nanostructured Mn-based oxides for electrochemical energy storage and conversion, Chem. Soc. Rev., 44 (2015) 699-728.

[25] D. Chen, C. Chen, Z.M. Baiyee, Z. Shao, F. Ciucci, Nonstoichiometric Oxides as Low-Cost and Highly-Efficient Oxygen Reduction/Evolution Catalysts for Low-Temperature Electrochemical Devices, Chem. Rev., 115 (2015) 9869-9921.

[26] L. Grande, E. Paillard, J. Hassoun, J.B. Park, Y.J. Lee, Y.K. Sun, S. Passerini, B. Scrosati, The Lithium/Air Battery: Still an Emerging System or a Practical Reality?, Adv. Mater., 27 (2015) 784-800.

[27] D. Aurbach, B.D. McCloskey, L.F. Nazar, P.G. Bruce, Advances in understanding mechanisms underpinning lithium-air batteries, Nat. Energy, 1 (2016) 16128.

[28] F. Meng, H. Zhong, D. Bao, J. Yan, X. Zhang, In Situ Coupling of Strung Co4N and Intertwined N-C Fibers toward Free-Standing Bifunctional Cathode for Robust, Efficient, and Flexible Zn-Air Batteries, J. Am. Chem. Soc., 138 (2016) 10226-10231.

[29] P. Geng, S. Zheng, H. Tang, R. Zhu, L. Zhang, S. Cao, H. Xue, H. Pang, Transition Metal Sulfides Based on Graphene for Electrochemical Energy Storage, Adv. Energy Mater., 8 (2018) 1703259.

[30] J. Liu, C. Xu, Z. Chen, S. Ni, Z.X. Shen, Progress in aqueous rechargeable batteries, Green Energy Environ., 3 (2018) 20-41.

[31] G. Fang, J. Zhou, A. Pan, S. Liang, Recent Advances in Aqueous Zinc-Ion Batteries, ACS Energy Lett., 3 (2018) 2480-2501.

[32] T. Zhang, Z. Tao, J. Chen, Magnesium-air batteries: from principle to application, Mater. Horiz., 1 (2014) 196-206.

[33] T.B. Reddy, Linden's Handbook of Batteries, 4th Edition, McGraw-Hill Companies, New York, 2011.

[34] Y. Li, H. Dai, Recent advances in zinc-air batteries, Chem. Soc. Rev., 43 (2014) 5257-5275.

[35] J. Fu, Z.P. Cano, M.G. Park, A.P. Yu, M. Fowler, Z.W. Chen, Electrically Rechargeable Zinc-Air Batteries: Progress, Challenges, and Perspectives, Adv. Mater., 29 (2017).

[36] G.G. Park, Y.J. Sohn, T.H. Yang, Y.G. Yoon, W.Y. Lee, C.S. Kim, Effect of PTFE contents in the gas diffusion media on the performance of PEMFC, J. Power Sources, 131 (2004) 182-187.

[37] J. Pan, Y.Y. Xu, H. Yang, Z.H. Dong, H.F. Liu, B.Y. Xia, Advanced Architectures and Relatives of Air Electrodes in Zn-Air Batteries, Adv. Sci., 5 (2018) 1700691.

[38] X. Wang, P.J. Sebastian, M.A. Smit, H. Yang, S.A. Gamboa, Studies on the oxygen reduction catalyst for zinc-air battery electrode, J. Power Sources, 124 (2003) 278-284.

[39] E.S. Davydova, I.N. Atamanyuk, A.S. Ilyukhin, E.I. Shkolnikov, A.Z. Zhuk, Nitrogen-doped carbonaceous catalysts for gas-diffusion cathodes for alkaline aluminum-air batteries, J. Power Sources, 306 (2016) 329-336.

[40] C. Yang, Preparation and characterization of electrochemical properties of air cathode electrode, Int. J. Hydrogen Energy, 29 (2004) 135-143.

[41] Z.F. Li, J.W. Yang, G.F. Xu, S.W. Wang, Non-precious cathode electrocatalyst for magnesium air fuel cells: Activity and durability of iron-polyphthalocyanine absorbed on carbon black, J. Power Sources, 242 (2013) 157-165.

[42] H. Zhang, H. Qiao, H. Wang, N. Zhou, J. Chen, Y. Tang, J. Li, C. Huang, Nickel cobalt oxide/carbon nanotubes hybrid as a high-performance electrocatalyst for metal/air battery, Nanoscale, 6 (2014) 10235-10242.

[43] A. Flegler, S. Hartmann, J. Settelein, K. Mandel, G. Sextl, Screen printed bifunctional gas diffusion electrodes for aqueous metal-air batteries: Combining the best of the catalyst and binder world, Electrochim. Acta, 258 (2017) 495-503.

[44] C.Z. Shu, E.D. Wang, L.H. Jiang, G.Q. Sun, High performance cathode based on carbon fiber felt for magnesium-air fuel cells, Int. J. Hydrogen Energy, 38 (2013) 5885-5893.

[45] Y. Xue, H. Miao, S. Sun, Q. Wang, S. Li, Z. Liu, Template-directed fabrication of porous gas diffusion layer for magnesium air batteries, J. Power Sources, 297 (2015) 202-207.

[46] W.Q. Yang, S.H. Yang, J.S. Guo, G.Q. Sun, Q. Xin, Comparison of CNF and XC-72 carbon supported palladium electrocatalysts for magnesium air fuel cell, Carbon, 45 (2007) 397-401.

[47] F. Li, X.Z. Xu, H. Song, J. Xiong, F. Wu, Impact of Polytetrafluoroethylene Emulsion Binder Pretreatment with Ethanol on the Performance of Gas Diffusion Electrodes, Acta Phys. Chim. Sin., 25 (2009) 2205-2210.

[48] J. Grbovic, Z. Lausevic, S. Mentus, New carbon materials as a support for oxygen electrode in fuel cells, in: D.P. Uskokovic, G.A. Battiston, S.K. Milonjic, D.I. Rakovic (Eds.) Contemporary Studies in Advanced Materials and Processes: Yucomat Iv, Trans Tech Publications Ltd, Zurich-Uetikon, 2003, pp. 225-230.

[49] K. Xu, A. Loh, B.G. Wang, X.H. Li, Enhancement of Oxygen Transfer by Design Nickel Foam Electrode for Zinc-Air Battery, J. Electrochem. Soc., 165 (2018) A809-A818.

[50] F. Chu, C. Zuo, Z. Tian, C. Ma, C. Zhao, Y. Wang, W. Dong, J. Long, Z. Wen, X. Yuan, Y. Cao, Solution combustion synthesis of mixed-phase Mn-based oxides nanoparticles and their electrocatalytic performances for Al-air batteries, J. Alloys Compd., 748 (2018) 375-381.

[51] V. Neburchilov, H. Wang, J.J. Martin, W. Qu, A review on air cathodes for zinc-air fuel cells, J. Power Sources, 195 (2010) 1271-1291.

[52] Z.H. Cheng, Q. Fu, C.X. Li, X.P. Wang, J. Gao, M.H. Ye, Y. Zhao, L.J. Dong, H.X. Luo, L.T. Qu, Controllable localization of carbon nanotubes on the holey edge of graphene: an efficient oxygen reduction electrocatalyst for Zn-air batteries, J. Mater. Chem. A, 4 (2016) 18240-18247.

[53] Y. Liang, Y. Li, H. Wang, J. Zhou, J. Wang, T. Regier, H. Dai, Co_3O_4 nanocrystals on graphene as a synergistic catalyst for oxygen reduction reaction, Nat. Mater., 10 (2011) 780-786.

[54] S.S. Shinde, J.Y. Yu, J.W. Song, Y.H. Nam, D.H. Kim, J.H. Lee, Highly active and durable carbon nitride fibers as metal-free bifunctional oxygen electrodes for flexible Zn-air batteries, Nanoscale Horiz., 2 (2017) 333-341.

[55] Y.F. Cheng, F. Liao, W. Shen, L.B. Liu, B.B. Jiang, Y.Q. Li, M.W. Shao, Carbon cloth supported cobalt phosphide as multifunctional catalysts for efficient overall water splitting and zinc-air batteries, Nanoscale, 9 (2017) 18977-18982.

[56] Z.S. Song, X.P. Han, Y.D. Deng, N.Q. Zhao, W.B. Hu, C. Zhong, Clarifying the Controversial Catalytic Performance of $Co(OH)_2$ and Co_3O_4 for Oxygen Reduction/Evolution Reactions toward Efficient Zn-Air Batteries, ACS Appl. Mater. Interfaces, 9 (2017) 22694-22703.

[57] F.L. Meng, H.X. Zhong, D. Bao, J.M. Yan, X.B. Zhang, In Situ Coupling of Strung Co_4N and Intertwined N-C Fibers toward Free-Standing Bifunctional Cathode for Robust, Efficient, and Flexible Zn Air-Batteries, J. Am. Chem. Soc., 138 (2016) 10226-10231.

[58] X. Chen, B. Liu, C. Zhong, Z. Liu, J. Liu, L. Ma, Y.D. Deng, X.P. Han, T.P. Wu, W.B. Hu, J. Lu, Ultrathin Co_3O_4 Layers with Large Contact Area on Carbon Fibers as High-Performance Electrode for Flexible Zinc-Air Battery Integrated with Flexible Display, Adv. Energy Mater., 7 (2017) 1700779.

[59] S.X. Qu, Z.S. Song, J. Liu, Y.B. Li, Y. Kou, C. Ma, X.P. Han, Y.D. Deng, N.Q. Zhao, W.B. Hu, C. Zhong, Electrochemical approach to prepare integrated air electrodes for highly stretchable zinc-air battery array with tunable output voltage and current for wearable electronics, Nano Energy, 39 (2017) 101-110.

[60] P. Tan, B. Chen, H. Xu, W. Cai, W. He, M. Ni, Investigation on the electrode design of hybrid Zn-Co_3O_4/air batteries for performance improvements, Electrochim. Acta, 283 (2018) 1028-1036.

[61] Y. Kou, J. Liu, Y.B. Li, S.X. Qu, C. Ma, Z.S. Song, X.P. Han, Y.D. Deng, W.B. Hu, C. Zhong, Electrochemical Oxidation of Chlorine-Doped $Co(OH)_2$ Nanosheet Arrays on Carbon Cloth as a Bifunctional Oxygen Electrode, ACS Appl. Mater. Interfaces, 10 (2018) 796-805.

[62] Z.H. Pu, Y. Xue, W.Q. Li, I.S. Amiinu, S.C. Mu, Efficient water splitting catalyzed by flexible NiP_2 nanosheet array electrodes under both neutral and alkaline solutions, New J. Chem., 41 (2017) 2154-2159.

[63] X. Du, Z. Yan, E. Wang, L. Li, A High Performance Air Cathode with the Hydrophobic Pores Distributed Continuously and in Gradient for Zinc-Air Fuel Cells, Energy Technol., 6 (2018) 1860-1864.

[64] Z.X. Zhang, Z.F. Li, C.Y. Sun, T.W. Zhang, S.W. Wang, Preparation and properties of an amorphous MnO_2/CNTs-OH catalyst with high dispersion and durability for magnesium-air fuel cells, Catal. Today, 298 (2017) 241-249.

[65] M. Jiang, H. He, C. Huang, B. Liu, W.J. Yi, Z.S. Chao, alpha-MnO_2 Nanowires/Graphene Composites with High Electrocatalytic Activity for Mg-Air Fuel Cell, Electrochim. Acta, 219 (2016) 492-501.

[66] Y.F. Li, K. Huang, J.D. MacGregor, Y.C. Xing, The Role of PTFE in Cathode Transition Layer in Aqueous Electrolyte Li-Air Battery, Electrochim. Acta, 191 (2016) 996-1000.

[67] L. Zhou, C. Zhang, X. Cai, Y. Qian, H. Jiang, B. Li, L. Lai, Z. Shen, W. Huang, N, P Co-doped Hierarchical Porous Graphene as a Metal-Free Bifunctional Air Cathode for Zn-Air Batteries, Chemelectrochem, 5 (2018) 1811-1816.

[68] J. Sun, D. Yang, S. Lowe, L. Zhang, Y. Wang, S. Zhao, P. Liu, Y. Wang, Z. Tang, H. Zhao, X. Yao, Sandwich-Like Reduced Graphene Oxide/Carbon Black/Amorphous Cobalt Borate Nanocomposites as Bifunctional Cathode Electrocatalyst in Rechargeable Zinc-Air Batteries, Adv. Energy Mater., 8 (2018) 1801495.

[69] N.N. Xu, J.L. Qiao, X. Zhang, C.Y. Ma, S.A. Jian, Y.Y. Liu, P.C. Pei, Morphology controlled La_2O_3/Co_3O_4/MnO_2-CNTs hybrid nanocomposites with durable bi-functional air electrode in high-performance zinc-air energy storage, Appl. Energy, 175 (2016) 495-504.

[70] D.U. Lee, J.Y. Choi, K. Feng, H.W. Park, Z.W. Chen, Advanced Extremely Durable 3D Bifunctional Air Electrodes for Rechargeable Zinc-Air Batteries, Adv. Energy Mater., 4 (2014) 5.

[71] W. Niu, S. Pakhira, K. Marcus, Z. Li, J.L. Mendoza-Cortes, Y. Yang, Apically Dominant Mechanism for Improving Catalytic Activities of N-Doped Carbon Nanotube Arrays in Rechargeable Zinc-Air Battery, Adv. Energy Mater., 8 (2018) 1800480.

[72] J. Fu, F.M. Hassan, J.D. Li, D.U. Lee, A.R. Ghannoum, G. Lui, M.A. Hoque, Z.W. Chen, Flexible Rechargeable Zinc-Air Batteries through Morphological Emulation of Human Hair Array, Adv. Mater., 28 (2016) 6421-6428.

[73] J.T. Ren, G.G. Yuan, C.C. Weng, Z.Y. Yuan, Rationally Designed Co_3O_4-C Nanowire Arrays on Ni Foam Derived From Metal Organic Framework as Reversible Oxygen Evolution Electrodes with Enhanced Performance for Zn-Air Batteries, Acs Sustainable Chem. Eng., 6 (2018) 707-718.

[74] X. Ren, M. Huang, S. Luo, Y. Li, L. Deng, H. Mi, L. Sun, P. Zhang, PdNi alloy decorated 3D hierarchically N, S co-doped macro-mesoporous carbon composites as efficient free-standing and binder-free catalysts for Li-O_2 batteries, J. Mater. Chem. A, 6 (2018) 10856-10867.

[75] Y. Liu, N. Li, K.M. Liao, Q. Li, M. Ishida, H.S. Zhou, Lowering the charge voltage of Li-O_2 batteries via an unmediated photoelectrochemical oxidation approach, J. Mater. Chem. A, 4 (2016) 12411-12415.

[76] J. Liu, Z.H. Wang, J.F. Zhu, Binder-free nitrogen-doped carbon paper electrodes derived from polypyrrole/cellulose composite for Li-O_2 batteries, J. Power Sources, 306 (2016) 559-566.

[77] Y. Li, Y.F. Huang, Z.L. Zhang, D.H. Duan, X.G. Hao, S.B. Liu, Preparation and structural evolution of well aligned-carbon nanotube arrays onto conductive carbon-black layer/carbon paper substrate with enhanced discharge capacity for Li-air batteries, Chem. Eng. J., 283 (2016) 911-921.

[78] B.B. Chen, D.Y.C. Leung, A Low-Cost Mechanically Rechargeable Aluminum-Air Cell for Energy Conversion Using Low-Grade Aluminum Foil, J. Electrochem. En. Conv. Stor., 13 (2016) 011001.

[79] X.B. Zhu, Y.G. Wu, W.H. Wan, Y.Z. Yan, Y. Wang, X.L. He, Z. Lu, CNF-grafted carbon fibers as a binder-free cathode for Lithium-Oxygen batteries with a superior performance, Int. J. Hydrogen Energy, 43 (2018) 739-747.

[80] Y.C. Yu, M. Chen, S.T. Wang, C. Hill, P. Joshi, T. Kuruganti, A.M. Hu, Laser Sintering of Printed Anodes for Al-Air Batteries, J. Electrochem. Soc., 165 (2018) A584-A592.

[81] L.M. Leng, J. Li, X.Y. Zeng, X.L. Tian, H.Y. Song, Z.M. Cui, T. Shu, H.S. Wang, J.W. Ren, S.J. Liao, Enhanced cyclability of Li-O_2 batteries with cathodes of Ir and MnO_2 supported on well-defined TiN arrays, Nanoscale, 10 (2018) 2983-2989.

[82] N. Bhandary, P.P. Ingole, S. Basu, Electrosynthesis of Mn-Fe oxide nanopetals on carbon paper as bi-functional electrocatalyst for oxygen reduction and oxygen evolution reaction, Int. J. Hydrogen Energy, 43 (2018) 3165-3171.

[83] Z.J. Liu, Z.H. Zhao, Y.Y. Wang, S. Dou, D.F. Yan, D.D. Liu, Z.H. Xia, S.Y. Wang, In Situ Exfoliated, Edge-Rich, Oxygen-Functionalized Graphene from Carbon Fibers for Oxygen Electrocatalysis, Adv. Mater., 29 (2017) 1606207.

[84] Z. Khan, B. Senthilkumar, S.O. Park, S. Park, J. Yang, J.H. Lee, H.K. Song, Y. Kim, S.K. Kwak, H. Ko, Carambola-shaped VO_2 nanostructures: a binder-free air electrode for an aqueous Na-air battery, J. Mater. Chem. A, 5 (2017) 2037-2044.

[85] H.Q. Wang, X.P. Fan, X.H. Zhang, Y.G. Huang, Q. Wu, Q.C. Pan, Q.Y. Li, In situ growth of NiO nanoparticles on carbon paper as a cathode for rechargeable Li-O_2 batteries, Rsc Adv., 7 (2017) 23328-23333.

[86] Q. Liu, Y.B. Wang, L.M. Dai, J.N. Yao, Scalable Fabrication of Nanoporous Carbon Fiber Films as Bifunctional Catalytic Electrodes for Flexible Zn-Air Batteries, Adv. Mater., 28 (2016) 3000-3006.

[87] X.Y. Wu, X.P. Han, X.Y. Ma, W. Zhang, Y.D. Deng, C. Zhong, W.B. Hu, Morphology-Controllable Synthesis of Zn-Co-Mixed Sulfide Nanostructures on Carbon Fiber Paper Toward Efficient Rechargeable Zinc-Air Batteries and Water Electrolysis, ACS Appl. Mater. Interfaces, 9 (2017) 12574-12583.

[88] X. Zhang, G.Q. Liu, C.J. Zhao, G.Z. Wang, Y.X. Zhang, H.M. Zhang, H.J. Zhao, Highly efficient electrocatalytic oxidation of urea on a Mn-incorporated $Ni(OH)_2$/carbon fiber cloth for energy-saving rechargeable Zn-air batteries, Chem. Commun., 53 (2017) 10711-10714.

[89] C. Tang, Y. Mao, J. Xie, Z. Chen, J. Tu, G. Cao, X. Zhao, $NiCo_2O_4$/MnO_2 core/shell arrays as a binder-free catalytic cathode for high-performance lithium-oxygen cells, Inorg. Chem. Front., 5 (2018) 1707-1713.

[90] S. Hyun, S. Shanmugam, Hierarchical Nickel-Cobalt Dichalcogenide Nanostructure as an Efficient Electrocatalyst for Oxygen Evolution Reaction and a Zn-Air Battery, Acs Omega, 3 (2018) 8621-8630.

[91] C. Guan, A. Sumboja, H.J. Wu, W.N. Ren, X.M. Liu, H. Zhang, Z.L. Liu, C.W. Cheng, S.J. Pennycook, J. Wang, Hollow Co_3O_4 Nanosphere Embedded in Carbon Arrays for Stable and Flexible Solid-State Zinc-Air Batteries, Adv. Mater., 29 (2017) 1704117.

[92] Y. Luo, C. Jin, Z.J. Wang, M.H. Wei, C.H. Yang, R.Z. Yang, Y. Chen, M.L. Liu, A high-performance oxygen electrode for Li-O_2 batteries: Mo_2C nanoparticles grown on carbon fibers, J. Mater. Chem. A, 5 (2017) 5690-5695.

[93] H.T. Wu, W. Sun, Y. Wang, F. Wang, J.F. Liu, X.Y. Yue, Z.H. Wang, J.S. Qiao, D.W. Rooney, K.N. Sun, Facile Synthesis of Hierarchical Porous Three-Dimensional Free-Standing $MnCo_2O_4$ Cathodes for Long-Life Li-O_2 Batteries, ACS Appl. Mater. Interfaces, 9 (2017) 12355-12365.

[94] M. Carboni, A.G. Marrani, R. Spezia, S. Brutti, Degradation of LiTfO/TEGME and LiTfO/DME Electrolytes in Li-O_2 Batteries, J. Electrochem. Soc., 165 (2018) A118-A125.

[95] D. Pletcher, X.H. Li, S.W.T. Price, A.E. Russell, T. Sonmez, S.J. Thompson, Comparison of the Spinels Co_3O_4 and $NiCo_2O_4$ as Bifunctional Oxygen Catalysts in Alkaline Media, Electrochim. Acta, 188 (2016) 286-293.

[96] G.P. Kim, H.H. Sun, A. Manthiram, Design of a sectionalized MnO_2-Co_3O_4 electrode via selective electrodeposition of metal ions in hydrogel for enhanced electrocatalytic activity in metal-air batteries, Nano Energy, 30 (2016) 130-137.

[97] X. Qin, Z. Wang, J. Han, Y. Luo, F. Xie, G. Cui, X. Guo, X. Sun, Fe-doped CoP nanosheet arrays: an efficient bifunctional catalyst for zinc-air batteries, Chem. Commun., 54 (2018) 7693-7696.

[98] X.Q. Wu, F.Y. Chen, N. Zhang, A. Qaseem, R.L. Johnston, A silver-copper metallic glass electrocatalyst with high activity and stability comparable to Pt/C for zinc-air batteries, J. Mater. Chem. A, 4 (2016) 3527-3537.

[99] K. Wang, P. Pei, Y. Wang, C. Liao, W. Wang, S. Huang, Advanced rechargeable zinc-air battery with parameter optimization, Appl. Energy, 225 (2018) 848-856.

[100] C. Hua, Z. Qian, M. Chen, C. Du, P. Zuo, X. Cheng, Y. Ma, G. Yin, 3D hierarchical Co/CoO/C nanocomposites with mesoporous microsheets grown on nickel foam as cathodes for Li-O_2 batteries, J. Alloys Compd., 749 (2018) 378-384.

[101] H.B. Huang, S.H. Luo, C.L. Liu, Q. Wang, Z.Y. Wang, Y.H. Zhang, A.M. Hao, Y.G. Liu, J.Z. Li, Y.C. Zhai, Y.N. Dai, Ag-decorated highly mesoporous Co_3O_4 nanosheets on nickel foam as an efficient free-standing cathode for Li-O_2 batteries, J. Alloys Compd., 726 (2017) 939-946.

[102] B. Li, J.Y. Ruan, A. Loh, J.W. Chai, Y. Chen, C.L. Tan, X.M. Ge, T.S.A. Hor, Z.L. Liu, H. Zhang, Y. Zong, A Robust Hybrid Zn-Battery with Ultralong Cycle Life, Nano Lett., 17 (2017) 156-163.

[103] S.M. Xu, Q.C. Zhu, J. Long, H.H. Wang, X.F. Xie, K.X. Wang, J.S. Chen, Low-Overpotential Li-O-2 Batteries Based on TFSI Intercalated Co-Ti Layered Double Oxides, Adv. Funct. Mater., 26 (2016) 1365-1374.

[104] Q.Y. Yu, Q.L. Yu, W. Sun, H.T. Wu, Z.H. Wang, D. Rooney, K.N. Sun, Novel Ni@Co_3O_4 Web-like Nanofiber Arrays as Highly Effective Cathodes for Rechargeable Li-O_2 Batteries, Electrochim. Acta, 220 (2016) 654-663.

[105] W.B. Luo, X.W. Gao, D.Q. Shi, S.L. Chou, J.Z. Wang, H.K. Liu, Binder-Free and Carbon-Free 3D Porous Air Electrode for Li-O_2 Batteries with High Efficiency, High Capacity, and Long Life, Small, 12 (2016) 3031-3038.

[106] M. He, P. Zhang, S. Xu, X.B. Yan, Morphology Engineering of Co_3O_4 Nanoarrays as Free-Standing Catalysts for Lithium-Oxygen Batteries, ACS Appl. Mater. Interfaces, 8 (2016) 23713-23720.

[107] T. Cetinkaya, H. Akbulut, M. Tokur, S. Ozcan, M. Uysal, High capacity Graphene/α-MnO_2 nanocomposite cathodes for Li-O_2 batteries, Int. J. Hydrogen Energy, 41 (2016) 9746-9754.

[108] M. Bockelmann, U. Kunz, T. Turek, Electrically rechargeable zinc-oxygen flow battery with high power density, Electrochem. Commun., 69 (2016) 24-27.

[109] Z.H. Yue, W.X. Zhu, Y.Z. Li, Z.Y. Wei, N. Hu, Y.R. Suo, J.L. Wang, Surface Engineering of a Nickel Oxide-Nickel Hybrid Nanoarray as a Versatile Catalyst for Both Superior Water and Urea Oxidation, Inorg. Chem., 57 (2018) 4693-4698.

[110] C.Z. Shu, Y.H. Liu, J.P. Long, X.F. Chen, Y. Su, 3D Array of Bi_2S_3 Nanorods Supported on Ni Foam as a Highly Efficient Integrated Oxygen Electrode for the Lithium-Oxygen Battery, Part. Part. Syst. Charact., 35 (2018) 1700433.

[111] Z. Yan, E.D. Wang, J.X. Gao, J.P. Yang, C.C. Wu, L.H. Jiang, M.Y. Zhu, G.Q. Sun, An Exceptionally Facile Synthesis of Highly Efficient Oxygen Evolution Electrodes for Zinc-Oxygen Batteries, Chemelectrochem, 4 (2017) 2190-2195.

[112] W. Sun, Y. Wang, H.T. Wu, Z.H. Wang, D. Rooney, K.N. Sun, 3D free-standing hierarchical $CuCo_2O_4$ nanowire cathodes for rechargeable lithium-oxygen batteries, Chem. Commun., 53 (2017) 8711-8714.

[113] Y.B. Ren, S.C. Zhang, H.L. Li, X. Wei, Y.L. Xing, Mesoporous Pd/Co_3O_4 nanosheets nanoarrays as an efficient binder/carbon free cathode for rechargeable Li-O_2 batteries, Appl. Surf. Sci., 420 (2017) 222-232.

[114] Z.Q. Liu, N.N. Feng, Z.H. Shen, F.J. Li, P. He, H.G. Zhang, H.S. Zhou, Carbon-Free O_2 Cathode with Three-Dimensional Ultralight Nickel Foam-Supported Ruthenium Electrocatalysts for Li-O_2 Batteries, Chemsuschem, 10 (2017) 2714-2719.

[115] T.V. Pham, H.P. Guo, W.B. Luo, S.L. Chou, J.Z. Wang, H.K. Liu, Carbon- and binder-free 3D porous perovskite oxide air electrode for rechargeable lithium-oxygen batteries, J. Mater. Chem. A, 5 (2017) 5283-5289.

[116] Y.Z. Sun, C.X. Liu, L.Y. Zhang, P.Y. Wan, S.X. Zhuang, Y. Tang, Y.M. Chen, J.Q. Pan, Ultrafast Electrodeposition of Ni-Fe Hydroxide Nanosheets on Nickel Foam as Oxygen Evolution Anode for Energy-Saving Electrolysis of Na_2CO_3/ $NaHCO_3$, Chemelectrochem, 4 (2017) 1044-1050.

[117] H. Wang, Y. Min, P. Li, J. Yang, J. Li, In situ integration of ultrathin PtRuCu alloy overlayer on copper foam as an advanced free-standing bifunctional cathode for rechargeable Zn-air batteries, Electrochim. Acta, 283 (2018) 54-62.

[118] P. Titscher, J.C. Riede, J. Wiedemann, U. Kunz, A. Kwade, Multiscale Structured Particle-Based Zinc Anodes in Non-Stirred Alkaline Systems for Zinc-Air Batteries, Energy Technol., 6 (2018) 773-780.

[119] D. Giacco, A.G. Marrani, S. Brutti, Enhancement of the performance in Li-O_2 cells of a $NiCo_2O_4$ based porous positive electrode by Cr(III) doping, Mater. Lett., 224 (2018) 113-117.

[120] A.A. Uludag, M. Tokur, H. Algul, T. Cetinkaya, M. Uysal, H. Akbulut, High stable Li-air battery cells by using PEO and PVDF additives in the TEGDME/$LiPF_6$ electrolytes, Int. J. Hydrogen Energy, 41 (2016) 6954-6964.

[121] H. Kim, Y.J. Gong, J. Yoo, Y.S. Kim, Highly stable lithium metal battery with an applied three-dimensional mesh structure interlayer, J. Mater. Chem. A, 6 (2018) 15540-15545.

[122] K.H. Kwak, D.W. Kim, Y. Kang, J. Suk, Hierarchical Ru- and RuO_2-foams as high performance electrocatalysts for rechargeable lithium-oxygen batteries, J. Mater. Chem. A, 4 (2016) 16356-16367.

[123] K.R. Yoon, K. Shin, J. Park, S.H. Cho, C. Kim, J.W. Jung, J.Y. Cheong, H.R. Byon, H.M. Lee, I.D. Kim, Brush-Like Cobalt Nitride Anchored Carbon Nanofiber Membrane: Current Collector Catalyst Integrated Cathode for Long Cycle Li-O_2 Batteries, Acs Nano, 12 (2018) 128-139.

[124] S. Suren, S. Kheawhom, Development of a High Energy Density Flexible Zinc-Air Battery, J. Electrochem. Soc., 163 (2016) A846-A850.

[125] S. Zeng, H.Y. Chen, H. Wang, X. Tong, M.H. Chen, J.T. Di, Q.W. Li, Crosslinked Carbon Nanotube Aerogel Films Decorated with Cobalt Oxides for Flexible Rechargeable Zn-Air Batteries, Small, 13 (2017) 1700518.

[126] G.R. Sun, Q. Zhao, T. Wu, W. Lu, M. Bao, L.Q. Sun, H.M. Xie, J. Liu, 3D Foam-Like Composites of Mo2C Nanorods Coated by N-Doped Carbon: A Novel Self-Standing and Binder-Free O_2 Electrode for Li-O_2 Batteries, ACS Appl. Mater. Interfaces, 10 (2018) 6327-6335.

[127] H.Y. Song, S.M. Xu, Y.J. Li, J.Q. Dai, A. Gong, M.W. Zhu, C.L. Zhu, C.J. Chen, Y.A. Chen, Y.G. Yao, B.Y. Liu, J.W. Song, G. Pastel, L.B. Hu, Hierarchically Porous, Ultrathick, "Breathable" Wood-Derived Cathode for Lithium-Oxygen Batteries, Adv. Energy Mater., 8 (2018) 1701203.

[128] J. Gao, J. Zou, X. Zeng, W. Ding, Carbon supported nano Pt-Mo alloy catalysts for oxygen reduction in magnesium-air batteries, Rsc Adv., 6 (2016) 83025-83030.

[129] C. Shu, E. Wang, L. Jiang, G. Sun, High performance cathode based on carbon fiber felt for magnesium-air fuel cells, Int. J. Hydrogen Energy, 38 (2013) 5885-5893.

[130] Y. Li, X. Zhang, H.-B. Li, H.D. Yoo, X. Chi, Q. An, J. Liu, M. Yu, W. Wang, Y. Yao, Mixed-phase mullite electrocatalyst for pH-neutral oxygen reduction in magnesium-air batteries, Nano Energy, 27 (2016) 8-16.

[131] D.F. Yan, Y.X. Li, J. Huo, R. Chen, L.M. Dai, S.Y. Wang, Defect Chemistry of Nonprecious-Metal Electrocatalysts for Oxygen Reactions, Adv. Mater., 29 (2017) 1606459.

[132] Z.F. Huang, J. Wang, Y.C. Peng, C.Y. Jung, A. Fisher, X. Wang, Design of Efficient Bifunctional Oxygen Reduction/Evolution Electrocatalyst: Recent Advances and Perspectives, Adv. Energy Mater., 7 (2017) 1700544.

[133] C.G. Hu, L.M. Dai, Carbon-Based Metal-Free Catalysts for Electrocatalysis beyond the ORR, Angew. Chem. Int. Ed., 55 (2016) 11736-11758.

[134] M. Zhu, H. Ge, X. Xu, Q. Wang, Investigation on the variation law of gas liquid solid three phase boundary in porous gas diffusion electrode, Heliyon, 4 (2018) e00729.

[135] R. Subbaraman, D. Strmcnik, V. Stamenkovic, N.M. Markovic, Three Phase Interfaces at Electrified Metal-Solid Electrolyte Systems 1. Study of the Pt(hkl)-Nafion Interface, J. Phys. Chem. C, 114 (2010) 8414-8422.

[136] H. Fukunaga, M. Ihara, K. Sakaki, K. Yamada, The relationship between overpotential and the three phase boundary length, Solid State Ionics, 86-8 (1996) 1179-1185.

[137] C. Zhao, M. Yu, Z. Yang, J. Liu, S. Chen, Z. Hong, H. Chen, W. Wang, Oxygen reduction reaction catalytic activity enhancement over mullite $SmMn_2O_5$ via interfacing with perovskite oxides, Nano Energy, 51 (2018) 91-101.

[138] S. Kukunuri, K. Naik, S. Sampath, Effects of composition and nanostructuring of palladium selenide phases, Pd4Se, Pd_7Se_4 and $Pd_{17}Se_{15}$, on ORR activity and their use in Mg-air batteries, J. Mater. Chem. A, 5 (2017) 4660-4670.

[139] M. Balaish, Y. Ein-Eli, Meso-pores carbon nano-tubes (CNTs) tissues-perfluorocarbons (PFCs) hybrid air-electrodes for Li-O_2 battery, J. Power Sources, 379 (2018) 219-227.

[140] E. Davari, D.G. Ivey, Bifunctional electrocatalysts for Zn-air batteries, Sustainable Energy Fuels, 2 (2018) 39-67.

[141] Q. Ren, H. Wang, X.F. Lu, Y.X. Tong, G.R. Li, Recent Progress on MOF-Derived Heteroatom-Doped Carbon-Based Electrocatalysts for Oxygen Reduction Reaction, Adv. Sci., 5 (2018) 1700515.

[142] D. Xiong, X. Li, L. Fan, Z. Bai, Three-Dimensional Heteroatom-Doped Nanocarbon for Metal-Free Oxygen Reduction Electrocatalysis: A Review, Catalysts, 8 (2018) 301.

[143] F. Cheng, J. Chen, Metal-air batteries: from oxygen reduction electrochemistry to cathode catalysts, Chem. Soc. Rev., 41 (2012) 2172-2192.

[144] Y.J. Wang, H. Fan, A. Ignaszak, L. Zhang, S. Shao, D.P. Wilkinson, J. Zhang, Compositing doped-carbon with metals, non-metals, metal oxides, metal nitrides and other materials to form bifunctional electrocatalysts to enhance metal-air battery oxygen reduction and evolution reactions, Chem. Eng. J., 348 (2018) 416-437.

[145] T. Asefa, X.X. Huang, Heteroatom-Doped Carbon Materials for Electrocatalysis, Chem. Eur. J., 23 (2017) 10703-10713.

[146] X.B. He, F.X. Yin, H. Wang, B.H. Chen, G.R. Li, Metal-organic frameworks for highly efficient oxygen electrocatalysis, Chinese J. Catal., 39 (2018) 207-227.

[147] D. Higgins, P. Zamani, A.P. Yu, Z.W. Chen, The application of graphene and its composites in oxygen reduction electrocatalysis: a perspective and review of recent progress, Energy Environ. Sci., 9 (2016) 357-390.

[148] Q.S. Hong, H.M. Lu, In-situ Electrodeposition of Highly Active Silver Catalyst on Carbon Fiber Papers as Binder Free Cathodes for Aluminum-air Battery, Sci. Rep., 7 (2017) 3378.

[149] M. Wu, Y. Wang, Z. Wei, L. Wang, M. Zhuo, J. Zhang, X. Han, J. Ma, Ternary doped porous carbon nanofibers with excellent ORR and OER performance for zinc-air batteries dagger, J. Mater. Chem. A, 6 (2018) 10918-10925.

[150] J. Guo, B. Ghen, Q. Hao, J. Nie, G. Ma, Pod-like structured Co/CoO_x nitrogen-doped carbon fibers as efficient oxygen reduction reaction electrocatalysts for Zn-air battery, Appl. Surf. Sci., 456 (2018) 959-966.

[151] Y.G. Cheng, D.M. Li, L. Shi, Z.H. Xiang, Efficient unitary oxygen electrode for air-based flow batteries, Nano Energy, 47 (2018) 361-367.

[152] W.L. Li, Y. Yao, F. Wu, C.Z. Zhang, Applications of Carbon Fiber Ultra-microelectrode and Powder Microelectrode in Exploring Influences of Non-aqueous Solvents and Cathode Materials on ORR and OER, Chem. J. Chinese U., 38 (2017) 642-652.

[153] Y.B. Yin, J.J. Xu, Q.C. Liu, X.B. Zhang, Macroporous Interconnected Hollow Carbon Nanofibers Inspired by Golden-Toad Eggs toward a Binder-Free, High-Rate, and Flexible Electrode, Adv. Mater., 28 (2016) 7494-7500.

[154] S.J. Hu, X.P. Fan, J. Chen, J.M. Peng, H.Q. Wang, Y.G. Huang, Q.Y. Li, Carbon Nanotubes/Carbon Fiber Paper Supported MnO_2 Cathode Catalyst for Li-Air Batteries, Chemelectrochem, 4 (2017) 2997-3003.

[155] Y. Fu, H.Y. Yu, C. Jiang, T.H. Zhang, R. Zhan, X.W. Li, J.F. Li, J.H. Tian, R.Z. Yang, NiCo Alloy Nanoparticles Decorated on N-Doped Carbon Nanofibers as Highly Active and Durable Oxygen Electrocatalyst, Adv. Funct. Mater., 28 (2018) 1705094.

[156] B. Amunategui, A. Ibanez, M. Sierra, M. Perez, Electrochemical energy storage for renewable energy integration: zinc-air flow batteries, J. Appl. Electrochem., 48 (2018) 627-637.

[157] X. Tong, Q.L. Wei, X.X. Zhan, G.X. Zhang, S.H. Sun, The New Graphene Family Materials: Synthesis and Applications in Oxygen Reduction Reaction, Catalysts, 7 (2017) 1-26.

[158] H.J. Cui, Z. Zhou, D.Z. Jia, Heteroatom-doped graphene as electrocatalysts for air cathodes, Mater. Horiz., 4 (2017) 7-19.

[159] L.W. Ji, P. Meduri, V. Agubra, X.C. Xiao, M. Alcoutlabi, Graphene-Based Nanocomposites for Energy Storage, Adv. Energy Mater., 6 (2016) 1502159.

[160] H. Yuan, L. Kong, T. Li, Q. Zhang, A review of transition metal chalcogenide/graphene nanocomposites for energy storage and conversion, Chin. Chem. Lett., 28 (2017) 2180-2194.

[161] Z. Yan, E.D. Wang, L.H. Jiang, G.Q. Sun, Superior cycling stability and high rate capability of three-dimensional Zn/Cu foam electrodes for zinc-based alkaline batteries, Rsc Adv., 5 (2015) 83781-83787.

[162] R. Singhal, V. Kalra, Cobalt Nanoparticle-Embedded Porous Carbon Nanofibers with Inherent N- and F-Doping as Binder-Free Bifunctional Catalysts for Oxygen Reduction and Evolution Reactions, Chemphyschem, 18 (2017) 223-229.

[163] Z.X. Feng, W.T. Hong, D.D. Fong, Y.L. Lee, Y. Yacoby, D. Morgan, Y. Shao-Horn, Catalytic Activity and Stability of Oxides: The Role of Near-Surface Atomic Structures and Compositions, Acc. Chem. Res., 49 (2016) 966-973.

[164] V. Vij, S. Sultan, A.M. Harzandi, A. Meena, J.N. Tiwari, W.G. Lee, T. Yoon, K.S. Kim, Nickel-Based Electrocatalysts for Energy-Related Applications: Oxygen Reduction, Oxygen Evolution, and Hydrogen Evolution Reactions, Acs Catal., 7 (2017) 7196-7225.

[165] W.P. Xiao, W. Lei, M.X. Gong, H.L. Xin, D.L. Wang, Recent Advances of Structurally Ordered Intermetallic Nanoparticles for Electrocatalysis, Acs Catal., 8 (2018) 3237-3256.

[166] W. Xia, A. Mahmood, Z.B. Liang, R.Q. Zou, S.J. Guo, Earth-Abundant Nanomaterials for Oxygen Reduction, Angew. Chem. Int. Ed., 55 (2016) 2650-2676.

[167] Y. Liang, Y. Li, H. Wang, H. Dai, Strongly coupled inorganic/nanocarbon hybrid materials for advanced electrocatalysis, J. Am. Chem. Soc., 135 (2013) 2013-2036.

[168] N.A. Anastasijevic, V. Vesovic, R.R. Adzic, Determination of The Kinetic-parametrs of The Oxygen Reduction Reaction Using The Rotating-Ring-Disk Electrode. Part I. Theory, J. Electroanal. Chem., 229 (1987) 305-316.

[169] K. Kinoshita, Electrochemical oxygen technology, John Wiley & Sons, 1992.

[170] N. Ramaswamy, S. Mukerjee, Influence of Inner- and Outer-Sphere Electron Transfer Mechanisms during Electrocatalysis of Oxygen Reduction in Alkaline Media, J. Phys. Chem. C, 115 (2011) 18015-18026.

[171] M.T.M. Koper, Theory of multiple proton–electron transfer reactions and its implications for electrocatalysis, Chem. Sci., 4 (2013) 2710.

[172] J. Suntivich, K.J. May, H.A. Gasteiger, J.B. Goodenough, Y. Shao-Horn, A perovskite oxide optimized for oxygen evolution catalysis from molecular orbital principles, Science, 334 (2011) 1383-1385.

[173] H.B. Tao, L. Fang, J. Chen, H.B. Yang, J. Gao, J. Miao, S. Chen, B. Liu, Identification of Surface Reactivity Descriptor for Transition Metal Oxides in Oxygen Evolution Reaction, J. Am. Chem. Soc., 138 (2016) 9978-9985.

[174] M.S. Burke, L.J. Enman, A.S. Batchellor, S. Zou, S.W. Boettcher, Oxygen Evolution Reaction Electrocatalysis on Transition Metal Oxides and (Oxy)hydroxides: Activity Trends and Design Principles, Chem. Mater., 27 (2015) 7549-7558.

[175] L. Du, C.Y. Du, G.Y. Chen, F.P. Kong, G.P. Yin, Y. Wang, Metal-Organic Coordination Networks: Prussian Blue and Its Synergy with Pt Nanoparticles to Enhance Oxygen Reduction Kinetics, ACS Appl. Mater. Interfaces, 8 (2016) 15250-15257.

[176] W. Xiao, M.A.L. Cordeiro, G. Gao, A. Zheng, J. Wang, W. Lei, M. Gong, R. Lin, E. Stavitski, H.L. Xin, D. Wang, Atomic rearrangement from disordered to ordered Pd-Fe nanocatalysts with trace amount of Pt decoration for efficient electrocatalysis, Nano Energy, 50 (2018) 70-78.

[177] R. Illathvalappil, V.M. Dhavale, S.N. Bhange, S. Kurungot, Nitrogen-doped graphene anchored with mixed growth patterns of CuPt alloy nanoparticles as a highly efficient and durable electrocatalyst for the oxygen reduction reaction in an alkaline medium, Nanoscale, 9 (2017) 9009-9017.

[178] J. Gao, J.X. Zou, X.Q. Zeng, W.J. Ding, Carbon supported nano Pt-Mo alloy catalysts for oxygen reduction in magnesium-air batteries, Rsc Adv., 6 (2016) 83025-83030.

[179] Y.J. Xue, S.S. Sun, Q. Wang, H. Miao, S.H. Li, Z.P. Liu, $La_{0.7}(Sr_{0.3-x}Pd_x)MnO_3$ as a highly efficient electrocatalyst for oxygen reduction reaction in aluminum air battery, Electrochim. Acta, 230 (2017) 418-427.

[180] W.P. Xiao, M.A.L. Cordeiro, M.X. Gong, L.L. Han, J. Wang, C. Bian, J. Zhu, H.L. Xin, D.L. Wang, Optimizing the ORR activity of Pd based nanocatalysts by tuning their strain and particle size, J. Mater. Chem. A, 5 (2017) 9867-9872.

[181] Z.W. Zhang, H.N. Li, J. Hu, B.Z. Liu, Q.R. Zhang, C. Fernandez, Q.M. Peng, High oxygen reduction reaction activity of C-N/Ag hybrid composites for Zn-air battery, J. Alloys Compd., 694 (2017) 419-428.

[182] N. Li, C. Wang, T. Li, B. Latimer, Z. Liu, Z. Tang, Au@Ag Core-shell Nanoparticles Supported on Carbon Nanotubes as Promising Catalysts for Oxygen Electroreduction, Int. J. Electrochem. Sci., 13 (2018) 6756-6770.

[183] N. Zhang, F.Y. Chen, X.Q. Wu, Q. Wang, A. Qaseem, Z.H. Xia, The activity origin of core-shell and alloy AgCu bimetallic nanoparticles for the oxygen reduction reaction, J. Mater. Chem. A, 5 (2017) 7043-7054.

[184] X.Q. Wu, F.Y. Chen, N. Zhang, A. Qaseem, R.L. Johnston, Engineering Bimetallic Ag-Cu Nanoalloys for Highly Efficient Oxygen Reduction Catalysts: A Guideline for Designing Ag-Based Electrocatalysts with Activity Comparable to Pt/C-20%, Small, 13 (2017) 1603876.

[185] Q.S. Hong, H.M. Lu, J.R. Wang, Self-Reduction Synthesis of Silver Nanoparticles/Carbon Fiber Paper Air Cathodes for Improving Al-Air Battery Performance, J. Electrochem. Soc., 164 (2017) A1425-A1430.

[186] S. Hu, T. Han, C. Lin, W.K. Xiang, Y.H. Zhao, P. Gao, F.P. Du, X.P. Li, Y.H. Sun, Enhanced Electrocatalysis via 3D Graphene Aerogel Engineered with a Silver Nanowire Network for Ultrahigh-Rate Zinc-Air Batteries, Adv. Funct. Mater., 27 (2017) 1700041.

[187] D. Ji, Y. Wang, S. Chen, Y. Zhang, L. Li, W. Ding, Z. Wei, Nitrogen-doped graphene wrapped around silver nanowires for enhanced catalysis in oxygen reduction reaction, J. Solid State Electrochem., 22 (2018) 2287-2296.

[188] S.H. Li, H. Miao, Q. Xu, Y.J. Xue, S.S. Sun, Q. Wang, Z.P. Liu, Silver nanoparticles supported on a nitrogen-doped graphene aerogel composite catalyst for an oxygen reduction reaction in aluminum air batteries, Rsc Adv., 6 (2016) 99179-99183.

[189] J. Ryu, H. Jang, J. Park, Y. Yoo, M. Park, J. Cho, Seed-mediated atomic-scale reconstruction of silver manganate nanoplates for oxygen reduction towards high-energy aluminum-air flow batteries, Nat. Commun., 9 (2018) 3715.

[190] S.S. Sun, H. Miao, Y.J. Xue, Q. Wang, S.H. Li, Z.P. Liu, Oxygen reduction reaction catalysts of manganese oxide decorated by silver nanoparticles for aluminum-air batteries, Electrochim. Acta, 214 (2016) 49-55.

[191] S.S. Sun, H. Miao, Y.J. Xue, Q. Wang, Q.H. Zhang, Z.H. Dong, S.H. Li, H.R. Huang, Z.P. Liu, High Electrocatalytic Activity of Silver-Doped Manganese Dioxide toward Oxygen Reduction Reaction in Aluminum-Air Battery, J. Electrochem. Soc., 164 (2017) F768-F774.

[192] S.S. Sun, Y.J. Xue, Q. Wang, S.H. Li, H.R. Huang, H. Miao, Z.P. Liu, Electrocatalytic activity of silver decorated ceria microspheres for the oxygen reduction reaction and their application in aluminium-air batteries, Chem. Commun., 53 (2017) 7921-7924.

[193] Y.Z. Sun, M. Yang, J.Q. Pan, P.Y. Wang, W. Li, P.Y. Wan, Manganese dioxide-supported silver bismuthate as an efficient electrocatalyst for oxygen reduction reaction in zinc-oxygen batteries, Electrochim. Acta, 197 (2016) 68-76.

[194] X.Q. Wu, F.Y. Chen, N. Zhang, Y.M. Lei, Y.C. Jin, A. Qaseem, R.L. Johnston, Activity Trends of Binary Silver Alloy Nanocatalysts for Oxygen Reduction Reaction in Alkaline Media, Small, 13 (2017) 1603387.

[195] Y.Q. Zhang, H.B. Tao, J. Liu, Y.F. Sun, J. Chen, B. Hua, T. Thundat, J.L. Luo, A rational design for enhanced oxygen reduction: Strongly coupled silver nanoparticles and engineered perovskite nanofibers, Nano Energy, 38 (2017) 392-400.

[196] Q.M. Wu, L.H. Jiang, L.T. Qi, L.Z. Yuan, E.D. Wang, G.Q. Sun, Electrocatalytic activity and stability of Ag-MnO_x/C composites toward oxygen reduction reaction in alkaline solution, Electrochim. Acta, 123 (2014) 167-175.

[197] L.Z. Yuan, L.H. Jiang, J. Liu, Z.X. Xia, S.L. Wang, G.Q. Sun, Facile synthesis of silver nanoparticles supported on three dimensional graphene oxide/carbon black composite and its application for oxygen reduction reaction, Electrochim. Acta, 135 (2014) 168-174.

[198] D.M. Chen, P.Y. Wang, X. Zeng, Y.Z. Sun, B.X. Zhu, J.Q. Pan, Preparation of Nano-$Ag_4Bi_2O_5$ with Co-precipitation Method and Study of Its Application for Oxygen Reduction Reaction, Int. J. Electrochem. Sci., 11 (2016) 10581-10591.

[199] M. Jiang, H. He, W.J. Yi, W. Huang, X. Pan, M.Y. Wang, Z.S. Chao, ZIF-67 derived Ag-Co_3O_4@N-doped carbon/carbon nanotubes composite and its application in Mg-air fuel cell, Electrochem. Commun., 77 (2017) 5-9.

[200] Y.J. Xue, H. Miao, S.S. Sun, Q. Wang, S.H. Li, Z.P. Liu, $La_{1-x}Ag_xMnO_3$ electrocatalyst with high catalytic activity for oxygen reduction reaction in aluminium air batteries, Rsc Adv., 7 (2017) 5214-5221.

[201] L.Z. Yuan, L.H. Jiang, T.R. Zhang, G.X. Wang, S.L. Wang, X.H. Bao, G. Sun, Electrochemically synthesized freestanding 3D nanoporous silver electrode with high electrocatalytic activity, Catal. Sci. Technol., 6 (2016) 7163-7171.

[202] X.Y. Cai, L.F. Lai, J.Y. Lin, Z.X. Shen, Recent advances in air electrodes for Zn-air batteries: electrocatalysis and structural design, Mater. Horiz., 4 (2017) 945-976.

[203] X.Y. Cai, L.F. Lai, J.Y. Lin, Z.X. Shen, Recent advances in air electrodes for Zn-air batteries: electrocatalysis and structural design, Mater. Horiz., 5 (2018) 577.

[204] R. Cao, J.S. Lee, M.L. Liu, J. Cho, Recent Progress in Non-Precious Catalysts for Metal-Air Batteries, Adv. Energy Mater., 2 (2012) 816-829.

[205] M.J. Chen, L. Wang, H.P. Yang, S. Zhao, H. Xu, G. Wu, Nanocarbon/oxide composite catalysts for bifunctional oxygen reduction and evolution in reversible alkaline fuel cells: A mini review, J. Power Sources, 375 (2018) 277-290.

[206] G. Li, M.A. Mezaal, R. Zhang, K. Zhang, L. Lei, Electrochemical Performance of MnO_2-based Air Cathodes for Zinc-air Batteries, Fuel Cells, 16 (2016) 395-400.

[207] P.C. Li, C.C. Hu, T.C. Lee, W.S. Chang, T.H. Wang, Synthesis and characterization of carbon black/manganese oxide air cathodes for zinc-air batteries, J. Power Sources, 269 (2014) 88-97.

[208] A.L. Loh, K. Xu, X.H. Li, B.G. Wang, Influence of synthesis parameters on amorphous manganese dioxide catalyst electrocatalytic performance, Electrochim. Acta, 245 (2017) 615-624.

[209] S.S. Sun, Y.J. Xue, Q. Wang, H.R. Huang, H. Miao, Z.P. Liu, Cerium ion intercalated MnO_2 nanospheres with high catalytic activity toward oxygen reduction reaction for aluminum-air batteries, Electrochim. Acta, 263 (2018) 544-554.

[210] L. Kuai, E.J. Kan, W. Cao, M. Huttula, S. Ollikkala, T. Ahopelto, A.P. Honkanen, S. Huotari, W.H. Wang, B.Y. Geng, Mesoporous $LaMnO_{3+\delta}$ perovskite from spray-pyrolysis with superior performance for oxygen reduction reaction and Zn-air battery, Nano Energy, 43 (2018) 81-90.

[211] K. Liu, X.B. Huang, H.Y. Wang, F.Z. Li, Y.G. Tang, J.S. Li, M.H. Shao, Co_3O_4-CeO_2/C as a Highly Active Electrocatalyst for Oxygen Reduction Reaction in Al-Air Batteries, ACS Appl. Mater. Interfaces, 8 (2016) 34422-34430.

[212] F. Xiang, X. Chen, J. Yu, W. Ma, Y. Li, N. Yang, Synthesis of three-dimensionally ordered porous perovskite type $LaMnO_3$ for Al-air battery, J. Mater. Sci. Technol., 34 (2018) 1532-1537.

[213] Y.J. Xue, H.R. Huang, H. Miao, S.S. Sun, Q. Wang, S.H. Li, Z.P. Liu, One-pot synthesis of $La_{0.7}Sr_{0.3}MnO_3$ supported on flower-like CeO_2 as electrocatalyst for oxygen reduction reaction in aluminum-air batteries, J. Power Sources, 358 (2017) 50-60.

[214] Y.J. Xue, H.R. Huang, H. Miao, S.S. Sun, Q. Wang, S.H. Li, Z.P. Liu, Electrostatic Self-Assembly of the Composite $La_{0.7}Sr_{0.3}MnO_3$@$Ce_{0.75}Zr_{0.25}O_2$ as Electrocatalyst for the Oxygen Reduction Reaction in Aluminum-Air Batteries, Energy Technol., 5 (2017) 2226-2233.

[215] Y.J. Xue, H. Miao, B.H. Li, S.S. Sun, Q. Wang, S.H. Li, L. Chen, Z.P. Liu, Promoting effects of $Ce_{0.75}Zr_{0.25}O_2$ on the $La_{0.7}Sr_{0.3}MnO_3$ electrocatalyst for the oxygen reduction reaction in metal-air batteries, J. Mater. Chem. A, 5 (2017) 6411-6415.

[216] Y.J. Xue, H. Miao, S.S. Sun, Q. Wang, S.H. Li, Z.P. Liu, $(La_{1-x}Sr_x)_{0.98}MnO_3$ perovskite with A-site deficiencies toward oxygen reduction reaction in aluminum-air batteries, J. Power Sources, 342 (2017) 192-201.

[217] Z. Huang, X. Qin, X. Gu, G. Li, Y. Mu, N. Wang, K. Ithisuphalap, H. Wang, Z. Guo, Z. Shi, G. Wu, M. Shao, Mn3O4 Quantum Dots Supported on Nitrogen-Doped Partially Exfoliated Multiwall Carbon Nanotubes as Oxygen Reduction Electrocatalysts for High-Performance Zn-Air Batteries, ACS Appl. Mater. Interfaces, 10 (2018) 23900-23909.

[218] Q. Xue, Z.X. Pei, Y. Huang, M.S. Zhu, Z.J. Tang, H.F. Li, Y. Huang, N. Li, H.Y. Zhang, C.Y. Zhi, Mn3O4 nanoparticles on layer-structured Ti_3C_2 MXene towards the oxygen reduction reaction and zinc-air batteries, J. Mater. Chem. A, 5 (2017) 20818-20823.

[219] Y. Zhou, S.N. Sun, S.B. Xi, Y. Duan, T. Sritharan, Y.H. Du, Z.C.J. Xu, Superexchange Effects on Oxygen Reduction Activity of Edge-Sharing $Co_xMn_{1-x}O_6$ Octahedra in Spinel Oxide, Adv. Mater., 30 (2018).

[220] Z.T. Li, W.N. Zhao, C.Z. Yin, L.Q. Wei, W.T. Wu, Z.P. Hu, M.B. Wu, Synergistic Effects between Doped Nitrogen and Phosphorus in Metal-Free Cathode for Zinc-Air Battery from Covalent Organic Frameworks Coated CNT, ACS Appl. Mater. Interfaces, 9 (2017) 44519-44528.

[221] Y. Wang, H.Y. Liu, K. Wang, S.Q. Song, P. Tsiakaras, 3D interconnected hierarchically porous N-doped carbon with NH_3 activation for efficient oxygen reduction reaction, Appl. Catal. B Environ., 210 (2017) 57-66.

[222] M. Zhang, M.M. Zhang, Y.S. Wei, X.Y. Dong, S.Q. Zang, Facile Synthesis of a Heteroatoms' Quaternary-Doped Porous Carbon as an Efficient and Stable Metal-Free Catalyst for Oxygen Reduction, Chemistryselect, 2 (2017) 6129-6134.

[223] M.R. Wang, X.K. Lei, L.T. Hu, P. Zhang, H.X. Hu, J. Fang, High-performance Waste Biomass-derived Microporous Carbon Electrocatalyst with a Towel-like Surface for Alkaline Metal/air batteries, Electrochim. Acta, 250 (2017) 384-392.

[224] W. Yuan, A. Xie, P. Chen, F. Huang, S. Li, Y. Shen, Combustion reaction-derived nitrogen-doped porous carbon as an effective metal-Free catalyst for the oxygen reduction reaction, Energy, 152 (2018) 333-340.

[225] L. Qin, L.C. Wang, X. Yang, R.M. Ding, Z.F. Zheng, X.H. Chen, B.L. Lv, Synergistic enhancement of oxygen reduction reaction with BC3 and graphitic-N in boron- and nitrogen-codoped porous graphene, J. Catal., 359 (2018) 242-250.

[226] L.W. Zhu, J. Wu, Q. Zhang, X.K. Li, Y.M. Li, X.B. Cao, Chemical-free fabrication of N, P dual-doped honeycomb-like carbon as an efficient electrocatalyst for oxygen reduction, J. Colloid Interface Sci., 510 (2018) 32-38.

[227] X.K. Lei, M.R. Wang, Y.Q. Lai, L.T. Hu, H. Wang, Z. Fang, J. Li, J. Fang, Nitrogen-doped micropore-dominant carbon derived from waste pine cone as a promising metal-free electrocatalyst for aqueous zinc/air batteries, J. Power Sources, 365 (2017) 76-82.

[228] L.Y. Zhang, M.R. Wang, Y.Q. Lai, X.Y. Li, Nitrogen-doped microporous carbon: An efficient oxygen reduction catalyst for Zn-air batteries, J. Power Sources, 359 (2017) 71-79.

[229] L. Yu, Q. Yi, G. Li, Y. Chen, X. Yang, FeCo-Doped Hollow Bamboo-Like C-N Composites as Cathodic Catalysts for Zinc-Air Battery in Neutral Media, J. Electrochem. Soc., 165 (2018) A2502-A2509.

[230] G.M. Jiang, B. Peng, Waste cotton-derived N-doped carbon as a sustainable metal-free electrocatalyst for oxygen reduction, Mater. Lett., 188 (2017) 33-36.

[231] Y.H. Qian, T. An, K.E. Birgersson, Z.L. Liu, D. Zhao, Web-Like Interconnected Carbon Networks from NaCl-Assisted Pyrolysis of ZIF-8 for Highly Efficient Oxygen Reduction Catalysis, Small, 14 (2018) 1704169.

[232] H. Yadegari, X. Sun, Recent Advances on Sodium-Oxygen Batteries: A Chemical Perspective, Acc. Chem. Res., 51 (2018) 1532-1540.

[233] X. Han, X. Li, J. White, C. Zhong, Y. Deng, W. Hu, T. Ma, Metal-Air Batteries: From Static to Flow System, Adv. Energy Mater., 8 (2018) 1801396.

[234] X. Li, S. Zheng, L. Jin, Y. Li, P. Geng, H. Xue, H. Pang, Q. Xu, Metal-Organic Framework-Derived Carbons for Battery Applications, Adv. Energy Mater., 8 (2018) 1800716.

[235] B. Yao, J. Zhang, T.Y. Kou, Y. Song, T.Y. Liu, Y. Li, Paper-Based Electrodes for Flexible Energy Storage Devices, Adv. Sci., 4 (2017) 1700107.

[236] Z. Wang, D. Cheng, C. Chen, K. Zhou, Hierarchically porous carbon microspheres with fully open and interconnected super-macropores for air cathodes of Zn-Air batteries, Carbon, 136 (2018) 54-62.

[237] G.X. Zhang, Q.L. Wei, X.H. Yang, A.C. Tavares, S.H. Sun, RRDE experiments on noble-metal and noble-metal-free catalysts: Impact of loading on the activity and selectivity of oxygen reduction reaction in alkaline solution, Appl. Catal. B Environ., 206 (2017) 115-126.

[238] J.J. Xu, B. Li, S.M. Li, J.H. Liu, From melamine sponge towards 3D sulfur-doping carbon nitride as metal-free electrocatalysts for oxygen reduction reaction, Mater. Res. Express, 4 (2017) 076305.

[239] J. Zhang, Y. Sun, J. Zhu, Z. Kou, P. Hu, L. Liu, S. Li, S. Mu, Y. Huang, Defect and pyridinic nitrogen engineering of carbon-based metal-free nanomaterial toward oxygen reduction, Nano Energy, 52 (2018) 307-314.

[240] Y.X. Zhao, Q.X. Lai, Y. Wang, J.J. Zhu, Y.Y. Liang, Interconnected Hierarchically Porous Fe, N-Codoped Carbon Nanofibers as Efficient Oxygen Reduction Catalysts for Zn-Air Batteries, ACS Appl. Mater. Interfaces, 9 (2017) 16178-16186.

[241] K. Yuan, S. Sfaelou, M. Qiu, D. Lutzenkirchen-Hecht, X.D. Zhuang, Y.W. Chen, C. Yuan, X.L. Feng, U. Scherft, Synergetic Contribution of Boron and Fe-N_x Species in Porous Carbons toward Efficient Electrocatalysts for Oxygen Reduction Reaction, ACS Energy Lett., 3 (2018) 252-260.

[242] J.X. Xu, C.X. Wu, Q.M. Yu, Y. Zhao, X. Li, L.H. Guan, Ammonia Defective Etching and Nitrogen-Doping of Porous Carbon toward High Exposure of Heme-Derived Fe-N_x Site for Efficient Oxygen Reduction, Acs Sustainable Chem. Eng., 6 (2018) 551-560.

[243] C. Cheng, S. Li, Y. Xia, L. Ma, C. Nie, C. Roth, A. Thomas, R. Haag, Atomic Fe-Nx Coupled Open-Mesoporous Carbon Nanofibers for Efficient and Bioadaptable Oxygen Electrode in Mg-Air Batteries, Adv. Mater., (2018) e1802669.

[244] G. Anandhababu, S.C. Abbas, J.Q. Lv, K. Ding, Q. Liu, D.D. Babu, Y.Y. Huang, J.F. Xie, M.X. Wu, Y.B. Wang, Highly exposed Fe-N4 active sites in porous poly-iron-phthalocyanine based oxygen reduction electrocatalyst with ultrahigh performance for air cathode, Dalton Trans., 46 (2017) 1803-1810.

[245] X. Zhang, R.R. Liu, Y.P. Zang, G.Q. Liu, S.W. Liu, G.Z. Wang, Y.X. Zhang, H.M. Zhang, H.J. Zhao, Shrimp-shell derived carbon nanodots as precursors to fabricate Fe,N-doped porous graphitic carbon electrocatalysts for efficient oxygen reduction in zinc-air batteries, Inorg. Chem. Front., 3 (2016) 910-918.

[246] Y.Q. Lai, Q.Y. Wang, M.R. Wang, J. Li, J. Fang, Z.A. Zhang, Facile synthesis of mesoporous Fe-N-C electrocatalyst for high performance alkaline aluminum-air battery, J. Electroanal. Chem., 801 (2017) 72-76.

[247] X. Deng, M.L. Xiao, R.O. Yang, F. Guo, H.Q. Chen, Y. Hu, Y. Li, C.C. Zhu, Y.P. Deng, Z. Jiang, Z. Xu, C. Gao, Q.G. He, J.J. Ge, Y. Hou, X.W. Zhang, Z.W. Chen, The Effect of CNTs on Performance Improvement of rGO Supported Fe-N_x/C Electrocatalysts for the Oxygen Reduction Reaction, J. Electrochem. Soc., 165 (2018) F401-F407.

[248] J.M. Ang, Y.H. Du, B.Y. Tay, C.Y. Zhao, J.H. Kong, L.P. Stubbs, X.H. Lu, One-Pot Synthesis of Fe(III)-Polydopamine Complex Nanospheres: Morphological Evolution, Mechanism, and Application of the Carbonized Hybrid Nanospheres in Catalysis and Zn-Air Battery, Langmuir, 32 (2016) 9265-9275.

[249] M.J. Wu, Q.W. Tang, F. Dong, Y.Z. Wang, D.H. Li, Q.P. Guo, Y.Y. Liu, J.L. Qiao, The design of Fe, N-doped hierarchically porous carbons as highly active and durable electrocatalysts for a Zn-air battery, Phys. Chem. Chem. Phys., 18 (2016) 18665-18669.

[250] Z.K. Yang, L. Lin, A.W. Xu, 2D Nanoporous Fe-N/C Nanosheets as Highly Efficient Non-Platinum Electrocatalysts for Oxygen Reduction Reaction in Zn-Air Battery, Small, 12 (2016) 5710-5719.

[251] H. Liu, M.Q. Wang, Z.Y. Chen, H. Chen, M.W. Xu, S.J. Bao, Design and synthesis of Co-N-C porous catalyst derived from metal organic complexes for highly effective ORR, Dalton Trans., 46 (2017) 15646-15650.

[252] K. Fu, Y. Wang, L. Mao, X. Yang, J. Jin, S. Yang, G. Li, Strongly coupled Co, N co-doped carbon nanotubes/graphene-like carbon nanosheets as efficient oxygen reduction electrocatalysts for primary Zinc-air battery, Chem. Eng. J., 351 (2018) 94-102.

[253] Y. Zhou, Q.Q. Cheng, Q.H. Huang, Z.Q. Zou, L.M. Yan, H. Yang, Highly Dispersed Cobalt-Nitrogen Co-doped Carbon Nanofiber as Oxygen Reduction Reaction Catalyst, Acta Phys. Chim. Sin., 33 (2017) 1429-1435.

[254] J.C. Li, X.T. Wu, L.J. Chen, N. Li, Z.Q. Liu, Bifunctional MOF-derived Co-N-doped carbon electrocatalysts for high-performance zinc-air batteries and MFCs, Energy, 156 (2018) 95-102.

[255] Z. Wang, H. Jin, T. Meng, K. Liao, W. Meng, J. Yang, D. He, Y. Xiong, S. Mu, Fe, Cu-Coordinated ZIF-Derived Carbon Framework for Efficient Oxygen Reduction Reaction and Zinc-Air Batteries, Adv. Funct. Mater., 28 (2018) 1802596.

[256] H.H. Wu, H.B. Li, X.F. Zhao, Q.F. Liu, J. Wang, J.P. Xiao, S.H. Xie, R. Si, F. Yang, S. Miao, X.G. Guo, G.X. Wang, X.H. Bao, Highly doped and exposed Cu(I)-N active sites within graphene towards efficient oxygen reduction for zinc-air batteries, Energy Environ. Sci., 9 (2016) 3736-3745.

[257] Q.X. Lai, J.J. Zhu, Y.X. Zhao, Y.Y. Liang, J.P. He, J.H. Chen, MOF-Based Metal-Doping-Induced Synthesis of Hierarchical Porous Cu-N/C Oxygen Reduction Electrocatalysts for Zn-Air Batteries, Small, 13 (2017) 1700740.

[258] J.S. Li, N. Zhou, J.Y. Song, L. Fu, J. Yan, Y.G. Tang, H.Y. Wang, Cu-MOF-Derived Cu/Cu_2O Nanoparticles and CuN_xC_y Species to Boost Oxygen Reduction Activity of Ketjenblack Carbon in Al-Air Battery, Acs Sustainable Chem. Eng., 6 (2018) 413-421.

[259] F.Z. Li, J.S. Li, Q.J. Feng, J. Yan, Y.G. Tang, H.Y. Wang, Significantly enhanced oxygen reduction activity of Cu/CuN_xC_y co-decorated ketjenblack catalyst for Al-air batteries, J. Energy Chem., 27 (2018) 419-425.

[260] J. Wei, Y. Liang, Y.X. Hu, B.A. Kong, G.P. Simon, J. Zhang, S.P. Jiang, H.T. Wang, A Versatile Iron-Tannin-Framework Ink Coating Strategy to Fabricate Biomass-Derived Iron Carbide/Fe-N-Carbon Catalysts for Efficient Oxygen Reduction, Angew. Chem. Int. Ed., 55 (2016) 1355-1359.

[261] Z.Y. Chen, Y.N. Li, L.L. Lei, S.J. Bao, M.Q. Wang, L. Heng, Z.L. Zhao, M.W. Xu, Investigation of Fe_2N@carbon encapsulated in N-doped graphene-like carbon as a catalyst in sustainable zinc-air batteries, Catal. Sci. Technol., 7 (2017) 5670-5676.

[262] C. Lin, S.S. Shinde, Z. Jiang, X.K. Song, Y. Sun, L.L. Guo, H. Zhang, J.Y. Jung, X.P. Li, J.H. Lee, In situ directional formation of Co@CoO_x-embedded 1D carbon nanotubes as an efficient oxygen electrocatalyst for ultra-high rate Zn-air batteries, J. Mater. Chem. A, 5 (2017) 13994-14002.

[263] L. Ye, G.L. Chai, Z.H. Wen, Zn-MOF-74 Derived N-Doped Mesoporous Carbon as pH-Universal Electrocatalyst for Oxygen Reduction Reaction, Adv. Funct. Mater., 27 (2017).

[264] H.B. Aiyappa, S.N. Bhange, V.P. Sivasankaran, S. Kurungot, Single Cell Fabrication Towards the Realistic Evaluation of a CNT-Strung ZIF-Derived Electrocatalyst as a Cathode Material in Alkaline Fuel Cells and Metal-Air Batteries, Chemelectrochem, 4 (2017) 2928-2933.

[265] Y.F. Ye, F. Cai, C.C. Yan, Y.S. Li, G.X. Wang, X.H. Bao, Two-step pyrolysis of ZIF-8 functionalized with ammonium ferric citrate for efficient oxygen reduction reaction, J. Energy Chem., 26 (2017) 1174-1180.

[266] C. Xuan, B. Hou, W. Xia, Z. Peng, T. Shen, H.L. Xin, G. Zhang, D. Wang, From a ZIF-8 polyhedron to three-dimensional nitrogen doped hierarchical porous carbon: an efficient electrocatalyst for the oxygen reduction reaction dagger, J. Mater. Chem. A, 6 (2018) 10731-10739.

[267] J.P. Wang, G.K. Han, L.G. Wang, L. Du, G.Y. Chen, Y.Z. Gao, Y.L. Ma, C.Y. Du, X.Q. Cheng, P.J. Zuo, G.P. Yin, ZIF-8 with Ferrocene Encapsulated: A Promising Precursor to Single-Atom Fe Embedded Nitrogen-Doped Carbon as Highly Efficient Catalyst for Oxygen Electroreduction, Small, 14 (2018).

[268] L. Cao, Z.H. Li, Y. Gu, D.H. Li, K.M. Su, D.J. Yang, B.W. Cheng, Rational design of N-doped carbon nanobox-supported Fe/Fe_2N/Fe_3C nanoparticles as efficient oxygen reduction catalysts for Zn-air batteries, J. Mater. Chem. A, 5 (2017) 11340-11347.

[269] G.H. Jin, S.Q. Liu, Y.M. Li, Y. Guo, Z.Y. Ding, Co_3O_4 Nanoparticles-Modified alpha-MnO_2 Nanorods Supported on Reduced Graphene Oxide as Cathode Catalyst for Oxygen Reduction Reaction in Alkaline Media, Nano, 11 (2016) 1650126.

[270] J. Yang, J.T. Hu, M.Y. Weng, R. Tan, L.L. Tian, J.L. Yang, J. Amine, J.X. Zheng, H.B. Chen, F. Pan, Fe-Cluster Pushing Electrons to N-Doped Graphitic Layers with Fe_3C(Fe) Hybrid Nanostructure to Enhance O_2 Reduction Catalysis of Zn-Air Batteries, ACS Appl. Mater. Interfaces, 9 (2017) 4587-4596.

[271] Q.M. Yu, J.X. Xu, C.X. Wu, J.S. Zhang, L.H. Guan, MnO_2 Nanofilms on Nitrogen-Doped Hollow Graphene Spheres as a High-Performance Electrocatalyst for Oxygen Reduction Reaction, ACS Appl. Mater. Interfaces, 8 (2016) 35264-35269.

[272] S.S. Zeng, F.C. Lyu, H.J. Nie, Y.W. Zhan, H.D. Bian, Y.Y. Tian, Z. Li, A.W. Wang, J. Lu, Y.Y. Li, Facile fabrication of N/S-doped carbon nanotubes with Fe_3O_4 nanocrystals enchased for lasting synergy as efficient oxygen reduction catalysts, J. Mater. Chem. A, 5 (2017) 13189-13195.

[273] K. Liu, Z. Zhou, H.Y. Wang, X.B. Huang, J.Y. Xu, Y.G. Tang, J.S. Li, H.L. Chu, J.J. Chen, N-Doped carbon supported Co_3O_4 nanoparticles as an advanced electrocatalyst for the oxygen reduction reaction in Al-air batteries, Rsc Adv., 6 (2016) 55552-55559.

[274] J. Zhang, H. Zhou, J.W. Zhu, P. Hu, C. Hang, J.L. Yang, T. Peng, S.C. Mu, Y.H. Huang, Facile Synthesis of Defect-Rich and S/N Co-Doped Graphene-Like Carbon Nanosheets as an Efficient Electrocatalyst for Primary and All-Solid-State Zn-Air Batteries, ACS Appl. Mater. Interfaces, 9 (2017) 24545-24554.

[275] Q. Wang, Z. Zhang, M. Wang, J. Li, J. Fang, Y. Lai, Self-assembled three-dimensional carbon networks with accessorial Lewis base sites and variational electron characteristics as efficient oxygen reduction reaction catalysts for alkaline metal-air batteries, Chinese J. Catal., 39 (2018) 1210-1218.

[276] L.N. Xu, H. Fan, L.X. Huang, J.L. Xia, S.H. Li, M. Li, H.Y. Ding, K. Huang, Chrysanthemum-derived N and S co-doped porous carbon for efficient oxygen reduction reaction and aluminum-air battery, Electrochim. Acta, 239 (2017) 1-9.

[277] T. Zhang, Z. Tao, J. Chen, Magnesium-air batteries: from principle to application, Mater. Horiz., 1 (2014) 196-206.

[278] C.S. Li, Y. Sun, W.H. Lai, J.Z. Wang, S.L. Chou, Ultrafine Mn_3O_4 Nanowires/Three-Dimensional Graphene/Single-Walled Carbon Nanotube Composites: Superior Electrocatalysts for Oxygen Reduction and Enhanced Mg/Air Batteries, ACS Appl. Mater. Interfaces, 8 (2016) 27710-27719.

[279] P.F. Yue, Z.F. Li, S.W. Wang, Y.X. Wang, MnO_2 nanorod catalysts for magnesium air fuel cells: Influence of different supports, Int. J. Hydrogen Energy, 40 (2015) 6809-6817.

[280] C.C. Zhao, Y.H. Jin, W.B. Du, C.W. Ji, X. Du, Multi-walled carbon nanotubes supported binary PdSn nanocatalyst as effective catalytic cathode for Mg-air battery, J. Electroanal. Chem., 826 (2018) 217-224.

[281] Y.F. Li, X.X. Zhang, H.B. Li, H.D. Yoo, X.W. Chi, Q.Y. An, J.Y. Liu, M. Yu, W.C. Wang, Y. Yao, Mixed-phase mullite electrocatalyst for pH-neutral oxygen reduction in magnesium-air batteries, Nano Energy, 27 (2016) 8-16.

[282] R. Wang, Z. Chen, N. Hu, C. Xu, Z. Shen, J. Liu, Nanocarbon-Based Electrocatalysts for Rechargeable Aqueous Li/Zn-Air Batteries, Chemelectrochem, 5 (2018) 1745-1763.

[283] S.K. Singh, V. Kashyap, N. Manna, S.N. Bhange, R. Soni, R. Boukherroub, S. Szunerits, S. Kurungot, Efficient and Durable Oxygen Reduction Electrocatalyst Based on CoMn Alloy Oxide Nanoparticles Supported Over N-Doped Porous Graphene, Acs Catal., 7 (2017) 6700-6710.

[284] Y.L. Liu, F.J. Chen, W. Ye, M. Zeng, N. Han, F.P. Zhao, X.X. Wang, Y.G. Li, High-Performance Oxygen Reduction Electrocatalyst Derived from Polydopamine and Cobalt Supported on Carbon Nanotubes for Metal-Air Batteries, Adv. Funct. Mater., 27 (2017) 1606034.

[285] G. Liu, Z. Liu, J. Li, M. Zeng, Z. Li, L. He, F. Li, Chitosan/phytic acid hydrogel as a platform for facile synthesis of heteroatom-doped porous carbon frameworks for electrocatalytic oxygen reduction, Carbon, 137 (2018) 68-77.

[286] Q.S. Hong, H.M. Lu, J.R. Wang, CuO Nanoplatelets with Highly Dispersed Ce-Doping Derived from Intercalated Layered Double Hydroxides for Synergistically Enhanced Oxygen Reduction Reaction in Al-Air Batteries, Acs Sustainable Chem. Eng., 5 (2017) 9169-9175.

[287] J.R. Wang, H.M. Lu, Q.S. Hong, Y. Cao, X.D. Li, J.J. Bai, Porous N,S-codoped carbon architectures with bimetallic sulphide nanoparticles encapsulated in graphitic layers: Highly active and robust electrocatalysts for the oxygen reduction reaction in Al-air batteries, Chem. Eng. J., 330 (2017) 1342-1350.

[288] Z. Cui, Y. Li, G. Fu, X. Li, J.B. Goodenough, Robust Fe_3Mo_3C Supported IrMn Clusters as Highly Efficient Bifunctional Air Electrode for Metal-Air Battery, Adv. Mater., 29 (2017) 1702385.

[289] Z.M. Cui, G.T. Fu, Y.T. Li, J.B. Goodenough, Ni_3FeN-Supported Fe_3Pt Intermetallic Nanoalloy as a High-Performance Bifunctional Catalyst for Metal-Air Batteries, Angew. Chem. Int. Ed., 56 (2017) 9901-9905.

[290] Z.Q. Ding, Z.H. Tang, L.G. Li, K. Wang, W. Wu, X.N. Chen, X. Wu, S.W. Chen, Ternary PtVCo dendrites for the hydrogen evolution reaction, oxygen evolution reaction, overall water splitting and rechargeable Zn-air batteries, Inorg. Chem. Front., 5 (2018) 2425-2431.

[291] C.C. Zhao, X.X. Yan, G.Q. Wang, Y.H. Jin, X. Du, W.B. Du, L. Sun, C.W. Ji, PdCo bimetallic nano-electrocatalyst as effective air-cathode for aqueous metal-air batteries, Int. J. Hydrogen Energy, 43 (2018) 5001-5011.

[292] J. Park, M. Park, G. Nam, M.G. Kim, J. Cho, Unveiling the Catalytic Origin of Nanocrystalline Yttrium Ruthenate Pyrochlore as a Bifunctional Electrocatalyst for Zn-Air Batteries, Nano Lett., 17 (2017) 3974-3981.

[293] T.H. You, C.C. Hu, Designing Binary Ru-Sn Oxides with Optimized Performances for the Air Electrode of Rechargeable Zinc-Air Batteries, ACS Appl. Mater. Interfaces, 10 (2018) 10064-10075.

[294] J. Hu, Q.N. Liu, L.N. Shi, Z.W. Shi, H. Huang, Silver decorated $LaMnO_3$ nanorod/graphene composite electrocatalysts as reversible metal-air battery electrodes, Appl. Surf. Sci., 402 (2017) 61-69.

[295] Z.Y. Guo, C. Li, W.Y. Li, H. Guo, X.L. Su, P. He, Y.G. Wang, Y.Y. Xia, Ruthenium oxide coated ordered mesoporous carbon nanofiber arrays: a highly bifunctional oxygen electrocatalyst for rechargeable Zn-air batteries, J. Mater. Chem. A, 4 (2016) 6282-6289.

[296] H.S. Park, E. Seo, J. Yang, Y. Lee, B.S. Kim, H.K. Song, Bifunctional hydrous RuO_2 nanocluster electrocatalyst embedded in carbon matrix for efficient and durable operation of rechargeable zinc-air batteries, Sci. Rep., 7 (2017) 7150.

[297] Y. Cheng, S. Dou, J.P. Veder, S. Wang, M. Saunders, S.P. Jiang, Efficient and Durable Bifunctional Oxygen Catalysts Based on NiFeO@MnO_x Core-Shell Structures for Rechargeable Zn-Air Batteries, ACS Appl. Mater. Interfaces, 9 (2017) 8121-8133.

[298] Q. Wang, L. Shang, R. Shi, X. Zhang, Y.F. Zhao, G.I.N. Waterhouse, L.Z. Wu, C.H. Tung, T.R. Zhang, NiFe Layered Double Hydroxide Nanoparticles on Co,N-Codoped Carbon Nanoframes as Efficient Bifunctional Catalysts for Rechargeable Zinc-Air Batteries, Adv. Energy Mater., 7 (2017) 1700467.

[299] Z. Zhang, D. Zhou, L. Zhou, H. Yu, B. Huang, NiFe LDH-CoPc/CNTs as novel bifunctional electrocatalyst complex for zinc-air battery, Ionics, 24 (2018) 1709-1714.

[300] Z.H. Li, M.F. Shao, Q.H. Yang, Y. Tang, M. Wei, D.G. Evans, X. Duan, Directed synthesis of carbon nanotube arrays based on layered double hydroxides toward highly-efficient bifunctional oxygen electrocatalysis, Nano Energy, 37 (2017) 98-107.

[301] M. Kuang, G.F. Zheng, Nanostructured Bifunctional Redox Electrocatalysts, Small, 12 (2016) 5656-5675.

[302] Y.L. Zhu, W. Zhou, Z.P. Shao, Perovskite/Carbon Composites: Applications in Oxygen Electrocatalysis, Small, 13 (2017) 1603793.

[303] Q.F. Liu, Z.P. Chen, Z. Yan, Y. Wang, E.D. Wang, S. Wang, S.D. Wang, G.Q. Sun, Crystal-Plane-Dependent Activity of Spinel Co_3O_4 Towards Water Splitting and the Oxygen Reduction Reaction, Chemelectrochem, 5 (2018) 1080-1086.

[304] Z.Q. Liu, H. Cheng, N. Li, T.Y. Ma, Y.Z. Su, $ZnCo_2O_4$ Quantum Dots Anchored on Nitrogen-Doped Carbon Nanotubes as Reversible Oxygen Reduction/Evolution Electrocatalysts, Adv. Mater., 28 (2016) 3777-3784.

[305] X.R. Wang, J.Y. Liu, Z.W. Liu, W.C. Wang, J. Luo, X.P. Han, X.W. Du, S.Z. Qiao, J. Yang, Identifying the Key Role of Pyridinic-N-Co Bonding in Synergistic Electrocatalysis for Reversible ORR/OER, Adv. Mater., 30 (2018) 1800005.

[306] C.Y. Ma, N.N. Xu, J.L. Qiao, S.S. Jian, J.J. Zhang, Facile synthesis of $NiCo_2O_4$ nanosphere-carbon nanotubes hybrid as an efficient bifunctional electrocatalyst for rechargeable Zn-air batteries, Int. J. Hydrogen Energy, 41 (2016) 9211-9218.

[307] P. Moni, S. Hyun, A. Vignesh, S. Shanmugam, Chrysanthemum flower-like $NiCo_2O_4$-nitrogen doped graphene oxide composite: an efficient electrocatalyst for lithium-oxygen and zinc-air batteries, Chem. Commun., 53 (2017) 7836-7839.

[308] Y.P. Deng, Y. Jiang, D. Luo, R.L. Liang, S.B. Cheng, Z.Y. Bai, Y.S. Liu, W. Lei, L. Yang, J. Zhu, Z.W. Chen, Hierarchical Porous Double-Shelled Electrocatalyst with Tailored Lattice Alkalinity toward Bifunctional Oxygen Reactions for Metal-Air Batteries, ACS Energy Lett., 2 (2017) 2706-2712.

[309] X.J. Wang, Y. Li, T. Jin, J. Meng, L.F. Jiao, M. Zhu, J. Chen, Electrospun Thin-Walled $CuCo_2O_4$@C Nanotubes as Bifunctional Oxygen Electrocatalysts for Rechargeable Zn-Air Batteries, Nano Lett., 17 (2017) 7989-7994.

[310] Y. Li, W. Zhou, J.C. Dong, Y. Luo, P.F. An, J. Liu, X. Wu, G.L. Xu, H.B. Zhang, J. Zhang, Interface engineered in situ anchoring of Co_9S_8 nanoparticles into a multiple doped carbon matrix: highly efficient zinc-air batteries, Nanoscale, 10 (2018) 2649-2657.

[311] X.P. Han, X.Y. Wu, C. Zhong, Y.D. Deng, N.Q. Zhao, W.B. Hu, $NiCo_2S_4$ nanocrystals anchored on nitrogen-doped carbon nanotubes as a highly efficient bifunctional electrocatalyst for rechargeable zinc-air batteries, Nano Energy, 31 (2017) 541-550.

[312] S. Dou, X.Y. Li, L. Tao, J. Huo, S.Y. Wang, Cobalt nanoparticle-embedded carbon nanotube/porous carbon hybrid derived from MOF-encapsulated Co_3O_4 for oxygen electrocatalysis, Chem. Commun., 52 (2016) 9727-9730.

[313] Z.Y. Guo, F.M. Wang, Y. Xia, J.L. Li, A.G. Tamirat, Y.R. Liu, L. Wang, Y.G. Wang, Y.Y. Xia, In situ encapsulation of core-shell-structured $Co@Co_3O_4$ into nitrogen-doped carbon polyhedra as a bifunctional catalyst for rechargeable Zn-air batteries, J. Mater. Chem. A, 6 (2018) 1443-1453.

[314] T.T. Li, Y.X. Lu, S.S. Zhao, Z.D. Gao, Y.Y. Song, Co_3O_4-doped Co/CoFe nanoparticles encapsulated in carbon shells as bifunctional electrocatalysts for rechargeable Zn-Air batteries, J. Mater. Chem. A, 6 (2018) 3730-3737.

[315] N.N. Xu, Y.Y. Liu, X. Zhang, X.M. Li, A.J. Li, J.L. Qiao, J.J. Zhang, Self-assembly formation of Bi-functional Co_3O_4/MnO_2-CNTs hybrid catalysts for achieving both high energy/power density and cyclic ability of rechargeable zin-cair battery, Sci. Rep., 6 (2016) 33590.

[316] C.W. Wang, Z. Zhao, X.F. Li, R. Yan, J. Wang, A.N. Li, X.Y. Duan, J.Y. Wang, Y. Liu, J.Z. Wang, Three-Dimensional Framework of Graphene Nanomeshes Shell/Co_3O_4 Synthesized as Superior Bifunctional Electrocatalyst for Zinc-Air Batteries, ACS Appl. Mater. Interfaces, 9 (2017) 41273-41283.

[317] Q. Shen, J. Yang, K.L. Chen, H. Wang, J.B. Liu, H. Yan, Co_3O_4 nanorods-graphene composites as catalysts for rechargeable zinc-air battery, J. Solid State Electrochem., 20 (2016) 3331-3336.

[318] G. Li, X.L. Wang, J. Fu, J.D. Li, M.G. Park, Y.N. Zhang, G. Lui, Z.W. Chen, Pomegranate-Inspired Design of Highly Active and Durable Bifunctional Electrocatalysts for Rechargeable Metal-Air Batteries, Angew. Chem. Int. Ed., 55 (2016) 4977-4982.

[319] Y.B. Li, C. Zhong, J. Liu, X.Q. Zeng, S.X. Qu, X. Han, Y.P. Deng, W.B. Hu, J. Lu, Atomically Thin Mesoporous Co_3O_4 Layers Strongly Coupled with N-rGO Nanosheets as High-Performance Bifunctional Catalysts for 1D Knittable Zinc-Air Batteries, Adv. Mater., 30 (2018) 1703657.

[320] M. Khalid, A.M.B. Honorato, H. Varela, L.M. Dai, Multifunctional electrocatalysts derived from conducting polymer and metal organic framework complexes, Nano Energy, 45 (2018) 127-135.

[321] V. Kashyap, S. Kurungot, Zirconium-Substituted Cobalt Ferrite Nanoparticle Supported N-doped Reduced Graphene Oxide as an Efficient Bifunctional Electrocatalyst for Rechargeable Zn-Air Battery, Acs Catal., 8 (2018) 3715-3726.

[322] S. Kim, O. Kwon, C. Kim, O. Gwon, H.Y. Jeong, K.H. Kim, J. Shin, G. Kim, Strategy for Enhancing Interfacial Effect of Bifunctional Electrocatalyst: Infiltration of Cobalt Nanooxide on Perovskite, Adv. Mater. Interfaces, 5 (2018) 1800123.

[323] N.N. Xu, Q. Nie, Y.N. Wei, H. Xu, Y.D. Wang, X.D. Zhou, J.L. Qiao, Bi-functional composite electrocatalysts consisting of nanoscale (La, Ca) oxides and carbon nanotubes for long-term zinc-air fuel cells and rechargeable batteries, Sustainable Energy Fuels, 2 (2018) 91-95.

[324] A. Vignesh, M. Prabu, S. Shanmugam, Porous $LaCo_{1-x}Ni_xO_{3-\delta}$ Nanostructures as an Efficient Electrocatalyst for Water Oxidation and for a Zinc-Air Battery, ACS Appl. Mater. Interfaces, 8 (2016) 6019-6031.

[325] Y.F. Bu, O. Gwon, G. Nam, H. Jang, S. Kim, Q. Zhong, J. Cho, G. Kim, A Highly Efficient and Robust Cation Ordered Perovskite Oxide as a Bifunctional Catalyst for Rechargeable Zinc-Air Batteries, Acs Nano, 11 (2017) 11594-11601.

[326] Q. Wang, Y.J. Xue, S.S. Sun, S.H. Li, H. Miao, Z.P. Liu, $La_{0.8}Sr_{0.2}Co_{1-x}Mn_xO_3$ perovskites as efficient bi-functional cathode catalysts for rechargeable zinc-air batteries, Electrochim. Acta, 254 (2017) 14-24.

[327] J. Hu, Q.N. Liu, Z.W. Shi, L. Zhang, H. Huang, $LaNiO_3$-nanorod/graphene composite as an efficient bi-functional catalyst for zinc-air batteries, Rsc Adv., 6 (2016) 86386-86394.

[328] S. Peng, X. Han, L. Li, S. Chou, D. Ji, H. Huang, Y. Du, J. Liu, S. Ramakrishna, Electronic and Defective Engineering of Electrospun $CaMnO_3$ Nanotubes for Enhanced Oxygen Electrocatalysis in Rechargeable Zinc-Air Batteries, Adv. Energy Mater., 8 (2018) 1800612.

[329] G.T. Fu, X.X. Yan, Y.F. Chen, L. Xu, D.M. Sun, J.M. Lee, Y.W. Tang, Boosting Bifunctional Oxygen Electrocatalysis with 3D Graphene Aerogel-Supported Ni/MnO Particles, Adv. Mater., 30 (2018) 1704609.

[330] T.R. Zhang, X.M. Ge, Z. Zhang, N.N. Tham, Z.L. Liu, A. Fisher, J.Y. Lee, Improving the Electrochemical Oxygen Reduction Activity of Manganese Oxide Nanosheets with Sulfurization-Induced Nanopores, Chemcatchem, 10 (2018) 422-429.

[331] M. Xiong, D.G. Ivey, Sequentially Electrodeposited MnO_x/Co-Fe as Bifunctional Electrocatalysts for Rechargeable Zinc-Air Batteries, J. Electrochem. Soc., 164 (2017) A1012-A1021.

[332] X. Liu, M. Park, M.G. Kim, S. Gupta, X.J. Wang, G. Wu, J. Cho, High-performance non-spinel cobalt-manganese mixed oxide-based bifunctional electrocatalysts for rechargeable zinc-air batteries, Nano Energy, 20 (2016) 315-325.

[333] J. Bai, T.M. Meng, D.L. Guo, S.G. Wang, B.G. Mao, M.H. Cao, Co_9S_8@MoS_2 Core Shell Heterostructures as Trifunctional Electrocatalysts for Overall Water Splitting and Zn Air Batteries, ACS Appl. Mater. Interfaces, 10 (2018) 1678-1689.

[334] L. An, Y.X. Li, M.C. Luo, J. Yin, Y.Q. Zhao, C.L. Xu, F.Y. Cheng, Y. Yang, P.X. Xi, S.J. Guo, Atomic-Level Coupled Interfaces and Lattice Distortion on CuS/NiS2 Nanocrystals Boost Oxygen Catalysis for Flexible Zn-Air Batteries, Adv. Funct. Mater., 27 (2017) 1703779.

[335] M.R. Wang, Y.Q. Lai, J. Fang, F.R. Qin, Z.A. Zhang, J. Li, K. Zhang, Hydrangea-like $NiCo_2S_4$ hollow microspheres as an advanced bifunctional electrocatalyst for aqueous metal/air batteries, Catal. Sci. Technol., 6 (2016) 434-437.

[336] Y.X. Li, J. Yin, L. An, M. Lu, K. Sun, Y.Q. Zhao, F.Y. Cheng, P.X. Xi, Metallic $CuCo_2S_4$ nanosheets of atomic thickness as efficient bifunctional electrocatalysts for portable, flexible Zn-air batteries, Nanoscale, 10 (2018) 6581-6588.

[337] T.T. Gao, Z.Y. Jin, Y.J. Zhang, G.Q. Tan, H.Y. Yuan, D. Xiao, Coupling cobalt-iron bimetallic nitrides and N-doped multi-walled carbon nanotubes as high-performance bifunctional catalysts for oxygen evolution and reduction reaction, Electrochim. Acta, 258 (2017) 51-60.

[338] G.T. Fu, Z.M. Cui, Y.F. Chen, L. Xu, Y.W. Tang, J.B. Goodenough, Hierarchically mesoporous nickel-iron nitride as a cost-efficient and highly durable electrocatalyst for Zn-air battery, Nano Energy, 39 (2017) 77-85.

[339] Y.C. Fan, S. Ida, A. Staykov, T. Akbay, H. Hagiwara, J. Matsuda, K. Kaneko, T. Ishihara, Ni-Fe Nitride Nanoplates on Nitrogen-Doped Graphene as a Synergistic Catalyst for Reversible Oxygen Evolution Reaction and Rechargeable Zn-Air Battery, Small, 13 (2017).

[340] M. Xiong, M.P. Clark, M. Labbe, D.G. Ivey, A horizontal zinc-air battery with physically decoupled oxygen evolution/reduction reaction electrodes, J. Power Sources, 393 (2018) 108-118.

[341] X. Guo, T. Zheng, G. Ji, N. Hu, C. Xu, Y. Zhang, Core/shell design of efficient electrocatalysts based on $NiCo_2O_4$ nanowires and NiMn LDH nanosheets for rechargeable zinc-air batteries, J. Mater. Chem. A, 6 (2018) 10243-10252.

[342] X. Wang, X.Y. Liu, C.J. Tong, X.T. Yuan, W.J. Dong, T.Q. Lin, L.M. Liu, F.Q. Huang, An electron injection promoted highly efficient electrocatalyst of $FeNi_3$@GR@Fe-NiOOH for oxygen evolution and rechargeable metal-air batteries, J. Mater. Chem. A, 4 (2016) 7762-7771.

[343] Y.Y. Huang, Q. Liu, J.Q. Lv, D.D. Babu, W.J. Wang, M.X. Wu, D.Q. Yuan, Y.B. Wang, Co-intercalation of multiple active units into graphene by pyrolysis of hydrogen-bonded precursors for zinc-air batteries and water splitting, J. Mater. Chem. A, 5 (2017) 20882-20891.

[344] Y.G. Li, M. Gong, Y.Y. Liang, J. Feng, J.E. Kim, H.L. Wang, G.S. Hong, B. Zhang, H.J. Dai, Advanced zinc-air batteries based on high-performance hybrid electrocatalysts, Nat. Commun., 4 (2013) 7.

[345] T. Wang, G. Nam, Y. Jin, X. Wang, P. Ren, M.G. Kim, J. Liang, X. Wen, H. Jang, J. Han, Y. Huang, Q. Li, J. Cho, NiFe (Oxy) Hydroxides Derived from NiFe Disulfides as an Efficient Oxygen Evolution Catalyst for Rechargeable Zn-Air Batteries: The Effect of Surface S Residues, Adv. Mater., 30 (2018) e1800757.

[346] D. Bin, Z.Y. Guo, A.G. Tamirat, Y.Y. Ma, Y.G. Wang, Y.Y. Xia, Crab-shell induced synthesis of ordered macroporous carbon nanofiber arrays coupled with $MnCo_2O_4$ nanoparticles as bifunctional oxygen catalysts for rechargeable Zn-air batteries, Nanoscale, 9 (2017) 11148-11157.

[347] Q.C. Wang, Y.J. Ji, Y.P. Lei, Y.B. Wang, Y.D. Wang, Y.Y. Li, S.Y. Wang, Pyridinic-N-Dominated Doped Defective Graphene as a Superior Oxygen Electrocatalyst for Ultrahigh-Energy-Density Zn-Air Batteries, ACS Energy Lett., 3 (2018) 1183-1191.

[348] S.S. Shinde, C.H. Lee, A. Sami, D.H. Kim, S.U. Lee, J.H. Lee, Scalable 3-D Carbon Nitride Sponge as an Efficient Metal-Free Bifunctional Oxygen Electrocatalyst for Rechargeable Zn-Air Batteries, Acs Nano, 11 (2017) 347-357.

[349] T. Sun, J. Wang, C. Qiu, X. Ling, B. Tian, W. Chen, C. Su, B, N Codoped and Defect-Rich Nanocarbon Material as a Metal-Free Bifunctional Electrocatalyst for Oxygen Reduction and Evolution Reactions, Adv. Sci., 5 (2018) 1800036.

[350] Z.X. Pei, H.F. Li, Y. Huang, Q. Xue, Y. Huang, M.S. Zhu, Z.F. Wang, C.Y. Zhi, Texturing in situ: N, S-enriched hierarchically porous carbon as a highly active reversible oxygen electrocatalyst, Energy Environ. Sci., 10 (2017) 742-749.

[351] J. Zhang, Z. Zhao, Z. Xia, L. Dai, A metal-free bifunctional electrocatalyst for oxygen reduction and oxygen evolution reactions, Nat. Nanotechnol., 10 (2015) 444-452.

[352] H.B. Yang, J.W. Miao, S.F. Hung, J.Z. Chen, H.B. Tao, X.Z. Wang, L.P. Zhang, R. Chen, J.J. Gao, H.M. Chen, L.M. Dai, B. Liu, Identification of catalytic sites for oxygen reduction and oxygen evolution in N-doped graphene materials: Development of highly efficient metal-free bifunctional electrocatalyst, Sci. Adv., 2 (2016) e1501122.

[353] T. Meng, J.W. Qin, S.G. Wang, D. Zhao, B.G. Mao, M.H. Cao, In situ coupling of $Co_{0.85}Se$ and N-doped carbon via one-step selenization of metal-organic frameworks as a trifunctional catalyst for overall water splitting and Zn-air batteries, J. Mater. Chem. A, 5 (2017) 7001-7014.

[354] Y. Pan, S. Liu, K. Sun, X. Chen, B. Wang, K. Wu, X. Cao, W.C. Cheong, R. Shen, A. Han, Z. Chen, L. Zheng, J. Luo, Y. Lin, Y. Liu, D. Wang, Q. Peng, Q. Zhang, C. Chen, Y. Li, A Bimetallic Zn/Fe Polyphthalocyanine-Derived Single-Atom Fe-N_4 Catalytic Site:A Superior Trifunctional Catalyst for Overall Water Splitting and Zn-Air Batteries, Angew. Chem. Int. Ed., 57 (2018) 8614-8618.

[355] L.T. Ma, S.M. Chen, Z.X. Pei, Y. Huang, G.J. Liang, F.N. Mo, Q. Yang, J. Su, Y.H. Gao, J.A. Zapien, C.Y. Zhi, Single-Site Active Iron-Based Bifunctional Oxygen Catalyst for a Compressible and Rechargeable Zinc-Air Battery, Acs Nano, 12 (2018) 1949-1958.

[356] S. Han, X. Hu, J. Wang, X. Fang, Y. Zhu, Novel Route to Fe-Based Cathode as an Efficient Bifunctional Catalysts for Rechargeable Zn-Air Battery, Adv. Energy Mater., 8 (2018).

[357] J. Li, S. Lu, H. Huang, D. Liu, Z. Zhuang, C. Zhong, ZIF-67 as Continuous Self-Sacrifice Template Derived $NiCo_2O_4$/Co,N-CNTs Nanocages as Efficient Bifunctional Electrocatalysts for Rechargeable Zn-Air Batteries, Acs Sustainable Chem. Eng., 6 (2018) 10021-10029.

[358] I.S. Amiinu, X.B. Liu, Z.H. Pu, W.Q. Li, Q.D. Li, J. Zhang, H.L. Tang, H.N. Zhang, S.C. Mu, From 3D ZIF Nanocrystals to Co-N_x/C Nanorod Array Electrocatalysts for ORR, OER, and Zn-Air Batteries, Adv. Funct. Mater., 28 (2018) .

[359] S.H. Ahn, X.W. Yu, A. Manthiram, "Wiring" Fe-N-x-Embedded Porous Carbon Framework onto 1D Nanotubes for Efficient Oxygen Reduction Reaction in Alkaline and Acidic Media, Adv. Mater., 29 (2017) 1704638.

[360] S.H. Liu, Z.Y. Wang, S. Zhou, F.J. Yu, M.Z. Yu, C.Y. Chiang, W.Z. Zhou, J.J. Zhao, J.S. Qiu, Metal-Organic-Framework-Derived Hybrid Carbon Nanocages as a Bifunctional Electrocatalyst for Oxygen Reduction and Evolution, Adv. Mater., 29 (2017) 1700874.

[361] M.D. Zhang, Q.B. Dai, H.G. Zheng, M.D. Chen, L.M. Dai, Novel MOF-Derived Co@N-C Bifunctional Catalysts for Highly Efficient Zn-Air Batteries and Water Splitting, Adv. Mater., 30 (2018) 1705431.

[362] Y.H. Qian, Z.G. Hu, X.M. Ge, S.L. Yang, Y.W. Peng, Z.X. Kang, Z.L. Liu, J.Y. Lee, D. Zhao, A metal-free ORR/OER bifunctional electrocatalyst derived from metal-organic frameworks for rechargeable Zn-Air batteries, Carbon, 111 (2017) 641-650.

[363] C. Kim, O. Gwon, I.Y. Jeon, Y. Kim, J. Shin, Y.W. Ju, J.B. Baek, G. Kim, Cloud-like graphene nanoplatelets on $Nd_{0.5}Sr_{0.5}CoO_{3-\delta}$ nanorods as an efficient bifunctional electrocatalyst for hybrid Li-air batteries, J. Mater. Chem. A, 4 (2016) 2122-2127.

[364] D. Safanama, S. Adams, High efficiency aqueous and hybrid lithium-air batteries enabled by $Li_{1.5}Al_{0.5}Ge_{1.5}(PO_4)_3$ ceramic anode-protecting membranes, J. Power Sources, 340 (2017) 294-301.

[365] X. Liu, H. Gong, T. Wang, H. Guo, L. Song, W. Xia, B. Gao, Z.Y. Jiang, L.F. Feng, J.P. He, Cobalt-Doped Perovskite-Type Oxide LaMnO3 as Bifunctional Oxygen Catalysts for Hybrid Lithium-Oxygen Batteries, Chem. Asian J., 13 (2018) 528-535.

[366] A. Tan, M.V. Reddy, S. Adams, Synthesis and application of nanostructured MCo_2O_4(M=Co, Ni) for hybrid Li-air batteries, Ionics, 23 (2017) 2589-2602.

[367] M. Abirami, S.M. Hwang, J. Yang, S.T. Senthilkumar, J. Kim, W.S. Go, B. Senthilkumar, H.K. Song, Y. Kim, A Metal-Organic Framework Derived Porous Cobalt Manganese Oxide Bifunctional Electrocatalyst for Hybrid Na-Air/Seawater Batteries, ACS Appl. Mater. Interfaces, 8 (2016) 32778-32787.

[368] Y. Kang, D. Zou, J.Y. Zhang, F. Liang, K. Hayashi, H. Wang, D.F. Xue, K.F. Chen, K.R. Adair, X.L. Sun, Dual-phase Spinel $MnCo_2O_4$ Nanocrystals with Nitrogen-doped Reduced Graphene Oxide as Potential Catalyst for Hybrid Na-Air Batteries, Electrochim. Acta, 244 (2017) 222-229.

[369] Y. Wu, X. Qiu, F. Liang, Q. Zhang, A. Koo, Y. Dai, Y. Lei, X. Sun, A metal-organic framework-derived bifunctional catalyst for hybrid sodium-air batteries, Appl. Catal. B: Environ., 241 (2019) 407-414.

[370] J.Y. Cheon, K. Kim, Y.J. Sa, S.H. Sahgong, Y. Hong, J. Woo, S.D. Yim, H.Y. Jeong, Y. Kim, S.H. Joo, Graphitic Nanoshell/Mesoporous Carbon Nanohybrids as Highly Efficient and Stable Bifunctional Oxygen Electrocatalysts for Rechargeable Aqueous Na-Air Batteries, Adv. Energy Mater., 6 (2016) 1501794.

[371] G. Nam, Y. Son, S.O. Park, W.C. Jeon, H. Jang, J. Park, S. Chae, Y. Yoo, J. Ryu, M.G. Kim, S.K. Kwak, J. Cho, A Ternary $Ni_{46}Co_{40}Fe_{14}$ Nanoalloy-Based Oxygen Electrocatalyst for Highly Efficient Rechargeable Zinc-Air Batteries, Adv. Mater., (2018) e1803372.

[372] Y.Q. Zhang, M. Li, B. Hua, Y. Wang, Y.F. Sun, J.L. Luo, A strongly cooperative spinel nanohybrid as an efficient bifunctional oxygen electrocatalyst for oxygen reduction reaction and oxygen evolution reaction, Appl. Catal. B Environ., 236 (2018) 413-419.

[373] J.I. Jung, M. Risch, S. Park, M.G. Kim, G. Nam, H.Y. Jeong, Y. Shao-Horn, J. Cho, Optimizing nanoparticle perovskite for bifunctional oxygen electrocatalysis, Energy Environ. Sci., 9 (2016) 176-183.

[374] W.W. Liu, J. Zhang, Z.Y. Bai, G.P. Jiang, M. Li, K. Feng, L. Yang, Y.L. Ding, T.W. Yu, Z.W. Chen, A.P. Yu, Controllable Urchin-Like $NiCo_2S_4$ Microsphere Synergized with Sulfur-Doped Graphene as Bifunctional Catalyst for Superior Rechargeable Zn-Air Battery, Adv. Funct. Mater., 28 (2018).

[375] G.T. Fu, Z.M. Cui, Y.F. Chen, Y.T. Li, Y.W. Tang, J.B. Goodenough, Ni_3Fe-N Doped Carbon Sheets as a Bifunctional Electrocatalyst for Air Cathodes, Adv. Energy Mater., 7 (2017) 1601172.

[376] Y.-J. Cho, I.-J. Park, H.-J. Lee, J.-G. Kim, Aluminum anode for aluminum-air battery-Part I: Influence of aluminum purity, J. Power Sources, 277 (2015) 370-378.

[377] M. Jingling, W. Jiuba, Z. Hongxi, L. Quanan, Electrochemical performances of $Al_{0.5}Mg_{0.1}Sn_{0.02}In$ alloy in different solutions for Al-air battery, J. Power Sources, 293 (2015) 592-598.

[378] S.K. Das, S. Mahapatra, H. Lahan, Aluminium-ion batteries: developments and challenges, J. Mater. Chem. A, 5 (2017) 6347-6367.

[379] D. Muñoz-Torrero, P. Leung, E. García-Quismondo, E. Ventosa, M. Anderson, J. Palma, R. Marcilla, Investigation of different anode materials for aluminium rechargeable batteries, J. Power Sources, 374 (2018) 77-83.

[380] L. Fan, H. Lu, J. Leng, Performance of fine structured aluminum anodes in neutral and alkaline electrolytes for Al-air batteries, Electrochimica Acta, 165 (2015) 22-28.

[381] L. Fan, H. Lu, J. Leng, Z. Sun, C. Chen, The effect of crystal orientation on the aluminum anodes of the aluminum–air batteries in alkaline electrolytes, J. Power Sources, 299 (2015) 66-69.

[382] M. Pino, D. Herranz, J. Chacon, E. Fatas, P. Ocon, Carbon treated commercial aluminium alloys as anodes for aluminium-air batteries in sodium chloride electrolyte, J. Power Sources, 326 (2016) 296-302.

[383] J. Lee, B. Hwang, M.-S. Park, K. Kim, Improved reversibility of Zn anodes for rechargeable Zn-air batteries by using alkoxide and acetate ions, Electrochim. Acta, 199 (2016) 164-171.

[384] S.-M. Lee, Y.-J. Kim, S.-W. Eom, N.-S. Choi, K.-W. Kim, S.-B. Cho, Improvement in self-discharge of Zn anode by applying surface modification for Zn-air batteries with high energy density, J. Power Sources, 227 (2013) 177-184.

[385] Y.N. Jo, S.H. Kang, K. Prasanna, S.W. Eom, C.W. Lee, Shield effect of polyaniline between zinc active material and aqueous electrolyte in zinc-air batteries, Appl. Surf. Sci., 422 (2017) 406-412.

[386] M. Schmid, M. Willert-Porada, Electrochemical behavior of zinc particles with silica based coatings as anode material for zinc air batteries with improved discharge capacity, J. Power Sources, 351 (2017) 115-122.

[387] D. Stock, S. Dongmo, F. Walther, J. Sann, J. Janek, D. Schröder, Homogeneous Coating with an Anion-Exchange Ionomer Improves the Cycling Stability of Secondary Batteries with Zinc Anodes, ACS Appl. Mater. Interfaces, 10 (2018) 8640-8648.

[388] M. Schmid, M. Willert-Porada, Zinc particles coated with bismuth oxide based glasses as anode material for zinc air batteries with improved electrical rechargeability, Electrochim. Acta, 260 (2018) 246-253.

[389] P. Titscher, J.-C. Riede, J. Wiedemann, U. Kunz, A. Kwade, Multiscale Structured Particle-Based Zinc Anodes in Non-Stirred Alkaline Systems for Zinc–Air Batteries, Energy Technol., 6 (2018) 773-780.

[390] Z. Yan, E.D. Wang, L.H. Jiang, G.Q. Sun, Superior cycling stability and high rate capability of three-dimensional Zn/Cu foam electrodes for zinc-based alkaline batteries, Rsc Adv., 5 (2015) 83781-83787.

[391] Z. Zhang, Z.H. Yang, J.H. Huang, Z.B. Feng, X.E. Xie, Enhancement of electrochemical performance with Zn-Al-Bi layered hydrotalcites as anode material for Zn/Ni secondary battery, Electrochim. Acta, 155 (2015) 61-68.

[392] L.S. Sun, Z. Yi, J. Lin, F. Liang, Y.M. Wu, Z.Y. Cao, L.M. Wang, Fast and energy efficient synthesis of ZnO@RGO and its application in Ni–Zn secondary battery, J. Phys. Chem. C, 120 (2016) 12337-12343.

[393] C. Yang, Z.J. Zhang, Z.L. Tian, K. Zhang, J. Li, Y.Q. Lai, Polydopamine-coated nano-ZnO for high-performance rechargeable Zn–Ni battery, Materials Letters, 197 (2017) 163-166.

[394] A.M. Zamarayeva, A.M. Gaikwad, I. Deckman, M. Wang, B. Khau, D.A. Steingart, A.C. Arias, Fabrication of a high‐performance flexible Silver–Zinc wire battery, Adv. Electron.Mater., 2 (2016) 1500296.

[395] C.W. Li, Q.C. Zhang, J. Sun, T.T. Li, S.F. E, Z.Z. Zhu, B. He, Z.Y. Zhou, Q.L. Li, Y.G. Yao, High-performance quasi-solid-state flexible aqueous rechargeable Ag–Zn battery based on metal–organic framework-derived Ag nanowires, ACS Energy Lett., 3 (2018) 2761-2768.

[396] M. Deng, D. Höche, S.V. Lamaka, D. Snihirova, M.L. Zheludkevich, Mg-Ca binary alloys as anodes for primary Mg-air batteries, J. Power Sources, 396 (2018) 109-118.

[397] D. Höche, S.V. Lamaka, B. Vaghefinazari, T. Braun, R.P. Petrauskas, M. Fichtner, M.L. Zheludkevich, Performance boost for primary magnesium cells using iron complexing agents as electrolyte additives, Sci. Rep., 8 (2018) 7578.

[398] N. Wang, R. Wang, Y. Feng, W. Xiong, J. Zhang, M. Deng, Discharge and corrosion behaviour of Mg-Li-Al-Ce-Y-Zn alloy as the anode for Mg-air battery, Corros. Sci., 112 (2016) 13-24.

[399] H. Xiong, K. Yu, X. Yin, Y. Dai, Y. Yan, H. Zhu, Effects of microstructure on the electrochemical discharge behavior of Mg-6wt%Al-1wt%Sn alloy as anode for Mg-air primary battery, J. Alloys Compounds, 708 (2017) 652-661.

[400] J. Li, B. Zhang, Q. Wei, N. Wang, B. Hou, Electrochemical behavior of Mg-Al-Zn-In alloy as anode materials in 3.5wt.% NaCl solution, Electrochim. Acta, 238 (2017) 156-167.

[401] X. Liu, S. Liu, J. Xue, Discharge performance of the magnesium anodes with different phase constitutions for Mg-air batteries, J. Power Sources, 396 (2018) 667-674.

[402] D.M. See, R.E. White, Temperature and Concentration Dependence of the Specific Conductivity of Concentrated Solutions of Potassium Hydroxide, J. Chem. Eng. Data, 42 (1997) 1266-1268.

[403] M.A. Deyab, 1-Allyl-3-methylimidazolium bis(trifluoromethylsulfonyl)imide as an effective organic additive in aluminum-air battery, Electrochim. Acta, 244 (2017) 178-183.

[404] D. Wang, H. Li, J. Liu, D. Zhang, L. Gao, L. Tong, Evaluation of AA5052 alloy anode in alkaline electrolyte with organic rare-earth complex additives for aluminium-air batteries, J. Power Sources, 293 (2015) 484-491.

[405] J. Liu, D. Wang, D. Zhang, L. Gao, T. Lin, Synergistic effects of carboxymethyl cellulose and ZnO as alkaline electrolyte additives for aluminium anodes with a view towards Al-air batteries, J. Power Sources, 335 (2016) 1-11.

[406] P. Pei, K. Wang, Z. Ma, Technologies for extending zinc–air battery's cyclelife: A review, Appl. Energy, 128 (2014) 315-324.

[407] J. Jindra, J. Mrha, M. Musilová, Zinc-air cell with neutral electrolyte, J. Appl. Electrochem., 3 (1973) 297-301.

[408] F.T. Goh, Z. Liu, T.A. Hor, J. Zhang, X. Ge, Y. Zong, A. Yu, W. Khoo, A near-neutral chloride electrolyte for electrically rechargeable zinc-air batteries, J. Electrochem. Soc., 161 (2014) A2080-A2086.

[409] Z.F. Pan, L. An, T.S. Zhao, Z.K. Tang, Advances and challenges in alkaline anion exchange membrane fuel cells, Prog. Energy Combust. Sci., 66 (2018) 141-175.

[410] S. Liu, W. Han, B. Cui, X. Liu, H. Sun, J. Zhang, M. Lefler, S. Licht, Rechargeable Zinc Air Batteries and Highly Improved Performance through Potassium Hydroxide Addition to the Molten Carbonate Eutectic Electrolyte, J. Electrochem. Soc., 165 (2018) A149-A154.

[411] Z. Pan, B. Huang, L. An, Performance of a hybrid direct ethylene glycol fuel cell, Int. J. Energy Res., 43 (2019) 2583-2591.

[412] M.D. Koninck, P. Manseau, B. Marsan, Preparation and characterization of Nb-doped TiO_2 nanoparticles used as a conductive support for bifunctional $CuCo_2O_4$ electrocatalyst, J. Electroanal. Chem., 611 (2007) 67-79.

[413] A. Sumboja, X. Ge, G. Zheng, F.W.T. Goh, T.S.A. Hor, Y. Zong, Z. Liu, Durable rechargeable zinc-air batteries with neutral electrolyte and manganese oxide catalyst, J. Power Sources, 332 (2016) 330-336.

[414] F. Wang, O. Borodin, T. Gao, X. Fan, W. Sun, F. Han, A. Faraone, J.A. Dura, K. Xu, C. Wang, Highly reversible zinc metal anode for aqueous batteries, Nat. Mater., 17 (2018) 543-549.

[415] M. Mayilvel Dinesh, K. Saminathan, M. Selvam, S.R. Srither, V. Rajendran, K.V.I.S. Kaler, Water soluble graphene as electrolyte additive in magnesium-air battery system, J. Power Sources, 276 (2015) 32-38.

[416] M.A. Deyab, Decyl glucoside as a corrosion inhibitor for magnesium-air battery, J. Power Sources, 325 (2016) 98-103.

[417] F.W. Richey, B.D. McCloskey, A.C. Luntz, Mg anode corrosion in aqueous electrolytes and implications for Mg-Air batteries, J. Electrochem. Soc., 163 (2016) A958-A963.

[418] Y. Zhao, G. Huang, C. Zhang, C. Peng, F. Pan, Effect of phosphate and vanadate as electrolyte additives on the performance of Mg-air batteries, Mater. Chem. Phys., 218 (2018) 256-261.

[419] X. Yu, M.M. Gross, S. Wang, A. Manthiram, Aqueous Electrochemical Energy Storage with a Mediator-Ion Solid Electrolyte, Adv. Energy Mater., 7 (2017) 1602454.

[420] J. Fu, J. Zhang, X. Song, H. Zarrin, X. Tian, J. Qiao, L. Rasen, K. Li, Z. Chen, A flexible solid-state electrolyte for wide-scale integration of rechargeable zinc-air batteries, Energy Environ. Sci., 9 (2016) 663-670.

[421] H.J. Hwang, W.S. Chi, O. Kwon, J.G. Lee, J.H. Kim, Y.G. Shul, Selective Ion Transporting Polymerized Ionic Liquid Membrane Separator for Enhancing Cycle Stability and Durability in Secondary Zinc-Air Battery Systems, ACS Appl. Mater. Interfaces, 8 (2016) 26298-26308.

[422] H.J. Lee, J.M. Lim, H.W. Kim, S.H. Jeong, S.W. Eom, Young T. Hong, S.Y. Lee, Electrospun polyetherimide nanofiber mat-reinforced, permselective polyvinyl alcohol composite separator membranes: A membrane-driven step closer toward rechargeable zinc-air batteries, J. Memb. Sci., 499 (2016) 526-537.

[423] H.W. Kim, J.M. Lim, H.J. Lee, S.W. Eom, Y.T. Hong, S.Y. Lee, Artificially engineered, bicontinuous anion-conducting/-repelling polymeric phases as a selective ion transport channel for rechargeable zinc-air battery separator membranes, J. Mater. Chem. A, 4 (2016) 3711-3720.

[424] A.R. Mainar, O. Leonet, M. Bengoechea, I. Boyano, I. de Meatza, A. Kvasha, A. Guerfi, J.A. Blazquez, Alkaline aqueous electrolytes for secondary zinc-air batteries: an overview, Int. J. Energy Res., 40 (2016) 1032-1049.

[425] P. Xie, M.Z. Rong, M.Q. Zhang, Moisture Battery Formed by Direct Contact of Magnesium with Foamed Polyaniline, Angew.Chem. Int.Ed., 55 (2016) 1805-1809.

[426] B. Pichler, S. Weinberger, L. Rescec, I. Grimmer, F. Gebetsroither, B. Bitschnau, V. Hacker, Bifunctional electrode performance for zinc-air flow cells with pulse charging, Electrochim. Acta, 251 (2017) 488-497.

[427] http://www.powerone-batteries.com/en/products/zinc-air-mercury-free-batteries. (accessed: January 2019)

[428] P. Tan, B. Chen, H.R. Xu, H.C. Zhang, W.Z. Cai, M. Ni, M.L. Liu, Z.P. Shao, Flexible Zn- and Li-air batteries: recent advances, challenges, and future perspectives, Energy Environ. Sci., 10 (2017) 2056-2080.

[429] A. Sumboja, X.M. Ge, Y. Zong, Z.L. Liu, Progress in development of flexible metal-air batteries, Funct. Mater. Lett., 9 (2016) 1630001.

[430] Y.H. He, B. Matthews, J.Y. Wang, L. Song, X.X. Wang, G. Wu, Innovation and challenges in materials design for flexible rechargeable batteries: from 1D to 3D, J. Mater. Chem. A, 6 (2018) 735-753.

[431] A.V. Ilyukhina, B.V. Kleymenov, A.Z. Zhuk, Development and study of aluminum-air electrochemical generator and its main components, J. Power Sources, 342 (2017) 741-749.

[432] W. Vielstich, A. Lamm, H.A.Gasteiger, Handbook of fuel cells : fundamentals, technology, and applications, Wiley, 2003.

[433] http://www.dafc.dicp.ac.cn/yanjiufangxiang/2010040759.html. (accessed: January 2019)

[434] Z. Yan, J.X. Gao, M. Liu, E.D. Wang, G.Q. Sun, Reducing the Cost of Zinc-Oxygen Batteries by Oxygen Recycling, Energy Technol., 6 (2018) 246-250.

[435] E. Wang, Z. Yan, Q. Liu, J. Gao, M. Liu, G. Sun, Research and Development of Metal-Air Fuel Cells, Springer International Publishing, Cham, Switzerland, 2018.

[436] B. Yirka. Phinergy demonstrates aluminum-air battery capable of fueling an electric vehicle for 1000 miles. https://phys.org/news/2013-03-phinergy-aluminum-air-battery-capable-fueling.html. (accessed: January 2019)